BULLETIN OF RUSSIAN STATE MEDICAL UNIVERSITY

BIOMEDICAL JOURNAL OF PIROGOV RUSSIAN NATIONAL RESEARCH MEDICAL UNIVERSITY

SUBMISSION http://vestnikrgmu.ru/login?lang=en
CORRESPONDENCE editor@vestnikrgmu.ru
COLLABORATION manager@vestnikrgmu.ru
ADDRESS ul. Ostrovityanova, d. 1, Moscow, Russia, 117997

Indexed in Scopus. CiteScore 2020: 0.4

Indexed in WoS. JCR 2020: 0.4

Five-year h-index is 6

Indexed in RSCI. IF 2018: 0,5

Listed in HAC 31.01.2020 (№ 507)

Open access to archive

Issue DOI: 10.24075/brsmu.2021-01
The mass media registration certificate no. 012769 issued on July 29, 1994
Founder and publisher is Pirogov Russian National Research Medical University (Moscow, Russia)

Approved for print 28.02.2021
Circulation: 100 copies. Printed by Print.Formula
www.print-formula.ru

ВЕСТНИК РОССИЙСКОГО ГОСУДАРСТВЕННОГО МЕДИЦИНСКОГО УНИВЕРСИТЕТА

НАУЧНЫЙ МЕДИЦИНСКИЙ ЖУРНАЛ РНИМУ ИМ. Н. И. ПИРОГОВА

ГЛАВНЫЙ РЕДАКТОР Денис Ребриков, д. б. н., профессор

ЗАМЕСТИТЕЛЬ ГЛАВНОГО РЕДАКТОРА Александр Эттингер, д. м. н., профессор

РЕДАКТОРЫ Валентина Гейдебрехт, Надежда Тихомирова

ТЕХНИЧЕСКИЙ РЕДАКТОР Нина Тюрина

ПЕРЕВОДЧИКИ Екатерина Третьякова, Вячеслав Витюк

ДИЗАЙН И ВЕРСТКА Марины Дорониной

ПОДАЧА РУКОПИСЕЙ http://vestnikrgmu.ru/login
ПЕРЕПИСКА С РЕДАКЦИЕЙ editor@vestnikrgmu.ru
СОТРУДНИЧЕСТВО manager@vestnikrgmu.ru
АДРЕС РЕДАКЦИИ ул. Островитянова, д. 1, г. Москва, 117997

Журнал включен в Scopus. CiteScore 2020: 0,4

Журнал включен в WoS. JCR 2020: 0,4

Индекс Хирша (h^{5}) журнала по оценке Google Scholar: 6

Журнал включен в РИНЦ. IF 2018: 0,5

Журнал включен в Перечень 31.01.2020 (№ 507)

Здесь находится открытый архив журнала

DOI выпуска: 10.24075/vrgmu.2021-01
Свидетельство о регистрации средства массовой информации № 012769 от 29 июля 1994 г.
Учредитель и издатель — Российский национальный исследовательский медицинский университет имени Н. И. Пирогова (Москва, Россия)

Подписано в печать 28.02.2021
Тираж 100 экз. Отпечатано в типографии Print.Formula
www.print-formula.ru

BULLETIN OF RSMU **1, 2021**
ВЕСТНИК РГМУ

Contents
Содержание

REVIEW 5

The features of HIV and SARS-CoV-2-coinfection in a pandemic
Oleynik AF, Revathy CG, Fazylov VH

Особенности течения сочетанной инфекции ВИЧ/SARS-CoV-2 в условиях пандемии
А. Ф. Олейник, Ч. Г. Реватхи, В. Х. Фазылов

ORIGINAL RESEARCH 13

The importance of determining SARS-CoV-2 N-Ag serodiagnostics for the management of COVID-19 pneumonia in hospital settings
Lebedin YuS, Lyang OV, Galstyan AG, Panteleeva AV, Belousov VV, Rebrikov DV

Важность определения N-антигена вируса SARS-CoV-2 для лечения пневмонии COVID-19 в условиях стационара
Ю. С. Лебедин, О. В. Лянг, А. Г. Галстян, А. В. Пантеелеева, В. В. Белоусов, Д. В. Ребриков

ORIGINAL RESEARCH 19

Associations between glutamate cysteine ligase catalytic subunit gene polymorphisms and clinical characteristics of ischemic stroke
Bocharova YA

Ассоциация полиморфных вариантов гена каталитической субъединицы глутаматцистеинлигазы с клиническими характеристиками ишемического инсульта
Ю. А. Бочарова

ORIGINAL RESEARCH 24

Characteristics of *BRCA*-associated breast cancer in the population of the Russian Federation
Novikova EI, Kudinova EA, Bozhenko VK, Solodkiy VA

Характеристика *BRCA*-ассоциированного рака молочной железы в российской популяции
Е. И. Новикова, Е. А. Кудинова, В. К. Боженко, В. А. Солодкий

ORIGINAL RESEARCH 30

Analysis of 13 *TP53* and *WRAP53* polymorphism frequencies in Russian populations
Olkova MV, Petrushenko VS, Ponomarev GYu

Анализ частот 13 полиморфизмов в генах *TP53* и *WRAP53* в российских популяциях
М. В. Олькова, В. С. Петрушенко, Г. Ю. Пономарев

ORIGINAL RESEARCH 40

Morphofunctional characteristics of cutaneous connective tissue scars in women with past history of childbirth after cesarian delivery
Mishina ES, Zatolokina MA, Mnikhovich MV, Kharchenko VV

Морфофункциональные особенности соединительнотканного рубца на коже у повторнородящих женщин после оперативного родоразрешения
Е. С. Мишина, М. А. Затолокина, М. В. Мнихович, В. В. Харченко

ORIGINAL RESEARCH 45

Elemental composition of blood of infertile patients participating in assisted reproduction programs
Syrkasheva AG, Frankevich VE, Dolgushina NV

Элементный состав крови пациенток с бесплодием в программах вспомогательных репродуктивных технологий
А. Г. Сыркашева, В. Е. Франкевич, Н. В. Долгушина

ORIGINAL RESEARCH 51

Oculomotor response to images in primary school children with mild intellectual disability
Nikishina VB, Prirodova OF, Petrash EA, Sevrukova IA

Глазодвигательные реакции при восприятии изображений младшими школьниками с легкой степенью умственной отсталости
В. Б. Никишина, О. Ф. Природова, Е. А. Петраш, И. А. Севрюкова

ORIGINAL RESEARCH 59

Bone turnover markers in patients with isolated femoral shaft fracture undergoing systemic ozone therapy
Osikov MV, Davidova EV, Abramov KS

Маркеры ремоделирования костной ткани при консолидации изолированного перелома бедренной кости в условиях системной озонотерапии
М. В. Осиков, Е. В. Давыдова, К. С. Абрамов

Refinement of noninvasive methods for diagnosing precancer and cancer of oral mucosa in general dental practice
Postnikov MA, Gabrielyan AG, Trunin DA, Kaganov OI, Kirillova VP, Khamadeeva AM, Osokin OV, Kopetskiy IS, Eremin DA

Совершенствование неинвазивных методов диагностики предраковых и злокачественных заболеваний слизистой оболочки рта на приеме у стоматолога
М. А. Постников, А. Г. Габриелян, Д. А. Трунин, О. И. Каганов, В. П. Кириллова, А. М. Хамадеева, О. В. Осокин, И. С. Копецкий, Д. А. Еремин

THE FEATURES OF HIV AND SARS-COV-2-COINFECTION IN A PANDEMIC

Oleynik AF[1,2] ✉, Revathy CG[2], Fazylov VH[1,3]

[1] Republic Center for AIDS and Infectious Diseases Prevention and Control, Kazan, Russia

[2] Kazan (Volga region) Federal University, Kazan, Russia

[3] Kazan State Medical University, Kazan, Russia

COVID-19 is known to undertake a severe course in several groups of patients. The review presents the latest data on the main features of COVID-19 course in HIV patients. People living with HIV, have not been found to be at a higher risk for acquiring COVID-19 and the disease runs a similar course compared to the general population in HIV patients on continuous antiretroviral therapy (ART) with a suppressed viral load and CD4+-T-lymphocytes count > 200cells/μl. Fewer than expected HIV patients have been reported to be hospitalised, this leads to hypothesize that infection may be majorly asymptomatic in this group of patients owing to their weak immune response. The patient's use of ART might also explain the comparatively milder disease course of COVID-19 seen in patients with HIV/SARS-CoV-2 coinfection. While ART use cannot be considered to be a protective factor against contracting the SARS-CoV-2, researchers assume that the therapy could stabilize the immune response in coinfected patients and thus prevent progression of the disease to the severe forms.

Keywords: COVID-19, SARS-CoV-2, HIV, human immunodeficiency virus, antiretroviral therapy, HIV/SARS-CoV-2-coinfection, PLHIV

Author contribution: Oleynik AF, Revathy Govindarajan C — literature review, manuscript authoring; Fazylov VH — manuscript authoring.

✉ **Correspondence should be addressed:** Alfiya F. Oleynik
Gvardeyskaya, 31/42-42, Kazan, 420073; alfiyaoleinik@yandex.ru

Received: 19.12.2020 **Accepted:** 26.01.2021 **Published online:** 08.02.2021

DOI: 10.24075/brsmu.2021.004

ОСОБЕННОСТИ ТЕЧЕНИЯ СОЧЕТАННОЙ ИНФЕКЦИИ ВИЧ/SARS-COV-2 В УСЛОВИЯХ ПАНДЕМИИ

А. Ф. Олейник[1,2] ✉, Ч. Г. Реватхи[2], В. Х. Фазылов[1,3]

[1] Республиканский центр по профилактике и борьбе со СПИД и инфекционными заболеваниями, Казань, Россия

[2] Казанский (Приволжский) федеральный университет, Казань, Россия

[3] Казанский государственный медицинский университет, Казань, Россия

Известно, что некоторые группы пациентов тяжело переносят COVID-19. В обзоре представлены последние данные об особенностях течения COVID-19 у пациентов, инфицированных вирусом иммунодефицита человека (ВИЧ). Установлено, что у людей с ВИЧ, находящихся на непрерывной антиретровирусной терапии (АРВТ), имеющих подавленную вирусную нагрузку и число CD4+-Т-лимфоцитов более 200 клеток/мкл, риск заражения и течение COVID-19 сопоставимы с таковыми в общей популяции. Пациенты с ВИЧ-инфекцией демонстрируют меньшую частоту госпитализаций, чем ожидалось, что предположительно может быть связано с бессимптомным течением COVID-19 на фоне слабого иммунного ответа у этих больных. Кроме того, сравнительно легкое течение заболевания у пациентов с коинфекцией, вызванной ВИЧ/SARS-CoV-2, может быть связано с применением АРВТ. Несмотря на отсутствие протективного действия АРВТ в отношении заражения вирусом SARS-CoV-2, исследователи предполагают, что АРВТ может стабилизировать иммунный ответ у коинфицированных пациентов, что препятствует прогрессированию заболевания до тяжелых форм.

Ключевые слова: COVID-19, SARS-CoV-2, ВИЧ, вирус иммунодефицита человека, антиретровирусная терапия, ВИЧ/SARS-CoV-2-коинфекция, лица живущие с ВИЧ, ЛЖВ

Вклад авторов: А. Ф. Олейник, Ч. Г. Реватхи — обзор литературы, подготовка рукописи; В. Х. Фазылов — подготовка рукописи.

✉ **Для корреспонденции:** Альфия Фаридовна Олейник
ул. Гвардейская, д. 31/42-42, г. Казань, 420073; alfiyaoleinik@yandex.ru

Статья получена: 19.12.2020 **Статья принята к печати:** 26.01.2021 **Опубликована онлайн:** 08.02.2021

DOI: 10.24075/vrgmu.2021.004

The coronavirus disease pandemic, announced by the World Health Organization in 2020, plays a central role in destabilizing health systems around the world, spreading rapidly and causing adverse outcomes. The SARS-CoV-2 high risk groups have been identified, yet pregnant women, children and chronic patients still constitute groups with "unclear" vulnerability, both socially and clinically, which is the reason for concern on the part of the medical community. Among the said groups, HIV patients form a separate category due to the immunodeficiency nature of the disease and its treatment peculiarities. Moreover, in many parts of the world it is difficult for HIV patients to get medical care, and with SARS-CoV-2 coinfection, their adherence to treatment protocols may become even more complicated. It is already known that the coronavirus infection manifestations in HIV patients were mainly limited to intestinal disorders, such as diarrhea, and rarely led to severe respiratory symptoms [1]. During the outbreak of SARS in 2003, only a few cases of the disease were registered in HIV-positive people, all of them mild [2]. In 2012, Middle East respiratory syndrome caused by MERS-CoV was a severe disease entailing high mortality, but it did not affect people living with HIV (PLHIV) significantly: the registered case describes patient's recovery [3]. The short duration of the aforementioned outbreaks has disallowed large-scale investigation of the ART's potential as the anticoronaviral therapy. Thus, it is important to clarify all the possible aspects of coinfection with two potentially dangerous viruses, their strength, interaction, the impact of ART and other issues.

Key features of COVID-19 and HIV infection

The first COVID-19 (Coronavirus Disease 2019) cases were registered in December 2019 in Wuhan (Hubei Province, China). The infectious agent was identified as a novel enveloped RNA beta coronavirus dubbed Severe Acute Respiratory Syndrome Coronavirus 2 (SARS-CoV-2). As of January 2021,

it caused a disease in over 93 million cases worldwide. While the susceptibility to COVID-19 seems to be high, the risk of severe COVID-19 course increases with age and peaks in those over 65. Studies have shown that men may be more susceptible to the infection than women, and the incidence in children is lower than in adults [4]. It was also established that concomitant diseases, including arterial hypertension, diabetes mellitus, chronic obstructive pulmonary disease, cardiovascular and cerebrovascular diseases, increase the risk of COVID-19 infection and the associated complications [5, 6].

The main routes of transmission of the disease from person to person are droplet and contact, with the former involving respiratory droplets and the latter virus transfer from a contaminated surface to the mucous membrane of the host. In 70% of patients, the symptoms of COVID-19 never manifest or manifest lightly; in 30% of patients the virus causes fever and a respiratory syndrome that can develop into a severe respiratory failure requiring intensive care [7]. The infection also frequently manifests as cardiovascular, neurological and gastrointestinal disorders. The most widely used diagnostic method relies on PCR (polymerase chain reaction). It aims to detect the nucleic acid of SARS-CoV-2. Serological methods are used to detect antibodies to SARS-CoV-2 in plasma and whole blood [7]. The recently developed T-Detect Assay, a T-cell test, offers higher accuracy in determining a pastinfection than antibody serology assay, and therefore can be regarded as a sensitive and reliable method to establish if a person has been infected earlier. This test confirms the special role of T-cells in the development of immunity to SARS-CoV-2 [8].

The treatment for COVID-19 is largely symptomatic and supportive, focused on preventive strategies. The antiviral agents involved are remdesivir and favipiravir, which can suppress SARS-CoV-2, improve the patient's clinical status and shorten the recovery period [9, 10]. In addition, based on the previous experience with SARS and MERS and the results of *in vitro* studies, researchers have also tested ribavirin, interferon, chloroquine/hydroxychloroquine, lopinavir-ritonavir for the purpose, with the latter seemingly delivering slightly better results than the former. [11]. In severe cases, it is recommended to administer corticosteroids [12].

HIV, transmitted during unprotected sex, through blood when sharing non-sterile tools and transfusing contaminated blood products, and transmitted from an HIV-positive mother to her child, has caused millions of deaths worldwide and continues to spread among the population. Having entered the body, HIV replicates in activated T-cells, migrates to the lymph nodes, which leads to a decrease in the overall $CD4^+$-T-cell count and inversion of the $CD4^+/CD8^+$ T-cells ratio. As a result, the host's immune response grows weaker, making it susceptible to various opportunistic diseases, mainly viral and mycotic by nature. ART suppresses the viral load, which translates into lower HIV transmission risk, immune system restoration, prevention of secondary diseases, HIV patient's life duration and quality improvement.

From both diagnostic and clinical points of view, HIV/SARS-CoV-2 coinfection is a combination of two separate diseases, so considering their peculiarities is critical to understanding how they interact. The clinical picture of the disease and the treatment protocols developed for the HIV/SARS-CoV-2 patient group may differ from those for the general population, therefore, a thorough study of cases from this group can give us valuable information about the behavior of viruses within a single host, the peculiarities of disease progression, effective treatment strategies.

COVID-19 course and outcomes in HIV patients: cases and discussion

Up to the present, the number of PLHIV infected with SARS-CoV-2 has remained low. However, it is best to practice caution in interpreting this fact: it does not prove that HIV-positive people are less susceptible to contracting the disease, it may simply be the result of HIV patients taking more serious precautions to limit their exposure to SARS-CoV-2 [13].

One of the first cases of HIV/SARS-CoV-2 coinfection was reported in Wuhan. The patient was 61-year-old man, longtime smoker with type 2 diabetes and long dry cough and fever manifestations. His blood test showed he suffered from mild lymphopenia, which grew severe (lymphocyte count 0.56×10^9/L, relative $CD4^+$-T-lymphocyte count 4.75%). Treatment included lopinavir/ritonavir on admission, moxifloxacin, gamma globulin, and methylprednisolone. The patient recovered and was discharged in 20 days after the first visit to the clinic [14].

A population study conducted in Wuhan among HIV/SARS-CoV-2-coinfected people revealed no difference in the severity of the disease and mortality associated with COVID-19 in HIV patients and general population. It is reported that the incidence of COVID-19 among PLHIV on ART is 0.52%, 2.20% among PLHIV who have interrupted ART, and 0.63% among PLHIV who have never had ART [15].

Based on the few HIV/SARS-CoV-2 coinfection studies available to date (Table), the international medical community has concluded that HIV infection is not an independent risk factor affecting COVID-19 infection possibility and the severity of the disease [16]. PLHIV on ART, with suppressed HIV viral load and over 200 cells/μl of $CD4^+$-T-lymphocytes, endure COVID-19 comparably to the general population [13, 17, 19]. Same as in the general population, the severity of the disease in coinfected individuals depends on age, gender, and concomitant diseases such as diabetes and hypertension [18, 19]. One of the findings is that HIV/SARS-CoV-2 patients often have a greater number of comorbidities than people not suffering the diseases [18].

However, a number of researchers report opposite results. For example, a retrospective study of HIV/SARS-CoV-2 coinfection cases conducted in New York clinics showed that, compared to the HIV-negative cohort, HIV-positive patients were more likely to need intensive care, invasive mechanical ventilation (IMV), died or were discharged to a hospice more often. At admission, radiological examination results of HIV patients commonly presented various pathologies. Three HIV/SARS-CoV-2 patients had bacterial complications and died. All HIV-positive patients, except one, were on ART and had the $CD4^+$-T-lymphocyte count of over 200 cells/μl [20].

A large cohort study that involved 22,308 patients in South Africa also reported a two-fold COVID-19-associated death risk increase in HIV-positive persons. However, the author of this study did not exclude the effect of confounding, which may cast doubt on the results [21].

Some other factors considered in addition to comorbidities as potentially capable of influencing the outcome are poor immune status, race, ART regimen. The authors of one of the prospective cohort studies involving 51 patients with controlled HIV infection conclude that an unfavorable outcome (severe course of COVID-19 and death) is probably associated with a $CD4^+$-T-lymphocyte count of less than 200 cells/μL [22].

A case series published by the King's College Hospital (UK) describes clinical characteristics of 18 PLHIV (mean age 52 years) who were admitted with COVID-19. It was found that the majority of patients belong to the Negroid race, have

Table. Studies researching the impact of HIV on COVID-19 course

Authors	Year	Region	Number of patients	Design	Key results
Shalev N et al.	2020	USA	31	Transverse	COVID-19 course and outcome in PLHIV on ART with CD4 >200 comparable to those in general population
Gudipati S et al.	2020	USA	14	Transverse	COVID-19 course and outcome in PLHIV comparable to those in general population
Stoeckle K et al.	2020	USA	120	Longitudinal	COVID-19 course and outcome in PLHIV comparable to those in general population
Karmen-Tuohy S et al.	2020	USA	63	Longitudinal	COVID-19 course and outcome in PLHIV comparable to those in general population
Inciarte A et al.	2020	Spain	62	Longitudinal	COVID-19 course and outcome in PLHIV comparable to those in general population. PLHIV exhibit lower incidence than the general population
Vizcarra P et al.	2020	Spain	51	Longitudinal	The risk of a severe course of COVID-19 among PLHIV is not lower than in the general population
Davies MA	2020	Western Cape Province, South Africa	22308	Longitudinal	Doubled risk of death of PLHIV from COVID-19
Huang J et al.	2020	China	35	Longitudinal	COVID-19 course and prognosis in PLHIV may be more adverse compared to those in general population
Suwanwongse K et al.	2020	USA	9	Transverse	HIV infection and low immune status may negatively impact COVID-19 outcomes
Gervasoni C et al.	2020	Italy	47	Transverse	Reduced risk of severe course and adverse outcomes of COVID-19 in PLHIV

a lower median number of CD4$^+$-T-cells and tend to use more protease inhibitors in the ART regimen than outpatients [23].

According to a study conducted in Turkey, out of 1224 HIV-positive individuals only four male patients contracted SARS-CoV-2, and three of them had no underlying conditions and recovered fully. All three patients were on ART; COVID-19 in their cases was mild. The fourth patient, a 44-year-old man, was on ART, with low HIV viral load, high CD4$^+$-T-cell counts and several comorbidities. This patient died, proving that from the point of view of comorbidities, HIV-positive people have the same predictors of adverse disease outcome as general population [24].

A number of other researchers report similarities in how people with controlled HIV (as evidenced by high CD4$^+$-T-cells and low viral load) and the general population endure COVID-19. The authors conclude that the reported deaths are caused by old age and multiple comorbidities [25, 26].

There are results of the analysis of all admissions of PLHIV with SARS-CoV-2 coinfection that are worth mentioning: most patients were on ART for a long time, their HIV viral load was suppressed or minimal, and the count of CD4$^+$-T-lymphocytes exceeded 200 cells/μL. Only a few patients were not on ART, had a detectable HIV viral load and CD4$^+$-T-cell count below 200 cells/μL. These patients recovered quickly [25].

Researchers from Spain described 5 cases of coinfection and reported interesting observations: a patient not on ART and with CD4$^+$-T-lymphocytes counting less than 200 cells/μL needed non-invasive ventilation only and was discharged without any complications, while another patient with a CD4$^+$-T-lymphocyte count of more than 200 cells/μL and a suppressed HIV load needed invasive mechanical ventilation [18].

Similarly, a 28-year-old male coinfected with SARS-CoV-2 and HIV, without comorbidities, showed no severity in his disease progression and improved smoothly in 9 days, eventhough his immune status from HIV infection was not well-controlled (CD4$^+$-T-cell count is 194 cells) due to a lack of ART [27].

A similar trend was reported in another retrospective cohort study of 23 patients with HIV/SARS-CoV-2 coinfection. Three patients from the cohort were discharged home without complications, while for the patients with undetectable viral load and relatively high CD4$^+$-T-lymphocyte counts (over 400 cells/μl) the outcome was unfavorable. In this case series, CD4$^+$-T-cell lymphopenia was recognized as a factor protecting COVID-19 progression to severe stages, and the ART regimen was stated to have no effect on the outcome [28].

A single-center prospective study conducted in Italy tracked the outcomes of HIV/SARS-CoV-2 coinfection cases; this effort also revealed no association between immunosuppression and the disease progressing to its severe forms. It is reported that the only patient with severe COVID-19 was a Caucasian male whose immunological profile was optimal (baseline CD4$^+$-T-lymphocyte count of 438 cells/μL), while two Negroid patients with severe immunodeficiency and comorbidities had the disease asymptomatic [29].

In another retrospective study, the majority of the participants from the coinfection cohort had the viral load suppressed and the count of CD4$^+$-T-lymphocyte acceptable; these patients had several comorbidities and were on average 10 years younger than the HIV-negative cohort. It was shown that the risk of severe COVID-19, admission to intensive care unit and death was significantly lower in HIV-positive patients. However, it should be borne in mind that this study included HIV patients with COVID-19 not confirmed by laboratory methods, so its results may be questionable [30].

The reports published suggested that HIV-associated immunosuppression may paradoxically protect against severe manifestations of COVID-19 [17, 30, 31]. In one of the studies, the HIV group exhibited low peak CRP levels, which, according to the researchers, signals difficulties with development of a pronounced immune response. It would seem like the relative immune dysfunction plays a protective role in case of COVID-19 contraction, which makes the need for non-invasive and invasive mechanical ventilation experienced by PLHIV less urgent [19].

Recent reports have shown that HIV/SARS-CoV-2 coinfected patients who had a fatal outcome had higher levels of soluble markers of immune activation and inflammation than those who survived, suggesting that PLHIV remain capable of a profound inflammatory reaction in response to SARS-CoV-2 coinfection [13, 22, 32].

An inverse relationship was noted between the number of CD4+-T-lymphocytes and the mortality rate. A case series covering HIV/SARS-CoV-2 patients admitted to the South Bronx Hospital, New York, describes nine participants (seven male, two female), aged 58, with multiple comorbidities, CD4+-T-lymphocyte count of 179–1827 cells/μL and HIV viral load from very low to undetectable [33]. In the context of the series, the researchers concluded that the predictors of disease progression to its severe form and death are similar in HIV-positive and HIV-negative groups. Comparing their findings to the data reported in other studies, the authors state the patients they worked with had a significantly lower CD4+-T-lymphocyte count, but their mortality rate was higher, which allows refuting the protective effect of immunosuppression. The results of the study, however, must be interpreted with caution, as the majority of the involved patients seeing adverse outcomes were not on ART, had CD4+-T-lymphocyte counts greater than 200 cells/μL and suffered multiple comorbidities [33].

Along with the conflicting reports on the peculiarities of COVID-19 in HIV-positive individuals, it is necessary to consider another theory that holds the possible effects lopinavir/ritonavir has on SARS-CoV-2, the initiation time and ART regimen balancing the immune response and clearance of coronavirus, thus preventing the development of an unfavorable hyperinflammatory condition in coinfected patients [34].

We hypothesize that severely immunocompromised patients themselves are not protected from COVID-19, they only may have the disease asymptomatic or manifesting mild symptoms because they are unable to develop a sufficiently strong inflammatory response to aggravate the symptoms. Thus, such patients are admitted to hospitals less often. However, such immunosuppression cannot be called a protective factor, as it can lead to prolonged viral clearance. With the virus clearance delayed and depending on a number of factors (comorbidities, patient age, timeliness of treatment, ART regimen etc), asymptomatic COVID-19 can progress to its mild to severe forms, sometimes leading to death.

A large-scale testing of HIV-positive individuals for antibodies (outpatients) could help clarify whether all immunosuppressed COVID-19 patients indeed have asymptomatic form of the disease [31].

At the same time, most of the HIV/SARS-CoV-2 patients involved in the studies had a CD4+-T-lymphocyte level in excess of 200 cells/μL, which, we assume, could add symptoms to the course of the disease. In this group of patients, COVID-19-induced lymphopenia was superimposed on the existing mild or moderate immunosuppression, which probably caused a stronger response against the background of previously prescribed ART, thus increasing the number of lymphocytes to the level of a stabilized immune response that prevents serious inflammation- or virus-caused damage.

There is another theory, which has the milder course of the disease a result of action of the viral interference mechanism, when HIV changes the host cells and creates the environment unfavorable for other viruses, thus modifying the course of COVID-19.

Immunological characteristics of HIV/SARS-CoV-2 patients

Transient lymphopenia is common against the background of COVID-19, but when combined with progressive HIV-associated lymphopenia, lymphocyte counts in HIV/SARS-CoV-2 coinfected patients improve only marginally after recovering from COVID-19 [35].

The relatively lower number of CD4+-T-lymphocytes in HIV/SARS-CoV-2 patients may be one of the reasons behind the blurred clinical picture, as well as delayed and insufficient production of antibodies to SARS-CoV-2. Moreover, the low levels of IgM and IgG to SARS-CoV-2 were associated with a higher HIV viral load, i. e. ≥ 20 copies/ml, as compared to patients with a viralload below 20 copies/ml [15].

A retrospective study of COVID-19 in PLHIV revealed severe lymphopenia and a decrease in the number of CD4+-T-lymphocytes, while the levels of CRP, fibrinogen, D-dimer, interleukin-6, interleukin-8 and TNFα were increased. Higher levels of inflammatory markers and more severe lymphopenia were reported in HIV patients for whom COVID-19 ended adversely compared to those who recovered [36]. While in general population higher interleukin-6 and d-dimer levels are associated with the severity of COVID-19, in PLHIV they may be interpreted as biomarkers of chronic HIV infection [37]. Nevertheless, there were no biomarker content differences registered between HIV/SARS-CoV-2 patients and HIV-negative COVID-19 patients.

Severe lymphopenia can be explained by the accelerated apoptosis of lymphocytes against the background of a viral infection that activates them in the context of antiviral response [38]. Another explanation for lymphopenia may be the direct effect SARS-CoV-2 produces on lymphocytes through ACE2-dependent and ACE2-independent pathways. It was reported earlier that less than 5% of oral mucosa lymphocytes can express ACE2 [39]. Besides, SARS-CoV-2 can use CD147 receptors to enter T-cells [40].

COVID-19 and antiretroviral therapy

Patients with ART-controlled HIV infection run roughly the same risk of contracting COVID-19 as the general population [14], however, the effect ART has on HIV/SARS-CoV-2 coinfection remains to be studied further. The main reason why earlier studies hypothesized about the protective effect of ART against COVID-19 in PLHIV was that antiviral drugs, such as tenofovir and lopinavir, showed anti-SARS-CoV-2 activity in vitro [41, 42]. This is indirectly confirmed by the results of a retrospective study that included 20 HIV/SARS-CoV-2 patients and reported lower ESR and CRP in those on ART compared to the patients who did not receive such therapy [43].

A clinical trial involving hospitalized adult HIV-negative patients with confirmed novel coronavirus infection showed no significant difference in the timing of clinical improvement backed by lopinavir/ritonavir treatment. However, the mortality rates at 28 days, the time in ICU/hospital registered by the researchers were generally lower, and more patients showed clinical improvement on day 14 in the lopinavir/ritonavir group compared to the standard treatment group. Compared to the standard supportive regimens, protocols including lopinavir/ritonavir enable reduction of SARS-CoV-2 RNA load and shorten the time when viral RNA remains detectable [44]. Despite the reported results suggesting the potential clinical benefits of lopinavir, it is necessary to evaluate the effectiveness of this drug in HIV/SARS-CoV-2 patients [34].

Another HIV/SARS-CoV-2 case series report describes the ART prescribed to the majority of patients and including of a protease inhibitor, predominantly darunavir, boosted with ritonavir or cobicistat [23].

It has also been reported that 800 mg darunavir has no protective effect against infection and progression of respiratory failure, while for the patients that mainly received integrase inhibitors COVID-19 ended favorably [30].

Spanish researchers have shown a higher prevalence of SARS-CoV-2 among those who resorted to pre-exposure prophylaxis regimen of tenofovir disoproxil fumarate or tenofovir alafenamide and emtricitabine (TDF/TAF+FTC); compared to the control group, they exhibited no significant differences in clinical manifestations [45], which refutes the hypothesis about the protective effect of tenofovir against SARS-CoV-2 [42]. Several other studies also report a higher proportion of HIV/SARS-CoV-2 patients on TDF-based ART compared to patients with HIV alone [17, 22].

More research is needed on nelfinavir mesylate, an HIV protease inhibitor that has recently been found to be an effective inhibitor of the SARS-CoV-2 S-protein, the main determinant of viral infectivity [46].

Conclusion

It is likely that in HIV-positive patients on virologically and immunologically effective ART, the course of COVID-19 is comparable to that in general population. Apparently, ART does not reduce the risk of SARS-CoV-2 infection, however, stabilization of the immune system during therapy can help reduce the incidence of adverse COVID-19 outcomes. SARS-CoV-2-associated lymphopenia superimposed on immunodeficiency can make the clinical picture blurred, delay virus clearance and production of antibodies to SARS-CoV-2 and make their count insufficient. It is unclear whether SARS-CoV-2-associated lymphopenia facilitates development of opportunistic diseases or not. The above is a powerful argument for taking all precautions in HIV-positive patients.

The available information on HIV/SARS-CoV-2 coinfection appears to be rather controversial and has many gaps. This reasons behind the situation being as it is may be associated with an insufficient sample size of HIV/SARS-CoV-2 patients in some studies, lack of a large-scale effort to diagnose asymptomatic cases, underestimation of the predisposing factors when comparing HIV/SARS-CoV-2 patients with people hosting HIV only, which leads to faulty estimation of the effects of confounding of comorbid conditions, ART regimen on the development of an adverse outcome in coinfection cases. Subsequently, the results of the study are distorted. Thus, more research is needed to confirm or refute some of the proposed hypotheses, as well as to assess the effectiveness of ART in HIV/SARS-CoV-2 coinfection cases.

References

1. Eis-Hübinger AM, Stifter G, Schneweis KE. Opportunistic infections with coronavirus-like particles in patients infected with the human immunodeficiency virus? Zentralbl Bakteriol. 1989 Sep; 271 (3): 351–5. DOI: 10.1016/s0934-8840(89)80034-9. PMID: 2553042; PMCID: PMC7135704.
2. Chen XP, Cao Y. Consideration of highly active antiretroviral therapy in the prevention and treatment of severe acute respiratory syndrome. Clin Infect Dis. 2004 Apr 1; 38 (7): 1030–2. DOI: 10.1086/386340. Epub 2004 Mar 15. PMID: 15034838.
3. Shalhoub S, AlZahrani A, Simhairi R, Mushtaq A. Successful recovery of MERS CoV pneumonia in a patient with acquired immunodeficiency syndrome: a case report. J Clin Virol. 2015 Jan; 62: 69–71. DOI: 10.1016/j.jcv.2014.11.030. Epub 2014 Nov 29. PMID: 25542475; PMCID: PMC7128447.
4. Channappanavar R, Fett C, Mack M, Ten Eyck PP, Meyerholz DK, Perlman S. Sex-Based Differences in Susceptibility to Severe Acute Respiratory Syndrome Coronavirus Infection. J Immunol. 2017 May 15; 198 (10): 4046–53. DOI: 10.4049/jimmunol.1601896. Epub 2017 Apr 3. PMID: 28373583; PMCID: PMC5450662.
5. Wang B, Li R, Lu Z, Huang Y. Does comorbidity increase the risk of patients with COVID-19: evidence from meta-analysis. Aging (Albany NY). 2020 Apr 8; 12 (7): 6049–57. DOI: 10.18632/aging.103000. Epub 2020 Apr 8. PMID: 32267833; PMCID: PMC7185114.
6. Promislow DEL. A Geroscience Perspective on COVID-19 Mortality. J Gerontol A BiolSci Med Sci. 2020 Sep 16; 75 (9): e30–e33. DOI: 10.1093/gerona/glaa094. PMID: 32300796; PMCID: PMC7184466.
7. Cascella M, Rajnik M, Cuomo A, et al. Features, Evaluation, and Treatment of Coronavirus. [Updated 2020 Oct 4]. In: StatPearls [Internet]. Treasure Island (FL): StatPearls Publishing; 2020 Jan. Available from: https://www.ncbi.nlm.nih.gov/books/NBK554776/.
8. Gittelman RM, Lavezzo E, Snyder TM, Zahid HJ, Elyanow R, Dalai S, et al. Diagnosis and Tracking of Past SARS-CoV-2 Infection in a Large Study of Vo', Italy Through T-Cell Receptor Sequencing. medRxiv [Preprint] 2020.11.09.20228023; 2020 [cited 2020 Nov 10] Available from: https://www.medrxiv.org/content/10.1101/2020.11.09.20228023v1.
9. Beigel JH, Tomashek KM, Dodd LE, Mehta AK, Zingman BS, Kalil AC, et al. Remdesivir for the Treatment of Covid-19 - Final Report. N Engl J Med. 2020 Nov 5; 383 (19): 1813–26. DOI: 10.1056/NEJMoa2007764. Epub 2020 Oct 8. PMID: 32445440; PMCID: PMC7262788.
10. Balykova LA, Granovskaya MV, Zaslavskaya KYa, Simakina EN, Agaf'ina AS, Ivanova AYu, et al. New possibilities for targeted antiviral therapy for COVID-19. Results of a multicenter clinical study of the efficacy and safety of using the drug Areplivir. Infectious diseases: news, opinions, training. 2020. 3 (34): 16–29. DOI: 10.33029/2305-3496-2020-9-3-16-29.
11. Chen N, Zhou M, Dong X, Qu J, Gong F, Han Y, et al. Epidemiological and clinical characteristics of 99 cases of 2019 novel coronavirus pneumonia in Wuhan, China: a descriptive study. Lancet. 2020 Feb 15; 395 (10223): 507–13. DOI: 10.1016/S0140-6736(20)30211-7. Epub 2020 Jan 30. PMID: 32007143; PMCID: PMC7135076.
12. World Health Organization (2020 Sep 2) [cited 2020 Nov 19] Available from: https://www.who.int/news-room/feature-stories/detail/who-updates-clinical-care-guidance-with-corticosteroid-recommendations.
13. Kanwugu ON, Adadi P. HIV/SARS-CoV-2 coinfection: A global perspective. J Med Virol. 2020 Jul 21. DOI: 10.1002/jmv.26321. Epub ahead of print. PMID: 32692406; PMCID: PMC7404432.
14. Zhu F, Cao Y, Xu S, Zhou M. Co-infection of SARS-CoV-2 and HIV in a patient in Wuhan city, China. J Med Virol. 2020 Jun; 92 (6): 529–30. DOI: 10.1002/jmv.25732. Epub 2020 Mar 11. PMID: 32160316; PMCID: PMC7228399.
15. Huang J, Xie N, Hu X, Yan H, Ding J, Liu P, et al. Epidemiological, virological and serological features of COVID-19 cases in people living with HIV in Wuhan City: A population-based cohort study. Clin Infect Dis. 2020 Aug 17: ciaa1186. DOI: 10.1093/cid/ciaa1186. Epub ahead of print. PMID: 32803216; PMCID: PMC7454403.
16. European AIDS Clinical Society. EACS-BHIVA, G. B statement (1 April 2020) [cited 2020 Nov 19]. Available from: https://www.eacsociety.org/home/eacs-bhiva-statement-1-april.html.
17. Shalev N, Scherer M, LaSota ED, Antoniou P, Yin MT, Zucker J, et al. Clinical Characteristics and Outcomes in People Living With Human Immunodeficiency Virus Hospitalized for Coronavirus Disease 2019. Clin Infect Dis. 2020 Nov 19; 71 (16): 2294–7. DOI: 10.1093/cid/ciaa635. PMID: 32472138; PMCID: PMC7314170.
18. Blanco JL, Ambrosioni J, Garcia F, Martínez E, Soriano A, Mallolas J, et al. COVID-19 in patients with HIV: clinical case series. Lancet HIV. 2020 May; 7 (5): e314–e316. DOI: 10.1016/S2352-3018(20)30111-9. Epub 2020 Apr 15. PMID: 32304642; PMCID: PMC7159872.

19. Stoeckle K, Johnston CD, Jannat-Khah DP, Williams SC, Ellman TM, Vogler MA, et al. COVID-19 in Hospitalized Adults With HIV. Open Forum Infect Dis. 2020 Aug 1; 7 (8): ofaa327. DOI: 10.1093/ofid/ofaa327. PMID: 32864388; PMCID: PMC7445584.
20. Karmen-Tuohy S, Carlucci PM, Zervou FN, Zacharioudakis IM, Rebick G, Klein E, et al. Outcomes Among HIV-Positive Patients Hospitalized With COVID-19. J Acquir Immune DeficSyndr. 2020 Sep 1; 85 (1): 6–10. DOI: 10.1097/QAI.0000000000002423. PMID: 32568770; PMCID: PMC7446982.
21. Davies MA. HIV and risk of COVID-19 death: a population cohort study from the Western Cape Province, South Africa. medRxiv [Preprint]. 2020 Jul 3: 2020.07.02.20145185. DOI: 10.1101/2020.07.02.20145185. PMID: 32637972; PMCID: PMC7340198.
22. Vizcarra P, Pérez-Elías MJ, Quereda C, Moreno A, Vivancos MJ, Dronda F, et al. Description of COVID-19 in HIV-infected individuals: a single-centre, prospective cohort. Lancet HIV. 2020 Aug; 7 (8): e554–e564. DOI: 10.1016/S2352-3018(20)30164-8. Epub 2020 May 28. PMID: 32473657; PMCID: PMC7255735.
23. Childs K, Post FA, Norcross C, Ottaway Z, Hamlyn E, Quinn K, et al. Hospitalized Patients With COVID-19 and Human Immunodeficiency Virus: A Case Series. Clin Infect Dis. 2020 Nov 5; 71 (8): 2021–2. DOI: 10.1093/cid/ciaa657. PMID: 32459833; PMCID: PMC7314116.
24. Altuntas Aydin O, Kumbasar Karaosmanoglu H, Kart Yasar K. HIV/SARS-CoV-2 coinfected patients in Istanbul, Turkey. J Med Virol. 2020 Nov; 92 (11): 2288–90. DOI: 10.1002/jmv.25955. Epub 2020 Jun 3. PMID: 32347975
25. Inciarte A, Gonzalez-Cordon A, Rojas J, Torres B, de Lazzari E, de la Mora L, et al. Clinical characteristics, risk factors, and incidence of symptomatic coronavirus disease 2019 in a large cohort of adults living with HIV: a single-center, prospective observational study. AIDS. 2020 Oct 1; 34 (12): 1775–80. DOI: 10.1097/QAD.0000000000002643. PMID: 32773471; PMCID: PMC7493771.
26. Gudipati S, Brar I, Murray S, McKinnon JE, Yared N, Markowitz N. Descriptive Analysis of Patients Living With HIV Affected by COVID-19. J Acquir Immune DeficSyndr. 2020 Oct 1; 85 (2): 123–6. DOI: 10.1097/QAI.0000000000002450. PMID: 32675771; PMCID: PMC7446990.
27. Nakamoto T, Kutsuna S, Yanagawa Y, Kanda K, Okuhama A, Akiyama Y, et al. A case of SARS-CoV-2 infection in an untreated HIV patient in Tokyo, Japan. J Med Virol. 2020 Jun 3: 10.1002/jmv.26102. DOI: 10.1002/jmv.26102. Epub ahead of print. PMID: 32492188; PMCID: PMC7300885.
28. Nagarakanti SR, Okoh AK, Grinberg S, Bishburg E. Clinical outcomes of patients with COVID-19 and HIV coinfection. J Med Virol. 2020 Sep 19. DOI: 10.1002/jmv.26533. Epub ahead of print. PMID: 32949148; PMCID: PMC7537324.
29. Mondi A, Cimini E, Colavita F, Cicalini S, Pinnetti C, Matusali G, et al. COVID-19 in people living with HIV: Clinical implications of dynamics of the immune response to SARS-CoV-2. J Med Virol. 2020 Sep 25. DOI: 10.1002/jmv.26556. Epub ahead of print. PMID: 32975842; PMCID: PMC7537181.
30. Gervasoni C, Meraviglia P, Riva A, Giacomelli A, Oreni L, Minisci D, et al. Clinical Features and Outcomes of Patients With Human Immunodeficiency Virus With COVID-19. Clin Infect Dis. 2020 Nov 19; 71 (16): 2276–78. DOI: 10.1093/cid/ciaa579. PMID: 32407467; PMCID: PMC7239244.
31. Zhao J, Liao X, Wang H, Wei L, Xing M, Liu L, et al. Early Virus Clearance and Delayed Antibody Response in a Case of Coronavirus Disease 2019 (COVID-19) With a History of Coinfection With Human Immunodeficiency Virus Type 1 and Hepatitis C Virus. Clin Infect Dis. 2020 Nov 19; 71 (16): 2233–35. DOI: 10.1093/cid/ciaa408. PMID: 32270178; PMCID: PMC7184426.
32. Hu Y, Ma J, Huang H, Vermund SH. Coinfection With HIV and SARS-CoV-2 in Wuhan, China: A 12-Person Case Series. J Acquir Immune Defic Syndr. 2020 Sep 1; 85 (1): 1–5. DOI: 10.1097/QAI.0000000000002424. PMID: 32568771; PMCID: PMC7446977.
33. Suwanwongse K, Shabarek N. Clinical features and outcome of HIV/SARS-CoV-2 coinfected patients in The Bronx, New York city. J Med Virol. 2020 Nov; 92 (11): 2387–9. DOI: 10.1002/jmv.26077. Epub 2020 Jun 9. PMID: 32462663; PMCID: PMC7283854.
34. Mascolo S, Romanelli A, Carleo MA, Esposito V. Could HIV infection alter the clinical course of SARS-CoV-2 infection? When less is better. J Med Virol. 2020 Oct; 92 (10): 1777–8. DOI: 10.1002/jmv.25881. Epub 2020 Jul 11. PMID: 32293709; PMCID: PMC7262314.
35. Yang R, Gui X, Zhang Y, Xiong Y, Gao S, Ke H. Clinical characteristics of COVID-19 patients with HIV coinfection in Wuhan, China. Expert Rev Respir Med. 2020 Oct 27: 1–7. DOI: 10.1080/17476348.2021.1836965. Epub ahead of print. PMID: 33074039; PMCID: PMC7605649.
36. Ho HE, Peluso MJ, Margus C, Matias Lopes JP, He C, Gaisa MM, et al. Clinical outcomes and immunologic characteristics of Covid-19 in people with HIV. J Infect Dis. 2020 Jun 30: jiaa380. DOI: 10.1093/infdis/jiaa380. Epub ahead of print. PMID: 32601704; PMCID: PMC7337732.
37. Neuhaus J, Jacobs DR Jr, Baker JV, Calmy A, Duprez D, La Rosa A, et al. Markers of inflammation, coagulation, and renal function are elevated in adults with HIV infection. J Infect Dis. 2010 Jun 15; 201 (12): 1788–95. DOI: 10.1086/652749. PMID: 20446848; PMCID: PMC2872049.
38. Feng X, Li S, Sun Q, Zhu J, Chen B, Xiong M, et al. Immune-Inflammatory Parameters in COVID-19 Cases: A Systematic Review and Meta-Analysis. Front Med (Lausanne). 2020 Jun 9; 7: 301. DOI: 10.3389/fmed.2020.00301. PMID: 32582743; PMCID: PMC7295898.
39. Xu H, Zhong L, Deng J, Peng J, Dan H, Zeng X, et al. High expression of ACE2 receptor of 2019-nCoV on the epithelial cells of oral mucosa. Int J Oral Sci. 2020 Feb 24; 12 (1): 8. DOI: 10.1038/s41368-020-0074-x. PMID: 32094336; PMCID: PMC7039956.
40. Biegler B, Kasinrerk W. Reduction of CD147 surface expression on primary T cells leads to enhanced cell proliferation. Asian Pac J Allergy Immunol. 2012 Dec; 30 (4): 259–67. PMID: 23393905.
41. Chan KS, Lai ST, Chu CM, Tsui E, Tam CY, Wong MM, et al. Treatment of severe acute respiratory syndrome with lopinavir/ritonavir: a multicentre retrospective matched cohort study. Hong Kong Med J. 2003 Dec; 9 (6): 399–406. PMID: 14660806.
42. Elfiky AA. Ribavirin, Remdesivir, Sofosbuvir, Galidesivir, and Tenofovir against SARS-CoV-2 RNA dependent RNA polymerase (RdRp): a molecular docking study. Life Sci. 2020 Jul 15; 253: 117592. DOI: 10.1016/j.lfs.2020.117592. Epub 2020 Mar 25. Erratum in: Life Sci. 2020 Oct 1; 258: 118350. PMID: 32222463; PMCID: PMC7102646.
43. Liu J, Zeng W, Cao Y, Cui Y, Li Y, Yao S, et al. Effect of a Previous History of Antiretroviral Treatment on Clinical Picture of Patients with Co-infection of SARS-CoV-2 and HIV: A Preliminary Study. Int J Infect Dis. 2020 Nov; 100: 141–8. DOI: 10.1016/j.ijid.2020.08.045. Epub 2020 Aug 20. PMID: 32829051; PMCID: PMC7439831.
44. Cao B, Wang Y, Wen D, Liu W, Wang J, Fan G, et al. A Trial of Lopinavir-Ritonavir in Adults Hospitalized with Severe Covid-19. N Engl J Med. 2020 May 7; 382 (19): 1787–99. DOI: 10.1056/NEJMoa2001282. Epub 2020 Mar 18. PMID: 32187464; PMCID: PMC7121492.
45. Ayerdi O, Puerta T, Clavo P, Vera M, Ballesteros J, Fuentes ME, et al. Preventive efficacy of Tenofovir/Emtricitabine against severe acute respiratory syndrome Coronavirus 2 among pre-exposure prophylaxis users. Open Forum Infect Dis. 2020 Sep 25; 7 (11): ofaa455. DOI: 10.1093/ofid/ofaa455. PMID: 33200081; PMCID: PMC7543639.
46. Musarrat F, Chouljenko V, Dahal A, Nabi R, Chouljenko T, Jois SD, et al. The anti-HIV drug nelfinavir mesylate (Viracept) is a potent inhibitor of cell fusion caused by the SARSCoV-2 spike (S) glycoprotein warranting further evaluation as an antiviral against COVID-19 infections. J Med Virol. 2020 Oct; 92 (10): 2087–95. DOI: 10.1002/jmv.25985. Epub 2020 May 17. PMID: 32374457; PMCID: PMC7267418.

Литература

1. Eis-Hübinger AM, Stifter G, Schneweis KE. Opportunistic infections with coronavirus-like particles in patients infected with the human immunodeficiency virus? Zentralbl Bakteriol. 1989 Sep; 271 (3): 351–5. DOI: 10.1016/s0934-8840(89)80034-9. PMID: 2553042; PMCID: PMC7135704.
2. Chen XP, Cao Y. Consideration of highly active antiretroviral therapy in the prevention and treatment of severe acute respiratory syndrome. Clin Infect Dis. 2004 Apr 1; 38 (7): 1030–2. DOI: 10.1086/386340. Epub 2004 Mar 15. PMID: 15034838.
3. Shalhoub S, AlZahrani A, Simhairi R, Mushtaq A. Successful recovery of MERS CoV pneumonia in a patient with acquired immunodeficiency syndrome: a case report. J Clin Virol. 2015 Jan; 62: 69–71. DOI: 10.1016/j.jcv.2014.11.030. Epub 2014 Nov 29. PMID: 25542475; PMCID: PMC7128447.
4. Channappanavar R, Fett C, Mack M, Ten Eyck PP, Meyerholz DK, Perlman S. Sex-Based Differences in Susceptibility to Severe Acute Respiratory Syndrome Coronavirus Infection. J Immunol. 2017 May 15; 198 (10): 4046–53. DOI: 10.4049/jimmunol.1601896. Epub 2017 Apr 3. PMID: 28373583; PMCID: PMC5450662.
5. Wang B, Li R, Lu Z, Huang Y. Does comorbidity increase the risk of patients with COVID-19: evidence from meta-analysis. Aging (Albany NY). 2020 Apr 8; 12 (7): 6049–57. DOI: 10.18632/aging.103000. Epub 2020 Apr 8. PMID: 32267833; PMCID: PMC7185114.
6. Promislow DEL. A Geroscience Perspective on COVID-19 Mortality. J Gerontol A Biol Sci Med Sci. 2020 Sep 16; 75 (9): e30–e33. DOI: 10.1093/gerona/glaa094. PMID: 32300796; PMCID: PMC7184466.
7. Cascella M, Rajnik M, Cuomo A, et al. Features, Evaluation, and Treatment of Coronavirus. [Updated 2020 Oct 4]. In: StatPearls [Internet]. Treasure Island (FL): StatPearls Publishing; 2020 Jan. Available from: https://www.ncbi.nlm.nih.gov/books/NBK554776/.
8. Gittelman RM, Lavezzo E, Snyder TM, Zahid HJ, Elyanow R, Dalai S, et al. Diagnosis and Tracking of Past SARS-CoV-2 Infection in a Large Study of Vo', Italy Through T-Cell Receptor Sequencing. medRxiv [Preprint] 2020.11.09.20228023; 2020 [cited 2020 Nov 10] Available from: https://www.medrxiv.org/content/10.1101/2020.11.09.20228023v1.
9. Beigel JH, Tomashek KM, Dodd LE, Mehta AK, Zingman BS, Kalil AC, et al. Remdesivir for the Treatment of Covid-19 - Final Report. N Engl J Med. 2020 Nov 5; 383 (19): 1813–26. DOI: 10.1056/NEJMoa2007764. Epub 2020 Oct 8. PMID: 32445440; PMCID: PMC7262788.
10. Балыкова Л. А., Грановская М. В., Заславская К. Я., Симакина Е. Н., Агафьина А. С., Иванова А. Ю. и др. Новые возможности направленной противовирусной терапии COVID-19: результаты многоцентрового клинического исследования эффективности и безопасности применения препарата Арепливир. Инфекционные болезни: новости, мнения, обучение. 2020. 3 (34): 16–29. DOI: 10.33029/2305-3496-2020-9-3-16-29.
11. Chen N, Zhou M, Dong X, Qu J, Gong F, Han Y, et al. Epidemiological and clinical characteristics of 99 cases of 2019 novel coronavirus pneumonia in Wuhan, China: a descriptive study. Lancet. 2020 Feb 15; 395 (10223): 507–13. DOI: 10.1016/S0140-6736(20)30211-7. Epub 2020 Jan 30. PMID: 32007143; PMCID: PMC7135076.
12. World Health Organization (2020 Sep 2) [cited 2020 Nov 19] Available from: https://www.who.int/news-room/feature-stories/detail/who-updates-clinical-care-guidance-with-corticosteroid-recommendations.
13. Kanwugu ON, Adadi P. HIV/SARS-CoV-2 coinfection: A global perspective. J Med Virol. 2020 Jul 21. DOI: 10.1002/jmv.26321. Epub ahead of print. PMID: 32692406; PMCID: PMC7404432.
14. Zhu F, Cao Y, Xu S, Zhou M. Co-infection of SARS-CoV-2 and HIV in a patient in Wuhan city, China. J Med Virol. 2020 Jun; 92 (6): 529–30. DOI: 10.1002/jmv.25732. Epub 2020 Mar 11. PMID: 32160316; PMCID: PMC7228399.
15. Huang J, Xie N, Hu X, Yan H, Ding J, Liu P, et al. Epidemiological, virological and serological features of COVID-19 cases in people living with HIV in Wuhan City: A population-based cohort study. Clin Infect Dis. 2020 Aug 17: ciaa1186. DOI: 10.1093/cid/ciaa1186. Epub ahead of print. PMID: 32803216; PMCID: PMC7454403.
16. European AIDS Clinical Society. EACS-BHIVA, G. B statement (1 April 2020) [cited 2020 Nov 19]. Available from: https://www.eacsociety.org/home/eacs-bhiva-statement-1-april.html.
17. Shalev N, Scherer M, LaSota ED, Antoniou P, Yin MT, Zucker J, et al. Clinical Characteristics and Outcomes in People Living With Human Immunodeficiency Virus Hospitalized for Coronavirus Disease 2019. Clin Infect Dis. 2020 Nov 19; 71 (16): 2294–7. DOI: 10.1093/cid/ciaa635. PMID: 32472138; PMCID: PMC7314170.
18. Blanco JL, Ambrosioni J, Garcia F, Martínez E, Soriano A, Mallolas J, et al. COVID-19 in patients with HIV: clinical case series. Lancet HIV. 2020 May; 7 (5): e314–e316. DOI: 10.1016/S2352-3018(20)30111-9. Epub 2020 Apr 15. PMID: 32304642; PMCID: PMC7159872.
19. Stoeckle K, Johnston CD, Jannat-Khah DP, Williams SC, Ellman TM, Vogler MA, et al. COVID-19 in Hospitalized Adults With HIV. Open Forum Infect Dis. 2020 Aug 1; 7 (8): ofaa327. DOI: 10.1093/ofid/ofaa327. PMID: 32864388; PMCID: PMC7445584.
20. Karmen-Tuohy S, Carlucci PM, Zervou FN, Zacharioudakis IM, Rebick G, Klein E, et al. Outcomes Among HIV-Positive Patients Hospitalized With COVID-19. J Acquir Immune Defic Syndr. 2020 Sep 1; 85 (1): 6–10. DOI: 10.1097/QAI.0000000000002423. PMID: 32568770; PMCID: PMC7446982.
21. Davies MA. HIV and risk of COVID-19 death: a population cohort study from the Western Cape Province, South Africa. medRxiv [Preprint]. 2020 Jul 3: 2020.07.02.20145185. DOI: 10.1101/2020.07.02.20145185. PMID: 32637972; PMCID: PMC7340198.
22. Vizcarra P, Pérez-Elías MJ, Quereda C, Moreno A, Vivancos MJ, Dronda F, et al. Description of COVID-19 in HIV-infected individuals: a single-centre, prospective cohort. Lancet HIV. 2020 Aug; 7 (8): e554–e564. DOI: 10.1016/S2352-3018(20)30164-8. Epub 2020 May 28. PMID: 32473657; PMCID: PMC7255735.
23. Childs K, Post FA, Norcross C, Ottaway Z, Hamlyn E, Quinn K, et al. Hospitalized Patients With COVID-19 and Human Immunodeficiency Virus: A Case Series. Clin Infect Dis. 2020 Nov 5; 71 (8): 2021–2. DOI: 10.1093/cid/ciaa657. PMID: 32459833; PMCID: PMC7314116.
24. Altuntas Aydin O, Kumbasar Karaosmanoglu H, Kart Yasar K. HIV/SARS-CoV-2 coinfected patients in Istanbul, Turkey. J Med Virol. 2020 Nov; 92 (11): 2288–90. DOI: 10.1002/jmv.25955. Epub 2020 Jun 3. PMID: 32347975
25. Inciarte A, Gonzalez-Cordon A, Rojas J, Torres B, de Lazzari E, de la Mora L, et al. Clinical characteristics, risk factors, and incidence of symptomatic coronavirus disease 2019 in a large cohort of adults living with HIV: a single-center, prospective observational study. AIDS. 2020 Oct 1; 34 (12): 1775–80. DOI: 10.1097/QAD.0000000000002643. PMID: 32773471; PMCID: PMC7493771.
26. Gudipati S, Brar I, Murray S, McKinnon JE, Yared N, Markowitz N. Descriptive Analysis of Patients Living With HIV Affected by COVID-19. J Acquir Immune Defic Syndr. 2020 Oct 1; 85 (2): 123–6. DOI: 10.1097/QAI.0000000000002450. PMID: 32675771; PMCID: PMC7446990.
27. Nakamoto T, Kutsuna S, Yanagawa Y, Kanda K, Okuhama A, Akiyama Y, et al. A case of SARS-CoV-2 infection in an untreated HIV patient in Tokyo, Japan. J Med Virol. 2020 Jun 3: 10.1002/jmv.26102. DOI: 10.1002/jmv.26102. Epub ahead of print. PMID: 32492188; PMCID: PMC7300885.
28. Nagarakanti SR, Okoh AK, Grinberg S, Bishburg E. Clinical outcomes of patients with COVID-19 and HIV coinfection. J Med Virol. 2020 Sep 19. DOI: 10.1002/jmv.26533. Epub ahead of print. PMID: 32949148; PMCID: PMC7537324.
29. Mondi A, Cimini E, Colavita F, Cicalini S, Pinnetti C, Matusali G, et al. COVID-19 in people living with HIV: Clinical implications of dynamics of the immune response to SARS-CoV-2. J Med Virol. 2020 Sep 25. DOI: 10.1002/jmv.26556. Epub ahead of print. PMID: 32975842; PMCID: PMC7537181.
30. Gervasoni C, Meraviglia P, Riva A, Giacomelli A, Oreni L, Minisci D, et al. Clinical Features and Outcomes of Patients With Human

Immunodeficiency Virus With COVID-19. Clin Infect Dis. 2020 Nov 19; 71 (16): 2276–78. DOI: 10.1093/cid/ciaa579. PMID: 32407467; PMCID: PMC7239244.
31. Zhao J, Liao X, Wang H, Wei L, Xing M, Liu L, et al. Early Virus Clearance and Delayed Antibody Response in a Case of Coronavirus Disease 2019 (COVID-19) With a History of Coinfection With Human Immunodeficiency Virus Type 1 and Hepatitis C Virus. Clin Infect Dis. 2020 Nov 19; 71 (16): 2233–35. DOI: 10.1093/cid/ciaa408. PMID: 32270178; PMCID: PMC7184426.
32. Hu Y, Ma J, Huang H, Vermund SH. Coinfection With HIV and SARS-CoV-2 in Wuhan, China: A 12-Person Case Series. J Acquir Immune Defic Syndr. 2020 Sep 1; 85 (1): 1–5. DOI: 10.1097/QAI.0000000000002424. PMID: 32568771; PMCID: PMC7446977.
33. Suwanwongse K, Shabarek N. Clinical features and outcome of HIV/SARS-CoV-2 coinfected patients in The Bronx, New York city. J Med Virol. 2020 Nov; 92 (11): 2387–9. DOI: 10.1002/jmv.26077. Epub 2020 Jun 9. PMID: 32462663; PMCID: PMC7283854.
34. Mascolo S, Romanelli A, Carleo MA, Esposito V. Could HIV infection alter the clinical course of SARS-CoV-2 infection? When less is better. J Med Virol. 2020 Oct; 92 (10): 1777–8. DOI: 10.1002/jmv.25881. Epub 2020 Jul 11. PMID: 32293709; PMCID: PMC7262314.
35. Yang R, Gui X, Zhang Y, Xiong Y, Gao S, Ke H. Clinical characteristics of COVID-19 patients with HIV coinfection in Wuhan, China. Expert Rev Respir Med. 2020 Oct 27: 1–7. DOI: 10.1080/17476348.2021.1836965. Epub ahead of print. PMID: 33074039; PMCID: PMC7605649.
36. Ho HE, Peluso MJ, Margus C, Matias Lopes JP, He C, Gaisa MM, et al. Clinical outcomes and immunologic characteristics of Covid-19 in people with HIV. J Infect Dis. 2020 Jun 30: jiaa380. DOI: 10.1093/infdis/jiaa380. Epub ahead of print. PMID: 32601704; PMCID: PMC7337732.
37. Neuhaus J, Jacobs DR Jr, Baker JV, Calmy A, Duprez D, La Rosa A, et al. Markers of inflammation, coagulation, and renal function are elevated in adults with HIV infection. J Infect Dis. 2010 Jun 15; 201 (12): 1788–95. DOI: 10.1086/652749. PMID: 20446848; PMCID: PMC2872049.
38. Feng X, Li S, Sun Q, Zhu J, Chen B, Xiong M, et al. Immune-Inflammatory Parameters in COVID-19 Cases: A Systematic Review and Meta-Analysis. Front Med (Lausanne). 2020 Jun 9; 7: 301. DOI: 10.3389/fmed.2020.00301. PMID: 32582743; PMCID: PMC7295898.
39. Xu H, Zhong L, Deng J, Peng J, Dan H, Zeng X, et al. High expression of ACE2 receptor of 2019-nCoV on the epithelial cells of oral mucosa. Int J Oral Sci. 2020 Feb 24; 12 (1): 8. DOI: 10.1038/s41368-020-0074-x. PMID: 32094336; PMCID: PMC7039956.
40. Biegler B, Kasinrerk W. Reduction of CD147 surface expression on primary T cells leads to enhanced cell proliferation. Asian Pac J Allergy Immunol. 2012 Dec; 30 (4): 259–67. PMID: 23393905.
41. Chan KS, Lai ST, Chu CM, Tsui E, Tam CY, Wong MM, et al. Treatment of severe acute respiratory syndrome with lopinavir/ritonavir: a multicentre retrospective matched cohort study. Hong Kong Med J. 2003 Dec; 9 (6): 399–406. PMID: 14660806.
42. Elfiky AA. Ribavirin, Remdesivir, Sofosbuvir, Galidesivir, and Tenofovir against SARS-CoV-2 RNA dependent RNA polymerase (RdRp): a molecular docking study. Life Sci. 2020 Jul 15; 253: 117592. DOI: 10.1016/j.lfs.2020.117592. Epub 2020 Mar 25. Erratum in: Life Sci. 2020 Oct 1; 258: 118350. PMID: 32222463; PMCID: PMC7102646.
43. Liu J, Zeng W, Cao Y, Cui Y, Li Y, Yao S, et al. Effect of a Previous History of Antiretroviral Treatment on Clinical Picture of Patients with Co-infection of SARS-CoV-2 and HIV: A Preliminary Study. Int J Infect Dis. 2020 Nov; 100: 141–8. DOI: 10.1016/j.ijid.2020.08.045. Epub 2020 Aug 20. PMID: 32829051; PMCID: PMC7439831.
44. Cao B, Wang Y, Wen D, Liu W, Wang J, Fan G, et al. A Trial of Lopinavir-Ritonavir in Adults Hospitalized with Severe Covid-19. N Engl J Med. 2020 May 7; 382 (19): 1787–99. DOI: 10.1056/NEJMoa2001282. Epub 2020 Mar 18. PMID: 32187464; PMCID: PMC7121492.
45. Ayerdi O, Puerta T, Clavo P, Vera M, Ballesteros J, Fuentes ME, et al. Preventive efficacy of Tenofovir/Emtricitabine against severe acute respiratory syndrome Coronavirus 2 among pre-exposure prophylaxis users. Open Forum Infect Dis. 2020 Sep 25; 7 (11): ofaa455. DOI: 10.1093/ofid/ofaa455. PMID: 33200081; PMCID: PMC7543639.
46. Musarrat F, Chouljenko V, Dahal A, Nabi R, Chouljenko T, Jois SD, et al. The anti-HIV drug nelfinavir mesylate (Viracept) is a potent inhibitor of cell fusion caused by the SARSCoV-2 spike (S) glycoprotein warranting further evaluation as an antiviral against COVID-19 infections. J Med Virol. 2020 Oct; 92 (10): 2087–95. DOI: 10.1002/jmv.25985. Epub 2020 May 17. PMID: 32374457; PMCID: PMC7267418.

THE IMPORTANCE OF DETERMINING SARS-COV-2 N-Ag SERODIAGNOSTICS FOR THE MANAGEMENT OF COVID-19 PNEUMONIA IN HOSPITAL SETTINGS

Lebedin YuS[1] ✉, Lyang OV[2], Galstyan AG[2], Panteleeva AV[1], Belousov VV[2, 3], Rebrikov DV[3]

[1] XEMA Co. Ltd., Moscow, Russia

[2] Federal Center of Brain Research and Neurotechnologies of the Federal Medical Biological Agency, Moscow, Russia

[3] Center for Precision Genome Editing and Genetic Technologies for Biomedicine, Pirogov Russian National Research Medical University, Moscow, Russia

A new coronavirus infection caused by the SARS-CoV-2 virus, which appeared in December 2019, has claimed the lives of 2.5 million people in almost a year. The high contagiousness of this virus has led to its wide and rapid spread around the world. As of February 2021, the total number of cases is 111 million people; more than 4 million cases of SARS-CoV-2 infection have been registered in the Russian Federation. To successfully combat the emerging pandemic, it is necessary to quickly diagnose the disease at an early stage, which will prevent the further spread of this virus and prescribe the necessary treatment on time. The aim of the work was to evaluate the use of the SARS-CoV-2 nucleocapsid antigen (N-Ag) and respective antibodies as diagnostic markers in pneumonia patients. The study was conducted at the height of COVID-19 pandemic in Moscow, Russia. It included 425 emergency patients with clinical signs of COVID-19 pneumonia, of which 280 (66%) were positive for either serum N-Ag and/or its respective antibodies. We demonstrate the total prevalence of N-Ag seroconversion in SARS-CoV-2-associated pneumonia patients within 3–5 days after hospital admission. The results indicate high feasibility of SARS-CoV-2 serodiagnostics in emergency patients.

Keywords: SARS-CoV-2, COVID-19, nucleocapsid antigen, seroconversion

Funding: this work was partially supported by a grant № 075-15-2019-1789 from the Ministry of Science and Higher Education of the Russian Federation allocated to the Center for Precision Genome Editing and Genetic Technologies for Biomedicine.

Acknowledgement: we acknowledge Natalia Usman for helpful discussions

Author contribution: Lebedin YS designed the study, performed the sampling, conducted molecular studies and drafted the manuscript, Lyang OV and Galstyan AG performed the clinical examinations and sampling, conducted biochemical and molecular studies, Panteleeva AV conducted molecular studies and drafted the manuscript, Belousov VV and Rebrikov DV designed the study and drafted the manuscript. All authors read and approved the final version of the manuscript.

Compliance with ethical standards: the study protocol was reviewed and approved by the Local Ethics Committee at the Pirogov Russian State Medical University (Protocol № 2020/07 dated March 16, 2020,); the study was conducted in accordance with the Declaration of Helsinki.

✉ **Correspondence should be addressed:** Yuri S. Lebedin
9-ya Parkovaya, 48, Moscow, 105264; lebedin@xema-medica.com

Preprint published: 25.09.2020 **DOI:** 10.1101/2020.09.24.20200303

Received: 11.02.2021 **Accepted:** 24.02.2021 **Published online:** 28.02.2021

DOI: 10.24075/brsmu.2021.009

ВАЖНОСТЬ ОПРЕДЕЛЕНИЯ N-АНТИГЕНА ВИРУСА SARS-COV-2 ДЛЯ ЛЕЧЕНИЯ ПНЕВМОНИИ COVID-19 В УСЛОВИЯХ СТАЦИОНАРА

Ю. С. Лебедин[1] ✉, О. В. Лянг[2], А. Г. Галстян[2], А. В. Пантеелеева[1], В. В. Белоусов[2, 3], Д. В. Ребриков[3]

[1] ООО «ХЕМА», Москва, Россия

[2] Федеральный центр мозга и нейротехнологий Федерального медико-биологического агентства, Москва, Россия

[3] Центр высокоточного редактирования и генетических технологий для биомедицины, Российский национальный исследовательский медицинский университет имени Н. И. Пирогова, Москва, Россия

Появившаяся в декабре 2019 г. новая коронавирусная инфекция, вызванная вирусом SARS-CoV-2, почти за год унесла жизни 2,5 млн человек. Высокая контагиозность вируса привела к его широкому и быстрому распространению по всему миру. По состоянию на февраль 2021 г. общее число заболевших достигает 111 млн человек; в РФ зарегистрировано более 4 млн случаев заражения SARS-CoV-2. Для успешной борьбы с возникшей пандемией необходимо быстро диагностировать заболевание на ранней стадии, что позволит предотвращать дальнейшее распространение этого вируса и своевременно назначать необходимое лечение. Целью работы было оценить использование нуклеокапсидного антигена (N-Ag) SARS-CoV-2 и соответствующих антител в качестве диагностических маркеров у больных пневмонией. Исследование проводили в разгар пандемии COVID-19 в Москве (Россия). В него вошли 425 экстренных пациентов с клиническими признаками пневмонии COVID-19, из которых 280 (66%) были положительны либо на сывороточный N-Ag, либо на соответствующие ему антитела. Продемонстрирована общая распространенность сероконверсии N-Ag у пациентов с пневмонией, ассоциированной с SARS-CoV-2, в течение 3–5 дней после госпитализации. Полученные результаты свидетельствуют о высокой целесообразности серодиагностики SARS-CoV-2 у экстренных больных.

Ключевые слова: SARS-CoV-2, COVID-19, нуклеокапсидный антиген, сероконверсия

Финансирование: работа выполнена при частичной поддержке гранта Министерства науки и высшего образования Российской Федерации № 075-15-2019-1789, выделенного Центру высокоточного редактирования и генетических технологий для биомедицины.

Благодарности: мы благодарим Наталью Усман за помощь в обсуждении.

Вклад авторов: Ю. С. Лебедин — разработка концепции, отбор проб, молекулярные исследования, редактирование рукописи; О. В. Лянг, А. Г. Галстян — клинические обследования, отбор проб, биохимические и молекулярные исследования; А. В. Пантелеева — молекулярные исследования; редактирование рукописи, В. В. Белоусов, Д. В. Ребриков — подготовка исследования; редактирование рукописи. Все авторы прочли и одобрили окончательный вариант рукописи.

Соблюдение этических стандартов: исследование одобрено этическим комитетом РНИМУ им. Н. И. Пирогова (протокол № 2020/07 от 16 марта 2020 г.), проведено в соответствии с требованиями Хельсинкской декларации.

✉ **Для корреспонденции:** Юрий Степанович Лебедин
9-я Парковая, д. 48, 105264, г. Москва; lebedin@xema-medica.com

Препринт опубликован: 25.09.2020 **DOI:** 10.1101/2020.09.24.20200303

Статья получена: 11.02.2021 **Статья принята к печати:** 24.02.2021 **Опубликована онлайн:** 28.02.2021

DOI: 10.24075/vrgmu.2021.009

Immunochemical detection of antigens in blood is widely used in the diagnostics of infectious diseases. The antigenemia tests are usually targeted at blood-borne pathogens (notably chronic viral infections including cytomegalovirus, hepatitis B and C viruses, and HIV [1–3]). In respiratory diseases, the penetration of the pathogen components (nucleic acids or proteins) into non-respiratory body fluids is likely, but their detection is usually considered of minor value because of the focal nature of the pathogenesis and its strong association with mucous immunity. Despite that, certain respiratory infections can be efficiently diagnosed and monitored by detection of corresponding antigens in the blood; the examples include galactomannan in pulmonary aspergillosis [4] and *L. pneumophila* antigen in urine of Legionnaires' disease patients [5]. In addition, the use of serological immunoassays for the management of virus-associated nosocomial pneumonias in intensive care unit patients has been reported [4, 6]. Serum nucleocapsid antigen (N-Ag) of SARS virus was described in SARS-associated pneumonia by Che et al [7, 8].

The aim of the work was to evaluate the use of the SARS-CoV-2 nucleocapsid antigen (N-Ag) and respective antibodies as diagnostic markers and demonstrate the total prevalence of N-Ag seroconversion in SARS-CoV-2-associated pneumonia patients.

METHODS

The study was carried out at the Federal Center of Brain Research and Neurotechnologies during the spring of 2020. At the height of the COVID-19 pandemic, the in-patient care facilities of the Center were redesigned for the emergency hospitalization and management of the SARS-CoV-2-associated pneumonia patients. The study involved patients with clinical signs of COVID-19 pneumonia (n = 425) flown by ambulance services from different districts of Moscow. Inclusion criteria: presence of clinical signs of COVID-19 pneumonia (fever with a combination of two or more clinical signs, including body temperature ≥ 38.5 °C, respiratory rate ≥ 30 breaths per minute, and/or SpO_2 ≤ 93%) [9]. Serum samples for the study were collected from each patient at least twice; sampling at the admission and at the discharge was carried out concomitantly with the mandatory procedure for routine blood tests. The in-patient care lasted 20 ± 2 days. Criteria for the discharge included a reduction in C-reactive protein levels at WBC counts within the normal range (above 4.0×10^9 L) and, notably, a clear tendency towards regression of characteristic signs revealed by computer tomography: the absence of new ground glass opacities, a decrease in the severity of the corresponding changes in the lung tissue and/or a decrease in the volume or degree of consolidation of the ground glass opacities (no more than three, each within 3 cm along the maximal dimension) [10]. The qualitative RT-PCR detection of SARS-CoV-2 RNA in nasopharyngeal swabs was carried out at the admission with the use of SARS-CoV-2/SARS-CoV Multiplex Real-Time PCR Detection Kit (DNA-Technology LLC; Russia); analytical sensitivity is 10 copies per amplification tube, diagnostic sensitivity — 100% (95% CI: 95.6–100%), diagnostic specificity — 100% (95% CI: 96.7–100%) according to the manufacturer's protocol.

SARS-Cov-2 nucleocapsid antigen (N-Ag) coding sequence

SARS-Cov-2 nucleocapsid antigen (N-Ag) coding sequence (NCBI accession number 045512.2) was cloned by NdeI/XhoI into pET-30b(+) vector, Novagen (EMD Millipore; USA); the plasmid was expanded in E. coli Top10 and transformed into *E. coli* Rosetta (DE3) for N-Ag expression.

The conditions were optimized for 37 °C bioreactor fermentation in 3000 mL of rich media (yeast extract, bacto peptone, glucose and trace salts). After 12 h incubation, the culture was induced with 2.5 mM imidazole for 4 h. The obtained biomass was resuspended in phosphate buffered saline (PBS) in 1 : 3 (w/v) proportion and disrupted using APV-2000 homogenizer (Spx Flow; USA) at 1200 bar. The solution was clarified by centrifugation at 12,000 g. The insoluble fraction (inclusion bodies) containing the target protein was washed sequentially with PBS, 2% Triton in PBS and a fresh portion of PBS to remove the residual detergent. The protein was dissolved in 8 M urea with 250 mM NaCl and 50 mM phosphate, pH 10.0. The solution was incubated at +4 °C overnight and centrifuged at 15,000 g; the collected supernatant was filtered and supplemented with 20 mM imidazole to prevent the non-specific binding of impurities. The polyhistidine-tagged N-Ag protein was purified by immobilized metal affinity chromatography using a nickel column High Density Nickel #6BCL-QHNi (ABT; Spain) equilibrated with the urea buffer. The protein was eluted with 250 mM imidazole buffer and filter-sterilized through filters with a diameter of 0.45 μm.

Serum IgG antibodies against nucleocapsid antigen (N-IgG)

Serum IgG antibodies against nucleocapsid antigen (N-IgG) were detected by solid-phase enzyme immunoassay. Briefly, the recombinant full-length SARS-CoV-2 nucleocapsid antigen produced in E. coli (XEMA; Russia) was coated onto the surface of polystyrene microwells. The sera pre-diluted 100-fold in the ELISA buffer (0.1% Tween-20 and 1% hydrolyzed casein in 0.1 M PBS) were placed in the microwells for 30 min at 37 °C. After 3 washes with 0.1% Tween-20 in 0.9% sodium chloride, the wells were exposed to the conjugate of murine monoclonal antibodies XG78 against human IgG (gamma chain) with horseradish peroxidase (XEMA; Russia) for 30 min. After 5 washes with 0.1% Tween-20 in 0.9% sodium chloride, the bound enzyme was revealed by addition of the substrate-chromogenic mix (TMB substrate, XEMA; Russia). The color development was stopped by 5% sulfuric acid and the optical density (OD) at 450 nm was measured in a plate reader Multiskan MC (Thermo Labsystems; Finland). The internal controls (stabilized human serum containing specific IgG antibodies) were included in all microplates to calculate the positivity threshold OD for each run individually. The results are expressed as positivity indexes (calculated as OD for a sample of interest related to OD for the internal control).

Serum IgM antibodies against nucleocapsid antigen (N-IgM)

Serum IgM antibodies against nucleocapsid antigen (N-IgM) were detected by reverse solid phase enzyme immunoassay. Briefly, murine monoclonal antibody against the mu chain of human IgM (clone X616, XEMA; Russia) was adsorbed on the surface of polystyrene microwells. The dilutions of sera (prepared in the same way as for the IgG assay) were placed in the microwells for 30 min at 37 °C. After 3 washes with 0.1% Tween-20 in 0.9% sodium chloride, a working dilution of the recombinant full-length SARS-CoV-2 nucleocapsid antigen conjugated with horseradish peroxidase in the ELISA buffer was placed in the microwells for 30 min at 37 °C. After

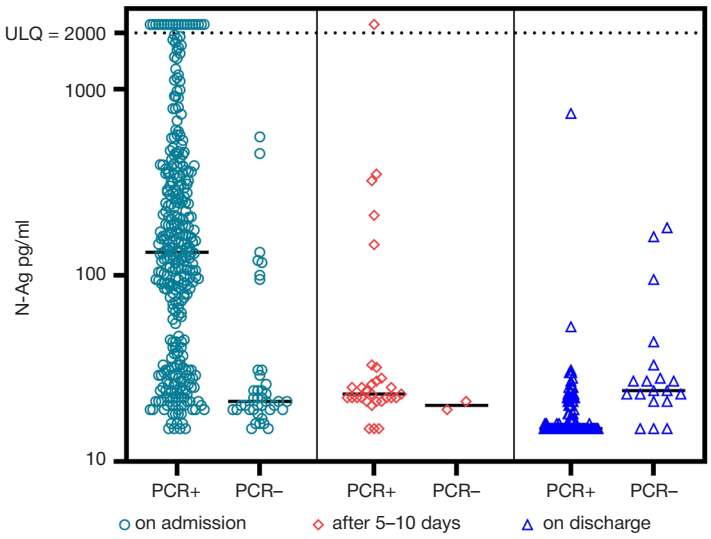

Fig. 1. Dynamics of serum N-Ag levels in the studied cohort of hospital patients. ULQ, upper limit of quantification. The 'PCR+' and 'PCR-' indications refer to the patient's status on admission

5 washes with 0.1% Tween-20 in 0.9% sodium chloride, the bound labeled antigen was detected by TMB substrate and OD reading. The calculation of positivity index (similarly with the IgG assay) was performed by using the internal IgM+ control.

Serum N-antigen (N-Ag) determination

Serum N-antigen (N-Ag) determination was performed by the two-site solid-phase sandwich method using monoclonal antibodies (mAbs) generously gifted by Hytest Ltd (Turku; Finland). The microwells were coated with the capture mAb NP1510. Serum samples or assay calibrators (solutions of nucleocapsid antigen in donor serum in the range 20–2000 pg/ml) were incubated with a working dilution of HRP-labeled tracer monoclonal antibody (clone NP1517) in ELISA buffer with the addition of heterophilic immunoglobulin elimination reagent (10 µg/ml, HIER-E-010, Fapon Biotech; China) for 2 h at 37 °C under continuous 600 rpm shaking in a PST-60HL-4 shaking incubator (Biosan; Latvia). The detection was performed with the use of TMB substrate (XEMA; Russia) and OD reading. The N-Ag concentrations were determined by calibration curve method using. N-Ag concentrations exceeding the upper limit of calibration curve (2000 pg/ml) were shown as 2222 pg/ml in calculations and graphic presentation. The samples with OD readings corresponding to concentrations lower than 20 pg/ml, lacking resolution from the zero calibrator, were conventionally assigned 15 pg/ml values in the presented data.

Statistical processing

The data were processed in GraphPad Prism 8.0 (GraphPad Software, Inc.; USA) and Microsoft Excel 2016 (Microsoft; USA).

The reference ranges were determined by analysis of serum samples collected from healthy donors (n = 250) before Dec 2019. In both assays, the threshold (cutoff) values were set to attain full specificity (none of the donors being considered positive).

RESULTS

The immunoassay-based detection of serum N-Ag in combination with its respective antibodies confirmed COVID-19 in 280 patients (66%) of the studied cohort. RT-PCR analysis of nasopharyngeal swabs confirmed COVID-19 in 76% of the patients; the interception constitutes 63% and corresponds to the concordance of 79%.

Several patients (n = 21; 5%) were identified as SARS-CoV-2 negative by both RT-PCR tests and serodiagnostics, and most likely represented cases on non-SARS-CoV-2-associated pneumonias. The small number of such patients is

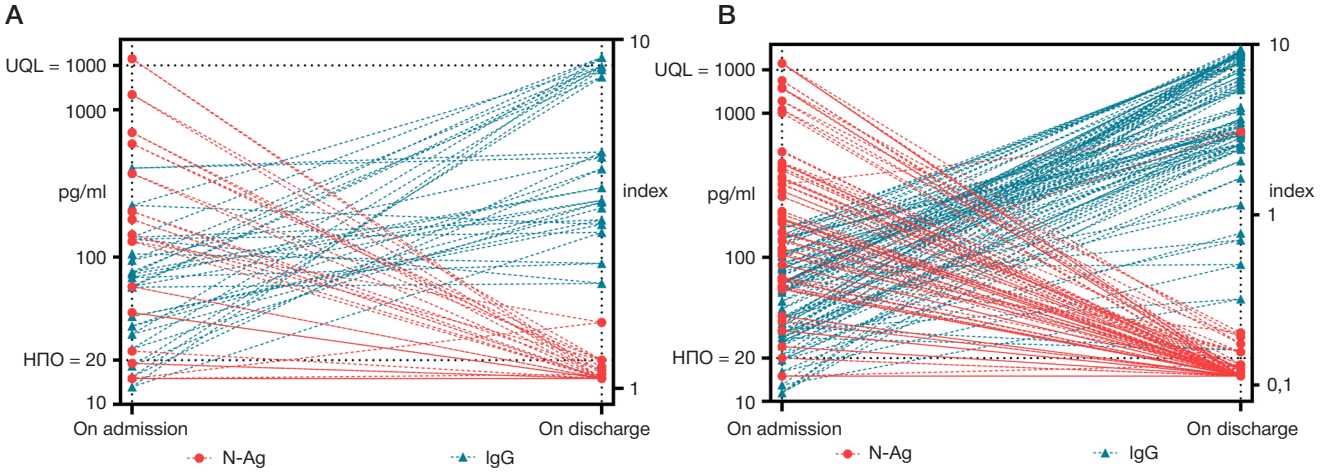

Fig. 2. Dynamics of serum N-Ag levels vs. respective IgG antibodies in patients IgG-seropositive on admission (**A**) and patients IgG-seronegative on admission (**B**). Vertical axes correspond to Ag concentration (on the *left*) and Ab index (on the *right*). ULQ, upper limit of quantification; LOD, (lower) limit of detection

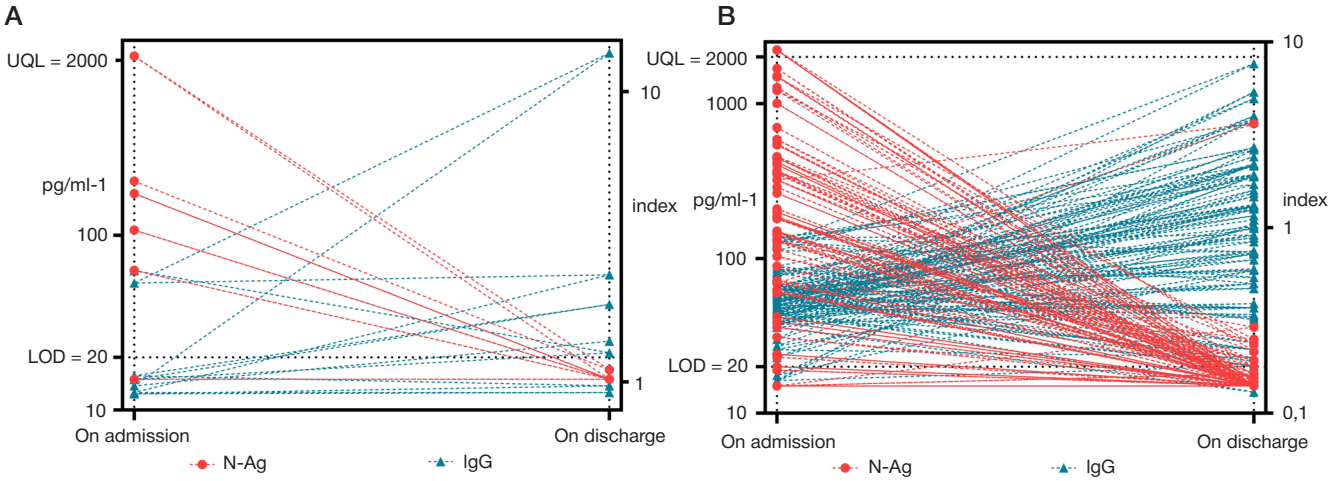

Fig. 3. Dynamics of serum N-Ag levels vs. respective IgM antibodies in patients IgM-seropositive on admission (**A**) and patients IgM-seronegative on admission (**B**). Vertical axes correspond to Ag concentration (on the *left*) and Ab index (on the *right*). ULQ, upper limit of quantification; LOD, (lower) limit of detection

explained by the fact that the study was carried out at the peak of the pandemic.

According to the data, N-Ag antigenemia is characteristic of the majority of patients with severe COVID-19 (63%).

The disease phase-related dynamics of serum N-Ag levels are shown in Fig 1. At the discharge, most of the patients N-Ag positive at the admission (104 of 116; 90%) showed serum N-Ag levels below the lower limit of the calibration curve (< 20 pg/ml; 104 of 116; 90%). However, some patients were clearly positive for serum N-Ag even at the discharge.

By the time of discharge, seroconversion was observed in most of the patients N-Ag positive at the admission (108 of 116; 93%), although the degree of seroconversion varied considerably.

DISCUSSION

To determine seroconversion patterns, we plotted serum N-Ag levels with two isotypes of antibody response for individual cases, dividing them in two subgroups by Ab-seropositivity on admission (Fig. 2A and 3A vs. 2B and 3B). The results indicate reciprocal patterns for N-Ag and respective antibodies, which is characteristic of classical seroconversion. The patients Ab-seronegative on admission (presumably being at the earlier stage of the disease) showed more distinct patterns of classical seroconversion. The IgG-antibody patterns were more pronounced than the IgM-antibody patterns in both groups.

Co-detection of N-Ag and anti-N-Ag antibodies in 92 (18%) of 503 serum samples demonstrates that the epitope recognized by immunoassay pair used for the antigen determination is at least not fully overlapped (masked) by the human antibody response.

For a subcohort of 20 patients, we had the opportunity to evaluate seroconversion within a shorter period of several days. According to the results shown in Figure 4, in the majority of cases the switch from Ag+Ab- to Ag-Ab+ status proceeded within 3–5 days after the emergency admission.

According to the results of the study, hospitalization of the patients with SARS-CoV-2-associated pneumonia at the height of pandemic most frequently occurred before the onset of seroconversion (i.e. against the background of detectable serum N-Ag concentrations). In the majority of patients the antigen prevailed at the time of admission and was "replaced" with respective antibodies by the time of discharge. Nevertheless, in some cases, by the time of emergency hospitalization, the level of antibodies to N-Ag in the patient's blood was already high, probably reflecting either delayed hospitalization or individual variation in the COVID-19 pathogenesis.

Overall, the obtained results indicate high feasibility of SARS-CoV-2 serodiagnostics in the emergency patients (along the

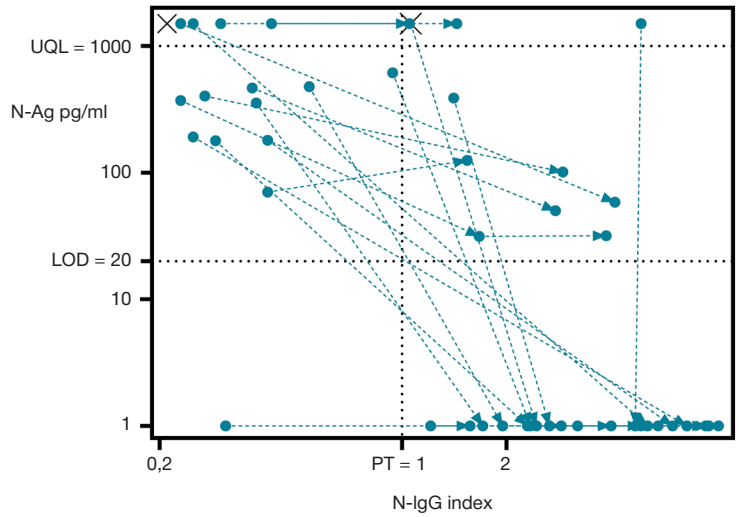

Fig. 4. Individual patterns of seroconversion in the course of 3–5 days after the admission. ULQ, upper limit of quantification; LOD, (lower) limit of detection; PT, positivity threshold

lines of 'rapid tests' Capillus HIV-1/HIV-2®, Determine HIV-1/2®, etc. currently proposed as a gold standard of HIV diagnostics instead of the more expensive and time-consuming western blot analysis [11]). Similar conclusions were drawn in the study of small groups of patients with confirmed SARS-CoV-2 using various methods of immunochemical analysis [12, 13].

It should be noted that false-positive results of SARS-CoV-2 serodiagnostics may appear in patients with high levels of rheumatoid factor or HAMA antibodies, which underscores the significance of personalized comprehensive diagnostics for the patients with severe COVID-19.

CONCLUSION

Overall, the results indicate high relevance of combined serological tests for SARS-CoV-2 N-Ag and the antibodies to SARS-CoV-2 antigens as applied to the infectious pneumonia emergency patients at the admission, since 1) sensitivity and specificity of the serological test for N-Ag is comparable to that of the RT-PCR analysis of nasopharyngeal swabs, and the use of serology tests in combination with PCR tests for SARS-CoV-2 provides a significant increase in the overall sensitivity; 2) processing of blood samples is safer for the personnel due to the negligible presence of SARS-CoV-2 infectious particles in the blood, by contrast with nasopharyngeal swabs; 3) serological tests are generally faster than RT-PCR tests (when accounting for the full cycle of biomaterial processing and sample preparation), which accelerates the determination of SARS-CoV-2 status for a prompt decision on the management mode and isolation measures; in addition, blood serum analyses are easier to automate; 4) collection of blood samples for serodiagnostics of SARS-CoV-2 in hospital settings is not an additional invasive procedure, but is performed as a part of the mandatory primary examination immediately upon the admission (as well as of the final examination upon the discharge from the hospital).

References

1. Dioverti MV, Razonable RR. Cytomegalovirus. Microbiol Spectr. 2016; 4 (4). DOI: 10.1128/microbiolspec.DMIH2-0022-2015.
2. Laing N, Tufton H, Ochola E, P'Kingston OG, Maini MK, Easom N. Hepatitis B assessment without hepatitis B virus DNA quantification: a prospective cohort study in Uganda. Trans R Soc Trop Med Hyg. 2019; 113 (1): 11–17. DOI: 10.1093/trstmh/try117.
3. Thai KTD, Götz H, Slingerland BCGC, Klaasse J, Schutten M, GeurtsvanKessel CH. An analysis of the predictive value of the HIV Ag/Ab screening assay within the performance characteristics of the DiaSorin LIAISON XL for the detection of blood-borne viruses. J Clin Virol. 2018; 102: 95–100. DOI: 10.1016/j.jcv.2018.02.018.
4. Loughlin L, Hellyer TP, White PL, et al. Pulmonary Aspergillosis in Patients with Suspected Ventilator-associated Pneumonia in UK Intensive Care Units [published online ahead of print, 2020 Jul 1]. Am J Respir Crit Care Med. 2020; 10.1164/rccm.202002-0355OC. DOI: 10.1164/rccm.202002-0355OC.
5. Edelstein PH, Jørgensen CS, Wolf LA. Performance of the ImmuView and BinaxNOW assays for the detection of urine and cerebrospinal fluid Streptococcus pneumoniae and Legionella pneumophila serogroup 1 antigen in patients with Legionnaires' disease or pneumococcal pneumonia and meningitis. PLoS One. 2020; 15 (8): e0238479. Published 2020 Aug 31. DOI: 10.1371/journal.pone.0238479.
6. Chiche L, Forel JM, Papazian L. The role of viruses in nosocomial pneumonia. Curr Opin Infect Dis. 2011; 24 (2): 152–56. DOI: 10.1097/QCO.0b013e328343b6e4.
7. Che XY, Qiu LW, Pan YX, Wen K, Hao W, Zhang LY, et al. Sensitive and specific monoclonal antibody-based capture enzyme immunoassay for detection of nucleocapsid antigen in sera from patients with severe acute respiratory syndrome. J Clin Microbiol. 2004 Jun; 42 (6): 2629–35. DOI: 10.1128/JCM.42.6.2629-2635.2004.
8. Xiao-yan Che, Biao Di, Guo-ping Zhao, Ya-di Wang, Li-wen Qiu, Wei Hao, et al. A Patient with Asymptomatic Severe Acute Respiratory Syndrome (SARS) and Antigenemia from the 2003–2004 Community Outbreak of SARS in Guangzhou, China, Clinical Infectious Diseases. 2006; 43 (1): e1–e5. DOI: 10.1086/504943.
9. Prikaz departamenta zdravoohranenija goroda Moskvy ot 22 marta 2020 g. # 230 «Ob utverzhdenii reglamentov (algoritmov) raboty medicinskih organizacij, podvedomstvennyh Departamentu zdravoohranenija goroda Moskvy v period s 23 po 30 marta 2020 g. po okazaniju medicinskoj pomoshhi pacientam, zabolevshim novoj koronavirusnoj infekciej (COVID-19), i kontaktnym s nimi licam». Available from: https://rg.ru/2020/03/24/moscow-prikaz230-reg-dok.html. Russian.
10. Prikaz Departamenta zdravoohranenija goroda Moskvy ot 06 aprelja 2020 g. # 351 «O porjadke vypiski iz medicinskih organizacij (stacionarov), podvedomstvennyh Departamentu zdravoohranenija goroda Moskvy, pacientov s vnebol'nichnoj pnevmoniej ili koronavirusnoj infekciej (COVID-19), dlja prodolzhenija lechenija v ambulatornyh uslovijah (na domu)». Available from: https://www.mos.ru/dzdrav/documents/department-acts/view/239550220/. Russian.
11. Huang X, Liu X, Chen J, et al. Evaluation of Blood-Based Antibody Rapid Testing for HIV Early Therapy: A Meta-Analysis of the Evidence. Front Immunol. 2018; 9: 1458. Published 2018 Jun 26. DOI: 10.3389/fimmu.2018.01458.
12. Le Hingrat Q, Visseaux B, Laouenan C, Tubiana S, Bouadma L, Yazdanpanah Y, et al. Detection of SARS-CoV-2 N-antigen in blood during acute COVID-19 provides a sensitive new marker and new testing alternatives. Clinical Microbiology and Infection. December 2020. DOI: 10.1016/j.cmi.2020.11.025.
13. Ogata AF, Maley AM, Wu C, Gilboa T, Norman M, Lazarovits R, et al. Ultra-Sensitive Serial Profiling of SARS-CoV-2 Antigens and Antibodies in Plasma to Understand Disease Progression in COVID-19 Patients with Severe Disease, Clinical Chemistry. 2020; 66 (12): 1562–72. DOI: 10.1093/clinchem/hvaa213.

Литература

1. Dioverti MV, Razonable RR. Cytomegalovirus. Microbiol Spectr. 2016; 4 (4). DOI: 10.1128/microbiolspec.DMIH2-0022-2015.
2. Laing N, Tufton H, Ochola E, P'Kingston OG, Maini MK, Easom N. Hepatitis B assessment without hepatitis B virus DNA quantification: a prospective cohort study in Uganda. Trans R Soc Trop Med Hyg. 2019; 113 (1): 11–17. DOI: 10.1093/trstmh/try117.
3. Thai KTD, Götz H, Slingerland BCGC, Klaasse J, Schutten M, GeurtsvanKessel CH. An analysis of the predictive value of the HIV Ag/Ab screening assay within the performance characteristics of the DiaSorin LIAISON XL for the detection of blood-borne viruses. J Clin Virol. 2018; 102: 95–100. DOI: 10.1016/j.jcv.2018.02.018.
4. Loughlin L, Hellyer TP, White PL, et al. Pulmonary Aspergillosis in Patients with Suspected Ventilator-associated Pneumonia in UK Intensive Care Units [published online ahead of print, 2020 Jul 1]. Am J Respir Crit Care Med. 2020; 10.1164/rccm.202002-0355OC. DOI: 10.1164/rccm.202002-0355OC.
5. Edelstein PH, Jørgensen CS, Wolf LA. Performance of the ImmuView and BinaxNOW assays for the detection of urine and

cerebrospinal fluid Streptococcus pneumoniae and Legionella pneumophila serogroup 1 antigen in patients with Legionnaires' disease or pneumococcal pneumonia and meningitis. PLoS One. 2020; 15 (8): e0238479. Published 2020 Aug 31. DOI: 10.1371/journal.pone.0238479.

6. Chiche L, Forel JM, Papazian L. The role of viruses in nosocomial pneumonia. Curr Opin Infect Dis. 2011; 24 (2): 152–56. DOI: 10.1097/QCO.0b013e328343b6e4.
7. Che XY, Qiu LW, Pan YX, Wen K, Hao W, Zhang LY, et al. Sensitive and specific monoclonal antibody-based capture enzyme immunoassay for detection of nucleocapsid antigen in sera from patients with severe acute respiratory syndrome. J Clin Microbiol. 2004 Jun; 42 (6): 2629–35. DOI: 10.1128/JCM.42.6.2629-2635.2004.
8. Xiao-yan Che, Biao Di, Guo-ping Zhao, Ya-di Wang, Li-wen Qiu, Wei Hao, et al. A Patient with Asymptomatic Severe Acute Respiratory Syndrome (SARS) and Antigenemia from the 2003–2004 Community Outbreak of SARS in Guangzhou, China, Clinical Infectious Diseases. 2006; 43 (1): e1–e5. DOI: 10.1086/504943.
9. Приказ департамента здравоохранения города Москвы от 22 марта 2020 г. № 230 «Об утверждении регламентов (алгоритмов) работы медицинских организаций, подведомственных Департаменту здравоохранения города Москвы в период с 23 по 30 марта 2020 г. по оказанию медицинской помощи пациентам, заболевшим новой коронавирусной инфекцией (COVID-19), и контактным с ними лицам». Доступно по ссылке: https://rg.ru/2020/03/24/moscow-prikaz230-reg-dok.html.
10. Приказ Департамента здравоохранения города Москвы от 06 апреля 2020 г. № 351 «О порядке выписки из медицинских организаций (стационаров), подведомственных Департаменту здравоохранения города Москвы, пациентов с внебольничной пневмонией или коронавирусной инфекцией (COVID-19), для продолжения лечения в амбулаторных условиях (на дому)». Доступно по ссылке: https://www.mos.ru/dzdrav/documents/department-acts/view/239550220/.
11. Huang X, Liu X, Chen J, et al. Evaluation of Blood-Based Antibody Rapid Testing for HIV Early Therapy: A Meta-Analysis of the Evidence. Front Immunol. 2018; 9: 1458. Published 2018 Jun 26. DOI: 10.3389/fimmu.2018.01458.
12. Le Hingrat Q, Visseaux B, Laouenan C, Tubiana S, Bouadma L, Yazdanpanah Y, et al. Detection of SARS-CoV-2 N-antigen in blood during acute COVID-19 provides a sensitive new marker and new testing alternatives. Clinical Microbiology and Infection. December 2020. DOI: 10.1016/j.cmi.2020.11.025.
13. Ogata AF, Maley AM, Wu C, Gilboa T, Norman M, Lazarovits R, et al. Ultra-Sensitive Serial Profiling of SARS-CoV-2 Antigens and Antibodies in Plasma to Understand Disease Progression in COVID-19 Patients with Severe Disease, Clinical Chemistry. 2020; 66 (12): 1562–72. DOI: 10.1093/clinchem/hvaa213.

ASSOCIATIONS BETWEEN GLUTAMATE CYSTEINE LIGASE CATALYTIC SUBUNIT GENE POLYMORPHISMS AND CLINICAL CHARACTERISTICS OF ISCHEMIC STROKE

Bocharova YA[1,2] ✉

[1] Belgorod State National Research University, Belgorod, Russia

[2] Kursk Regional Clinical Hospital, Kursk, Russia

An imbalance between the production of reactive oxygen species and their neutralization lies at the core of oxidative stress implicated in ischemic stroke (IS) and the subsequent brain tissue damage. The aim of this study was to investigate the effects of common polymorphic variants of the glutamate cysteine ligase catalytic subunit gene on the extent of brain damage and clinical manifestations in patients with ischemic stroke. A total of 589 ischemic stroke survivors were genotyped for 6 single nucleotide polymorphisms (SNPs) of the *GCLC* gene, including rs12524494, rs17883901, rs606548, rs636933, rs648595 and rs761142, using a MassARRAY-4 analyzer. The study found that genotypes rs636933-G/A-A/A (p = 0.009) and rs761142-A/C-C/C (p = 0.015) were associated with an enlargement of the cerebral lesion size. Genotypes rs12524494-G/G (p = 0.05) and rs606548-T/T (p = 0.003) were associated with a risk of 2 or more IS episodes. Genotype rs17883901-G/A was associated with early onset of IS (p = 0.004). The study revealed multiple associations of *GCLC* SNPs with the clinical manifestations of ischemic stroke. Thus, *GCLC* polymorphisms are important DNA markers affecting the size of the cerebral lesion in patients with ischemic stroke and are associated with age at onset, the number of past strokes and the clinical manifestations of the disease.

Keywords: ischemic stroke, cerebral infarction, redox homeostasis, glutathione, glutamate cysteine ligase, single nucleotide polymorphism

Acknowledgements: the author thanks Polonikov AV, Azarova YuE, Klyosova EYu, Bykanova MA and Bushueva OYu of the Research Institute of Genetic and Molecular Epidemiology (Kursk State Medical University) for their help in conducting molecular genetic studies.

Compliance with ethical standards: the study was approved by the Ethics Committee of Kursk State Medical University (Protocol № 5 dated June 25, 2012); all study participants gave voluntary informed consent to participate.

✉ **Correspondence should be addressed:** Yulia A. Bocharova
Sumskaya, 45a, Kursk, 305007; y_u_l_i_a_03@mail.ru

Received: 21.01.2021 **Accepted:** 06.02.2021 **Published online:** 23.02.2021

DOI: 10.24075/brsmu.2021.007

АССОЦИАЦИЯ ПОЛИМОРФНЫХ ВАРИАНТОВ ГЕНА КАТАЛИТИЧЕСКОЙ СУБЪЕДИНИЦЫ ГЛУТАМАТЦИСТЕИНЛИГАЗЫ С КЛИНИЧЕСКИМИ ХАРАКТЕРИСТИКАМИ ИШЕМИЧЕСКОГО ИНСУЛЬТА

Ю. А. Бочарова[1,2] ✉

[1] Белгородский государственный национальный исследовательский университет, Белгород, Россия

[2] Курская областная клиническая больница, Курск, Россия

Дисбаланс между образованием активных форм кислорода и их обезвреживанием лежит в основе окислительного стресса — патологического процесса, патогенетически связанного с развитием ишемического инсульта (ИИ) и последующими этапами постишемического повреждения тканей головного мозга. Целью настоящего исследования было изучение влияния частых полиморфных вариантов гена *GCLC* каталитической субъединицы глутаматцистеинлигазы на степень поражения головного мозга и клинические проявления у больных с ишемическим инсультом. У 589 пациентов с ишемическим инсультом было проведено генотипирование шести однонуклеотидных полиморфизмов (SNP) rs12524494, rs17883901, rs606548, rs636933, rs648595 и rs761142 гена *GCLC* с помощью генетического анализатора MassARRAY-4. Установлено, что генотипы rs636933-G/A-A/A (p = 0,009) и rs761142-A/C-C/C (p = 0,015) ассоциированы с увеличением зоны инфаркта мозга. Генотипы rs12524494-G/G (p = 0,05) и rs606548-T/T (p = 0,003) ассоциировались с возникновением двух и более эпизодов ИИ. Генотип rs17883901-G/A был ассоциирован с более ранним дебютом ИИ (p = 0,004). Выявлены многочисленные ассоциации SNP гена *GCLC* с клиническими проявлениями болезни. Таким образом, полиморфные варианты гена *GCLC* являются значимыми ДНК-маркерами, влияющими на зону инфаркта мозга у больных ишемическим инсультом, ассоциированы с возрастом дебюта первого инсульта, числом перенесенных инсультов и клиническими проявлениями болезни.

Ключевые слова: ишемический инсульт, инфаркт мозга, редокс-гомеостаз, глутатион, глутаматцистеинлигаза, однонуклеотидный полиморфизм

Благодарности: автор выражает благодарность сотрудникам научно-исследовательского института генетической и молекулярной эпидемиологии Курского государственного медицинского университета А. В. Полоникову, Ю. Э. Азаровой, Е. Ю. Клёсовой, М. А. Быкановой и О. Ю. Бушуевой за помощь в выполнении молекулярно-генетических исследований.

Соблюдение этических стандартов: исследование одобрено этическим комитетом Курского государственного медицинского университета (протокол № 5 от 25 июня 2012 г.); все участники подписали добровольное информированное согласие на участие в исследовании.

✉ **Для корреспонденции:** Юлия Александровна Бочарова
ул. Сумская, д. 45а, г. Курск, 305007; y_u_l_i_a_03@mail.ru

Статья получена: 21.01.2021 **Статья принята к печати:** 06.02.2021 **Опубликована онлайн:** 23.02.2021

DOI: 10.24075/vrgmu.2021.007

Cerebrovascular disease or, more specifically, ischemic stroke (IS) is among the leading causes of death and disability in high-income countries [1]. The etiology of IS is multifactorial, i.e. the disease is driven by the complex interplay of genetic and environmental factors [2]. Multiple studies have demonstrated that redox homeostasis disturbances manifesting as an imbalance between the production of reactive oxygen species and their neutralization lie at the core of oxidative stress implicated in IS and the subsequent brain tissue damage [3]. It is a well-known fact that oxidative stress plays a significant role in the pathogenesis of IS, especially in the acute stroke phase [4, 5]. Glutathione is a powerful body antioxidant; disorders of glutathione metabolism often result in disrupted redox homeostasis and oxidative stress, possibly contributing to postischemic brain damage [6, 7]. In patients predisposed to IS, glutathione deficiency might be associated with genetic variation that affects the activity of enzymes involved in glutathione synthesis [8, 9]. Glutamate cysteine ligase is the key

enzyme that catalyzes the first step of glutathione synthesis. It is composed of a catalytic and a modifier subunits encoded by several genes. Their polymorphic variants determine the variability in glutamate cysteine ligase activity and glutathione levels. However, so far no research studies have explored the effects of polymorphisms in glutathione metabolism genes on the extent of ischemic brain damage and the clinical manifestations of stroke. The aim of this study was to investigate the effects of common polymorphic variants of the glutamate cysteine ligase catalytic subunit gene on the extent of brain damage and the clinical manifestations of stroke in patients with IS.

METHODS

The study was carried out in 589 ischemic stroke survivors (330 men and 270 women; mean age 61.1–9.8 years) admitted to Kursk Regional Clinical Hospital between 2007 and 2017. The following inclusion criteria were applied: IS confirmed by clinical examination and imaging tests; Caucasian origin; voluntary informed consent to participate. Patients of non-Caucasian origin, with hemorrhagic stroke or those who did not give voluntary consent to participate were excluded from the study. Of all patients included in the study, 75% were Russian, i.e. at least 2 previous generations of the probands were Russian. IS was confirmed by qualified neurologists of Kursk Regional Clinical Hospital; the diagnosis was based on the neurological examination and imaging tests, including brain CT and MRI scans.

The patients were genotyped for 6 *GCLC* polymorphisms: rs12524494, rs17883901, rs606548, rs636933, rs648595, and rs761142. Candidate SNPs available in the HapMap catalogue were selected using the GenePipe tool [10]. Only those tagSNPs were selected that had at least 5% minor allele frequency and were in linkage disequilibrium with 2 or more SNPs. The functional significance of SNPs was assessed using the FuncPred software (SNPinfo Web Server) [11].

DNA was isolated from the frozen venous blood samples of the participants according to the standard protocol of phenol-chloroform extraction and ethanol precipitation. Molecular-genetic procedures, including SNP genotyping, were carried out at the Research Institute for Genetic and Molecular Epidemiology of Kursk State Medical University in 2016–2017. SNPs genotyping was performed using the iPLEX technology and a MALDI-TOF MassARRAY 4 analyzer (Agena Bioscience; USA).

The associations between the studied SNPs and the clinical manifestations of IS were analyzed by calculating the odds ratio and 95% CI using logistic regression with adjustments for age and sex; the statistical analysis was carried out in SNPStats (Catalan Institute of Oncology; Spain). Effects of the studied SNPs on the size of cerebral lesions measured by MRI and expressed in millimeters, on age at stroke onset and the number of previous cerebrovascular episodes were analyzed in SNPStats. The functional annotation of *GCLC* polymorphisms and the assessment of their regulatory potential from tissue-specific expression were performed using a battery of bioinformatic tools, including GTEx portal [12] and eQTLGen [13]. These databases host genomic and transcriptomic data that can be used to assess the effects of the analyzed SNPs on the levels of *GCLC* expression in the brain, arteries and blood.

RESULTS

The analysis of genotype frequencies revealed that only one *GCLC* polymorphism (rs648595) significantly deviated from the Hardy–Weinberg equilibrium due to a decrease in heterozygosity ($p < 0.05$). In patients with IS, genotype frequencies of the studied *GCLC* polymorphisms were as follows (the numbers represent genotypes homozygous for the reference allele, heterozygous, and homozygous for the minor allele, respectively): 93.5, 5.8, 0.7 (rs12524494); 85.4, 13.7, 1.0 (rs17883901); 93.7, 6.0, 0.3 (rs606548); 63.5, 31.6, 4.8 (rs636933); 16.3, 52.1, 31.6 (rs648595); 57.2, 37.8, 4.9 (rs761142). Clinically, it was interesting to explore the potential involvement of the studied polymorphisms in cerebral infarction growth, necrotic cell death and inflammation due to cerebral artery occlusion, and in some processes related to postischemic repair of damaged tissue. Using linear regression, we analyzed associations between the studied *GCLC* polymorphisms and the size of cerebral lesions (S, mm) in patients with IS. We found that polymorphisms rs636933 and rs761142 were significantly associated with the size of the cerebral lesion in patients with ischemic stroke regardless of their age or sex. Specifically, genotypes G/A-A/A of the rs636933 polymorphism (the dominance effect of SNP) were associated with a statistically significant (by 196.36 mm; $p = 0.009$) increase in the infarction size, in comparison with the wild type (G/G). Genotypes A/C-C/C of the rs761142 polymorphism also had a significant impact ($p = 0.015$) on the size of the lesion: we detected an increase in the lesion size by 173.92 mm in comparison with the A/A genotype (the dominance effect of SNP).

Then, we studied the associations of *GCLC* polymorphisms with the number of IS survived by the patients (Table 1). The participants were divided into two subgroups: group 1 included patients with a history of one stroke, group 2 comprised patients with a past history of 2 or more strokes. We were able to establish statistically significant associations between 2 SNPs and the number of past ischemic strokes. Carriers of the rs12524494-G/G and rs606548-T/T genotypes were at a higher risk of 2 or more IS than carriers of alternative genotypes (see Table 1).

It is known that the early onset of any multifactorial disease may be associated with genetic factors [14]. So, we attempted to investigate whether *GCLC* polymorphisms might affect age at ischemic stroke onset. Using linear regression with adjustments for age and sex, we discovered that rs17883901 was significantly associated with age at IS onset. Polymorphism rs17883901, and more specifically, the G/A genotype, was associated with earlier (56.8 ± 1.65 vs. 60.52 ± 0.42 years) onset of the first IS episode ($p = 0.0038$; see Figure).

Using logistic regression, we analyzed association between GCLC polymorphisms and the clinical manifestations of IS, including motor and sensory impairments. Multiple statistically significant associations were established between *GCLC* polymorphisms and the clinical manifestations of IS. Sensory symptoms were associated with rs636933 (OR = 2.72; 95% CI: 1.01–7.33; p = 0.032). The loss of temperature sensation was associated with rs17883901 (OR = 0.27; 95% CI: 0.09–0.86; $p = 0.006$) and rs12524494 (OR = 2.25; 95% CI: 1.13–4.46; $p = 0.032$). The loss of sense of touch was associated with rs12524494 (OR = 2.51; 95% CI: 1.27–4.99; $p = 0.016$) and rs606548 (OR = 2.36; 95% CI: 1.08–5.16; $p = 0.04$). Facial muscle impairment was associated with rs648595 (OR = 0.53; 95% CI: 0.34–0.81; $p = 0.0029$). Gait disturbances were associated with 3 GCLC SNPs: rs648595 (OR = 1.67; 95% CI: 1.03– 2.71; $p = 0.039$), rs761142 (OR = 1.50; 95% CI: 1.11–2.01; $p = 0.007$) and rs636933 (OR = 1.39; 95% CI: 1.03–1.88; $p = 0.03$). Muscle weakness was associated with rs761142 (OR = 1.46; 95% CI: 1.02–2.10; $p = 0.037$). Diplopia was associated with rs17883901 (OR = 0.12; 95% CI: 0.02–0.88; $p= 0.0028$). Strabismus was associated with 2 different SNPs:

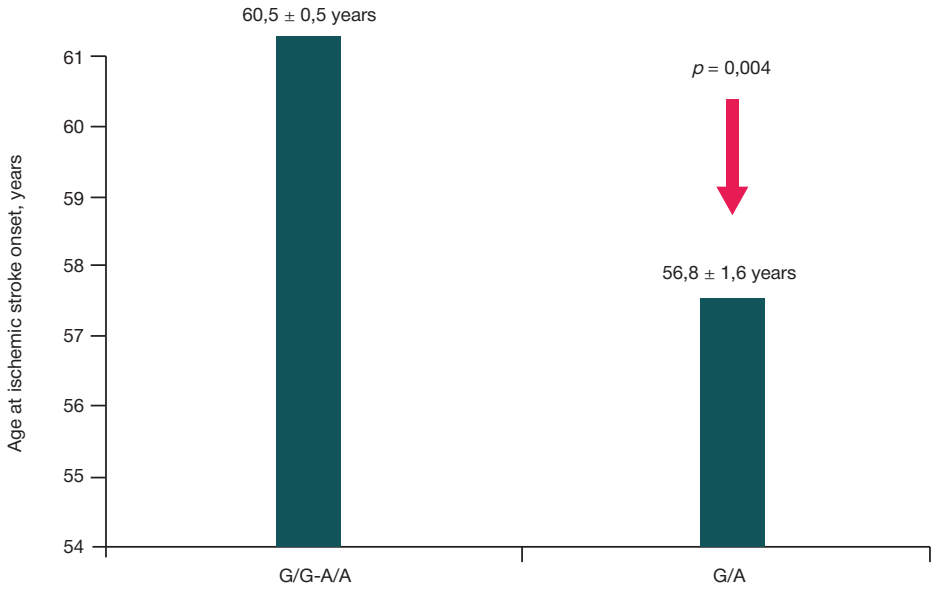

Fig. Associations between the rs17883901 polymorphism of the *GCLC* gene and age at ischemic stroke onset

rs606548 (OR = 7.68; 95% CI: 1.32–44.56; p = 0.04) and rs12524494 (OR = 6.67; 95% CI: 1.23–36.24; p = 0.05). Dysarthria was associated with rs636933 (OR = 0.69; 95% CI: 0.48–0.99; p = 0.04). Vision impairment was associated with rs636933 (OR = 0.61; 95% CI: 0.39–0.94; p = 0.023).

The analysis of genomic and transcriptomic data on the *GCLC* gene extracted from the GTEx database allowed us to establish statistically significant cis-eQTLs (expression Quantitative Trait Loci) linked to changes in the transcriptional activity of *GCLC*. Table 2 illustrates the effects of *GCLC* polymorphisms on the expression of this gene in different brain regions, arteries, and whole blood. We found that the rs648595-G allele was associated with reduced *GCLC* expression in basal ganglia (p = 0.00002), cerebral cortex (p = 0.000001) and blood (p = 1.2 × 10–70). The rs636933-A allele was associated with reduced GCLC in basal ganglia of the brain (p = 0.00005) and blood (p = 2.1 × 10–26). The rs761142-C allele was associated with reduced *GCLC* expression in the blood (p = 5.2 × 10–52), basal ganglia (p = 0.000002) and cerebral cortex (p = 0.000004). However, rs17883901 was not associated with *GCLC* expression in any of the analyzed tissue types involved in the pathogenesis of IS.

DISCUSSION

Our pilot study looked into the effects produced by the polymorphic variants of the gene encoding the key enzyme of glutathione synthesis (the catalytic subunit of glutamate cysteine ligase) on the extent of cerebral damage and the clinical manifestations of IS. The study found that the rs636933 and rs761142 polymorphisms of the *GCLC* gene are important DNA markers associated with the size of the cerebral lesion in patients with IS. Besides, the study demonstrates that rs12524494 and rs606548 are significantly associated with an increase in the frequency of IS episodes in the affected patients. The study shows that polymorphism rs17883901 is significantly associated with earlier onset of the first IS episode. The bioinformatic analysis uncovered the functional significance of some polymorphic loci associated with the studied phenotypes. Notably, the alternative alleles of the studied *GCLC* SNPs have a loss-of-function effect on *GCLC* expression, as revealed by the analysis of genomic and transcriptomic data from the GTEx database; this suggests a possible association between the expansion of the cerebral lesion and the reduced *GCLC* expression in the affected brain region. Thus, the obtained data indicate that the studied polymorphic variants of the glutamate cysteine ligase catalytic subunit gene are important DNA markers determining the size of the ischemic stroke lesion and the clinical manifestations of IS. Indeed, the analysis of possible associations between *GCLC* polymorphisms and the clinical manifestations of ischemic stroke is an important aspect of genetic and epidemiological research and can provide new evidence supporting the pathophysiological implication of the gene in ischemic stroke, thereby allowing researchers to deepen their understanding of molecular mechanisms underlying this pathology [15].

According to the literature, glutathione deficiency in the brain may be indirectly linked to the increased susceptibility of brain tissue to oxidative stress during cerebral artery occlusion. Experiments conducted in astrocyte cultures demonstrated that depletion of the glutathione pool in astrocytes did not affect their viability, at least during the first 24 hours of exposure, but

Table 1. Summary of the associations between GCLC polymorphisms and the number of past ischemic strokes

Gene (SNP ID)	Genotype, allele	*n* (%)		P^1	$_{cor}$OR (95%CI)[2]
		Patients with 1 IS	Patients with 2 or more IS		
GCLC A>G (rs12524494)	A/A-A/G	518 (99.6)	65 (97)	0.05	1.00
	G/G	2 (0.4)	2 (3.0)		7.78 (1.07–56.42)
GCLC C>T (rs606548)	C/C-C/T	470 (100.0)	58 (96.7)	0.003	1.00
	T/T	0 (0.0)	2 (3.3)		40.2 (1.91–847.9)

Note: [1] — indicates the significance of the association with the risk of 2 or more IS adjusted for age and sex; [2] — OR and 95% CI for the associations between the studied SNPs and the risk of 2 or more IS adjusted for age and sex.

Table 2. Effects of *GCLC* polymorphisms on its expression in the brain, arteries and blood (https://www.gtexportal.org)

Ген	Effect. Allele[1]	SNP ID	Whole blood*		Arteries		Basal ganglia		Cerebellum		Cerebral cortex	
			p	*Z*	*p*	*beta*	*p*	*beta*	*p*	*beta*	*p*	*beta*
GCLC	A>**G**	rs12524494	8.5×10^{-18}	–8.59	–	–	–	–	–	–	–	–
GCLC	G>**A**	rs17883901	–	–	–	–	–	–	–	–	–	–
GCLC	C>**T**	rs606548	8.8×10^{-16}	–8.04	–	–	–	–	–	–	–	–
GCLC	G>**A**	rs636933	2.1×10^{-26}	–10.63	–	–	0.00005	–0.25	–	–	–	–
GCLC	T>**G**	rs648595	1.2×10^{-70}	–17.77	–	–	0.00002	–0.24	–	–	0.000001	–0.21
GCLC	A>**C**	rs761142	5.2×10^{-52}	–15.04	–	–	0.000002	–0.27	–	–	0.000004	–0.23

Note: [1] The allele that was analyzed for the possible effect on *GCLC* expression is shown in bold. Significant effects of SNPs on *GCLC* expression ($p \leq 0.05$) are shown in bold. * — *p* — the level of statistical significance and the *Z* — score describing the effects of a given SNP on *GCLC* expression in the blood (eQTLGen, www.eqtlgen.org).

substantially increased their sensitivity to nitrogen or peroxynitrite [7]. *In vivo*, the selective depletion of glutathione develops during focal brain ischemia and persists during reperfusion [7]. The time and degree of glutathione depletion are associated with the risk of tissue infarction. A study established that the lesion size significantly decreased after intracerebroventricular infusions of glutathione monoethyl ester, the compound capable of raising mitochondrial glutathione levels [7]. Glutathione monoethyl ester was experimentally proved to have neuroprotective properties in the setting of focal brain ischemia [16]. Thus, changes in glutathione levels may contribute to the severity of tissue damage in patients with ischemic stroke. It is hypothesized that acrolein (a highly toxic α,β-unsaturated aldehyde) produced in the setting of oxidative cerebral tissue damage is one of the factors contributing to neuronal death linked to the depletion of the reduced intracellular glutathione pool in stroke patients [17].

CONCLUSION

The polymorphic variants rs636933 and rs761142 of the *GCLC* gene are important markers determining the size of cerebral infarction in patients with ischemic stroke. Genotypes rs12524494-G/G and rs606548-T/T are associated with an increase in the frequency of IS episodes; genotype rs17883901-G/A is associated with the early onset of the first IS episode. All SNPs of the *GCLC* gene studied in this work are significantly associated with the clinical manifestations of IS, including motor and sensory impairments, suggesting the involvement of these SNPs in the pathogenesis of IS. The loss-of-function effects of the studied alleles detected by means of bioinformatic analysis may indicate that the enlargement of the lesion area may be associated with reduced *GCLC* expression; glutathione deficiency is an unfavorable factor contributing to the severity of brain damage. Our findings provide rationale for clinical trials of the novel IS management and brain damage prevention strategy based on the intravenous injections of reduced glutathione. This may turn out to be an effective protection against neuronal damage provoked by oxidative stress in the setting of ischemia. Besides, the established clinical and genetic associations open up the possibilities for using DNA markers as a tool for assessing the progression of the pathology, predicting its outcomes and offering personalized treatment and prophylaxis to patients based on their ethnogenetics [18].

References

1. Feigin VL, Lawes CM, Bennett DA, Anderson CS. Stroke epidemiology: a review of population-based studies of incidence, prevalence, and case-fatality in the late 20th century. Lancet Neurol. 2003 Jan; 2 (1): 43–53.
2. Hassan A, Markus HS. Genetics and ischaemic stroke. Brain. 2000 Sep; 123 (Pt 9): 1784–812.
3. Ciancarelli I, Di Massimo C, De Amicis D, Carolei A, Tozzi Ciancarelli MG. Evidence of redox unbalance in post-acute ischemic stroke patients. Curr Neurovasc Res. 2012 May; 9 (2): 85–90.
4. Chehaibi K, Trabelsi I, Mahdouani K, Slimane MN. Correlation of Oxidative Stress Parameters and Inflammatory Markers in Ischemic Stroke Patients. J Stroke Cerebrovasc Dis. 2016 Nov; 25 (11): 2585–93.
5. Juurlink BH, Paterson PG. Review of oxidative stress in brain and spinal cord injury: suggestions for pharmacological and nutritional management strategies. J Spinal Cord Med. 1998 Oct; 21 (4): 309–34.
6. Rodrigo R, Fernández-Gajardo R, Gutiérrez R, Matamala JM, Carrasco R, Miranda-Merchak A, Feuerhake W. Oxidative stress and pathophysiology of ischemic stroke: novel therapeutic opportunities. CNS Neurol Disord Drug Targets. 2013 Aug; 12 (5): 698–714.
7. Sims NR, Nilsson M, Muyderman H. Mitochondrial glutathione: a modulator of brain cell death. J Bioenerg Biomembr. 2004 Aug; 36 (4): 329–33.
8. Bocharova IA. An association study of three polymorphisms in the glutathione synthase (GSS) gene with the risk of ischemic stroke. Research Results in Biomedicine. 2020; 6 (4): 476–87.
9. Bocharova YuA, Azarova YuE, Klesova EYu, Drozdova EL, Solodilova MA, Polonikov AV. Gen gamma-glutamilciklotransferazy — kljuchevogo fermenta katabolizma glutationa i predraspolozhennost' k ishemicheskomu insul'tu: analiz associacij s bolezn'ju i funkcional'noe annotirovanie DNK-polimorfizmov. Medicinskaja genetika. 2020; 19 (10): 32–39. Russian.
10. Bioinformaticheskij instrument GenePipe. Available from: https://snpinfo.niehs.nih.gov/snpinfo/selegene.html.
11. Bioinformaticheskaja programma FuncPred. Available from: https://snpinfo.niehs.nih.gov/snpinfo/snpfunc.html.
12. Bioinformaticheskij instrument GTEx portal. Available from: https://gtexportal.org.
13. Bioinformaticheskij instrument eQTLGen. Available from: www.eqtlgen.org.
14. Ruse CE, Parker SG. Molecular genetics and age-related disease. Age Ageing. 2001 Nov; 30 (6): 449–54.
15. Janssens AC, van Duijn CM. Genome-based prediction of common diseases: advances and prospects. Hum Mol Genet. 2008 Oct 15; 17 (R2): R166–73.
16. Anderson MF, Nilsson M, Eriksson PS, Sims NR. Glutathione monoethyl ester provides neuroprotection in a rat model of stroke. Neurosci Lett. 2004 Jan 9; 354 (2): 163–5.

17. Liu JH, Wang TW, Lin YY, Ho WC, Tsai HC, Chen SP, et al. Acrolein is involved in ischemic stroke-induced neurotoxicity through spermidine/spermine-N1-acetyltransferase activation. Exp Neurol. 2020 Jan; 323: 113066.
18. Mirzaev K, Abdullaev S, Akmalova K, Sozaeva J, Grishina E, Shuev G, et al. Interethnic differences in the prevalence of main cardiovascular pharmacogenetic biomarkers. Pharmacogenomics. 2020; 21 (10): 677–94.

Литература

1. Feigin VL, Lawes CM, Bennett DA, Anderson CS. Stroke epidemiology: a review of population-based studies of incidence, prevalence, and case-fatality in the late 20th century. Lancet Neurol. 2003 Jan; 2 (1): 43–53.
2. Hassan A, Markus HS. Genetics and ischaemic stroke. Brain. 2000 Sep; 123 (Pt 9): 1784–812.
3. Ciancarelli I, Di Massimo C, De Amicis D, Carolei A, Tozzi Ciancarelli MG. Evidence of redox unbalance in post-acute ischemic stroke patients. Curr Neurovasc Res. 2012 May; 9 (2): 85–90.
4. Chehaibi K, Trabelsi I, Mahdouani K, Slimane MN. Correlation of Oxidative Stress Parameters and Inflammatory Markers in Ischemic Stroke Patients. J Stroke Cerebrovasc Dis. 2016 Nov; 25 (11): 2585–93.
5. Juurlink BH, Paterson PG. Review of oxidative stress in brain and spinal cord injury: suggestions for pharmacological and nutritional management strategies. J Spinal Cord Med. 1998 Oct; 21 (4): 309–34.
6. Rodrigo R, Fernández-Gajardo R, Gutiérrez R, Matamala JM, Carrasco R, Miranda-Merchak A, Feuerhake W. Oxidative stress and pathophysiology of ischemic stroke: novel therapeutic opportunities. CNS Neurol Disord Drug Targets. 2013 Aug; 12 (5): 698–714.
7. Sims NR, Nilsson M, Muyderman H. Mitochondrial glutathione: a modulator of brain cell death. J Bioenerg Biomembr. 2004 Aug; 36 (4): 329–33.
8. Bocharova IA. An association study of three polymorphisms in the glutathione synthase (GSS) gene with the risk of ischemic stroke. Research Results in Biomedicine. 2020; 6 (4): 476–87.
9. Бочарова Ю. А., Азарова Ю. Э., Клёсова Е. Ю., Дроздова Е. Л., Солодилова М. А., Полоников А. В. Ген гамма-глутамилциклотрансферазы — ключевого фермента катаболизма глутатиона и предрасположенность к ишемическому инсульту: анализ ассоциаций с болезнью и функциональное аннотирование ДНК-полиморфизмов. Медицинская генетика. 2020; 19 (10): 32–39.
10. Биоинформатический инструмент GenePipe. Доступно по ссылке: https://snpinfo.niehs.nih.gov/snpinfo/selegene.html.
11. Биоинформатическая программа FuncPred. Доступно по ссылке: https://snpinfo.niehs.nih.gov/snpinfo/snpfunc.html.
12. Биоинформатический инструмент GTEx portal. Доступно по ссылке: https://gtexportal.org.
13. Биоинформатический инструмент eQTLGen. Доступно по ссылке: www.eqtlgen.org.
14. Ruse CE, Parker SG. Molecular genetics and age-related disease. Age Ageing. 2001 Nov; 30 (6): 449–54.
15. Janssens AC, van Duijn CM. Genome-based prediction of common diseases: advances and prospects. Hum Mol Genet. 2008 Oct 15; 17 (R2): R166–73.
16. Anderson MF, Nilsson M, Eriksson PS, Sims NR. Glutathione monoethyl ester provides neuroprotection in a rat model of stroke. Neurosci Lett. 2004 Jan 9; 354 (2): 163–5.
17. Liu JH, Wang TW, Lin YY, Ho WC, Tsai HC, Chen SP, et al. Acrolein is involved in ischemic stroke-induced neurotoxicity through spermidine/spermine-N1-acetyltransferase activation. Exp Neurol. 2020 Jan; 323: 113066.
18. Mirzaev K, Abdullaev S, Akmalova K, Sozaeva J, Grishina E, Shuev G, et al. Interethnic differences in the prevalence of main cardiovascular pharmacogenetic biomarkers. Pharmacogenomics. 2020; 21 (10): 677–94.

CHARACTERISTICS OF *BRCA*-ASSOCIATED BREAST CANCER IN THE POPULATION OF THE RUSSIAN FEDERATION

Novikova EI ✉, Kudinova EA, Bozhenko VK, Solodkiy VA

Federal State Budgetary Institution Russian Scientific Center of Roentgenoradiology (RSCR) of the Ministry of Healthcare of the Russian Federation, Moscow

"Standard" diagnostic panels allow identification of only a few of *BRCA1* and *BRCA2* gene mutations most common in a population. Therefore, tests relying on such panels may return false negative results, since the coding regions of these genes may have other defects. For breast cancer (BC) patients, false negative test results may translate into selection of inadequate therapy by their doctors. This study aimed to identify the features of *BRCA*-associated breast cancer in the population of the Russian Federation. The study included breast cancer patients (n = 4440). At the first stage, all patients were screened for the eight most common *BRCA1* and *BRCA2* genes mutations with the help of real-time PCR. Next, patients that exhibited clinical signs of a hereditary disease (CSHD) in the absence of common mutations (n = 290) had the entire coding regions of *BRCA1* and *BRCA2* genes studied with next generation sequencing (NGS). "Standard" mutations in the *BRCA1* and *BRCA2* genes were identified in 169 (3.8%) cases. In the CSHD group, such mutations were revealed in 15.4% of cases. NGS uncovered 33 rare pathogenic *BRCA1* and *BRCA2* gene mutations in 40 out of 290 breast cancer patients (13.8%). It was concluded that among the residents of the Russian Federation, the range of pathogenic variants of *BRCA*-associated breast cancer is wide, and it stretches beyond the mutations considered by the "standard" diagnostic panels. Analysis of the entire coding regions of *BRCA1* and *BRCA2* genes allows increasing efficiency of detection of germline mutations in breast cancer patients at least twofold.

Keywords: *BRCA1* and *BRCA2* mutations, next-generation sequencing, NGS, hereditary breast cancer

Author contribution: Novikova EI — collection of clinical material, conducting molecular genetic studies, analysis and statistical processing of the results, preparation and writing of the article; Kudinova EA — analysis of literature, analysis of the research results; Bozhenko VK — analysis of the results, article text editing; Solodkiy VA — planning and analysis of the research results, article test editing.

Compliance with ethical standards: the study was approved by the ethics committee of the RSCR (minutes #3 of March 27, 2020); all patients included in the study signed a voluntary informed consent.

✉ **Correspondence should be addressed:** Ekaterina I. Novikova
Profsoyuznaya, 86, Moscow, 117997; e.novikova.rncrr@mail.ru

Received: 02.01.2021 **Accepted:** 15.02.2021 **Published online:** 22.02.2021

DOI: 10.24075/brsmu.2021.006

ХАРАКТЕРИСТИКА *BRCA*-АССОЦИИРОВАННОГО РАКА МОЛОЧНОЙ ЖЕЛЕЗЫ В РОССИЙСКОЙ ПОПУЛЯЦИИ

Е. И. Новикова ✉, Е. А. Кудинова, В. К. Боженко, В. А. Солодкий

Российский научный центр рентгенорадиологии, Москва, Россия

Использование «стандартных» диагностических панелей, дающих возможность определять лишь несколько наиболее распространенных в популяции мутаций в генах *BRCA1* и *BRCA2*, может приводить к появлению ложноотрицательных результатов из-за наличия других повреждений в кодирующих областях данных генов, что, в свою очередь, может привести к неадекватному выбору тактики лечения у больных раком молочной железы (РМЖ). Целью работы было выявить особенности *BRCA*-ассоциированного рака молочной железы в российской популяции. В исследование вошли пациенты с диагнозом РМЖ (n = 4440). На первом этапе методом ПЦР в реальном времени проведено скрининговое исследование всех пациентов на наличие восьми наиболее распространенных мутаций в генах *BRCA1* и *BRCA2*. Далее при наличии у пациентов клинических признаков наследственного заболевания (КПНЗ) и отсутствии распространенных мутаций (n = 290) проводили исследование всей кодирующей части генов *BRCA1* и *BRCA2* методом секвенирования нового поколения (NGS). В 169 случаях (3,8%) были выявлены «стандартные» мутации в генах *BRCA1* и *BRCA2*. В группе пациентов с КПНЗ частота выявленных «стандартных» мутаций составила 15,4%. Методом NGS у 40 из 290 больных РМЖ (13,8%) были обнаружены 33 редкие патогенные мутации в генах *BRCA1* и *BRCA2*. Сделан вывод, что *BRCA*-ассоциированный РМЖ в российской популяции характеризуется широким спектром патогенных вариантов, который не ограничен мутациями, включенными в «стандартные» клинико-диагностические панели. Анализ всей кодирующей части генов *BRCA1* и *BRCA2* позволяет повысить эффективность выявления герминальных мутаций у больных РМЖ по крайней мере в 2 раза.

Ключевые слова: мутации в генах *BRCA1* и *BRCA2*, секвенирование нового поколения, NGS, наследственный рак молочной железы

Вклад авторов: Е. И. Новикова — сбор клинического материала, проведение молекулярно-генетических исследований, анализ и статистическая обработка результатов, подготовка и написание текста статьи; Е. А. Кудинова — анализ литературы, анализ результатов исследования; В. К. Боженко — анализ результатов, редактирование текста статьи; В. А. Солодкий — планирование и анализ результатов исследования, редактирование текста статьи.

Соблюдение этических стандартов: исследование одобрено этическим комитетом РНЦРР (протокол № 3 от 27 марта 2020 г.); все пациенты, включенные в исследование, подписали добровольное информированное согласие на его проведение.

✉ **Для корреспонденции:** Екатерина Ивановна Новикова
ул. Профсоюзная, д. 86, г. Москва, 117997; e.novikova.rncrr@mail.ru

Статья получена: 02.01.2021 **Статья принята к печати:** 15.02.2021 **Опубликована онлайн:** 22.02.2021

DOI: 10.24075/vrgmu.2021.006

Hormonal status and genetic predisposition are the key factors influencing breast cancer (BC) development [1].

In up to 90–95% of BC patients, the cancer is sporadic, non-hereditary by nature. Its hereditary forms, which are characterized by various mutations in genes *BRCA1*, *BRCA2*, *CHEK2*, *NBN*, ATM, PALB2 etc. [2, 3], are diagnosed in 5–10% of BC patients [2].

The most common hereditary reasons behind BC are *BRCA1* and *BRCA2* gene mutations. These genes encode proteins that enable double-strand DNA break repairs, control

cell cycle, regulate transcription and apoptosis, maintain genomic stability [4]. Damage to these genes increases the likelihood of development of cancer, with the majority of such progressions registered in young patients [5, 6]. The mutations registered in genes *BRCA1* and *BRCA2* largely determine the choice of therapy and preventive measures [7].

The current approach to diagnosing hereditary forms of BC adopted in the Russian Federation implies using "standard" diagnostic panels that, relying on PCR, make detection of the *BRCA1* and *BRCA2* gene mutations most common in our population quick and relatively inexpensive [8]. However, a number of studies points to other clinically significant mutations that cannot be detected with the "standard" panel but increase the risk of cancer development. Therefore, their presence requires a specialized approach in the treatment and prevention of diseases [9].

This research effort aimed to study the features of *BRCA*-associated breast cancer in the population of the Russian Federation.

METHODS

The study included 4440 patients who underwent examination and treatment at the Russian Scientific Center of Roentgenoradiology from 2010 to 2019. The inclusion criteria were: any age; diagnosed BC. The exclusion criterion was patient's refusal to participate in the study. The age of cancer onset varied from 20 to 90 years (Table 1). Samples of the tumors of all patients were subjected to histological examination and immunohistochemical analysis (IHC). Compiling the patients' medical histories, we paid special attention to the signals of possible hereditary nature of the disease.

Based on the medical histories and following recommendations of the US National Comprehensive Cancer Network (NCCN) [7], we formed a high-risk group exhibiting clinical signs of hereditary disease (CSHD). The group included 1026 breast cancer patients aged 20–90 years. The patient was added to the high-risk group if she had at least one CSHD: disease manifestation at any age under 50, multiple primary tumors (BC and/or ovarian cancer (OC)), cancer in the family history (BC and/or OC in first- and/or second-degree relatives), triple negative molecular subtype of the tumor.

At the first stage of the study, we employed real-time PCR (RT PCR) in search of the *BRCA1* and *BRCA2* mutations most common in the Russian Federation: 185delAG, 4153delA, 5382insC, 3819delGTAAA, 3875delGTCT, 300T>G, 2080delA (*BRCA1*) and 6174delT (*BRCA2*). All 4440 patients participating in the study were examined. For DNA isolation, we used the M-Sorb kits (Syntol; Russia). OncoGenetics BRCA reagent panel (DNA-Technology; Russia), which includes specific primers for detection of the eight studied mutations, was used to carry out RT PCR.

At the second stage, we examined 290 patients from the high-risk BC development group that had no "standard" mutations detected at the first stage of the study. The entire coding regions of their *BRCA1* and *BRCA2* genes were analyzed using next generation sequencing (NGS).

Using QIAamp DNA Blood Mini Kit reagents (Qiagen; Germany) and relying on the protocol suggested by the manufacturer, we isolated genomic DNA from peripheral blood. The minimal acceptable DNA concentration was 10 ng/μL. TruSight Cancer panel (Illumina; USA) and TruSight Rapid Capture reagent kit (Illumina; USA) allowed us to prepare the sequencing libraries. We followed manufacturer's instructions and used the selective DNA region capture method.

The prepared libraries were pair-end sequenced (2 × 151 base pairs) on a MiSeq system (Illumina; USA) using MiSeq Reagent Kits v2 (Illumina; USA). The average coverage of the target DNA regions was 100× and over.

The sequencing data were processed with the help of the standard MiSeq Reporter v2.5 (Illumina; USA) software. In some samples, the regions studied presented genetic abnormalities. To increase accuracy, we excluded poor quality sequencing reads from the analysis. Variant Studio 2.2 (Illumina; USA) software was used to annotate and classify the identified sequence variants.

Assessing the clinical significance of the genetic abnormalities identified, we relied on the sequence variant pathogenicity criteria suggested by the American College of Medical Genetics and Genomics (ACMG) [10] taking into account information published in accessible databases: dbSNP (The Single Nucleotide Polymorphism database), ClinVar (Clinical Variation), HGMD (Human Gene Mutation Database), BIC (Breast Cancer Information Core), OMIM (Online Mendelian Inheritance in Man), ExAC (Exome Aggregation Consortium), 1000G (1000 Genomes Project) and CADD (Combined Annotation Dependent Depletion), PolyPhen (Polymorphism Phenotyping) and Sift (Sorting Intolerant from Tolerant). We did not consider sequence variants that have no clinical significance, as well as those of unknown clinical significance.

The identified nucleotide sequence changes were verified with the help of the Sanger sequencing method. The analysis was enabled by the ABI PRISM 3100 automated capillary electrophoresis system (Applied Biosystems; USA).

RESULTS

Out of the total sample of RT PCR-diagnosed BC patients (n = 4440), 169 people (3.8%) had *BRCA1* and *BRCA2* gene mutations detectable with the "standard" diagnostic panels (Table 2). In the CSHD group, the share of patients with such "standard" gene mutations was 4 times higher: the analysis put it at 15.4%. The most common mutation was 5382insC in the *BRCA1* gene. In the overall sample, this variant was detected in 2.9% of patients, while for the high-risk CSHD group this figure was 11.5%, i.e., every 9th patient had the said mutation. Among the identified "standard" mutations, the 5382insC variant was found in 75% of cases. The remaining genetic variants included in the "standard" diagnostic panel were detected at least an order of magnitude less frequently (Table 2).

Next generation sequencing of the entire coding regions, as well as the *BRCA1* and *BRCA2* splicing regions, revealed 33 clinically significant variants in 40 out of 290 (13.8%) BC patients from the high-risk group. In 18 cases, the abnormalities were in the *BRCA1* gene: nine variants of nonsense mutations, three variants of frameshift deletions, and two abnormalities in splice sites. *BRCA2* pathogenic sequence variants were found in 22 patients; there were seven nonsense mutations, eight variants of frameshift deletions and insertions, and two splice site abnormalities (Table 3).

Among the identified genetic disorders, the most common abnormal nucleotide sequence change was the c.3607C>T mutation in *BRCA1* (7.5% of cases, three patients). The following pathogenic mutations were detected in approximately 5% of cases: c.4689C>G and c.5224C>T in *BRCA1*, c.1301_1304delAAAG, c.9089_9090insA and c.3283C>T in *BRCA2*.

With the exception of mutation 5382insC in *BRCA1*, the frequency of occurrence of each pathogenic variant detected through NGS is comparable to the frequency of "standard"

Table 1. Clinical characteristics of the examined BC patients group

Characteristic	BC patients (n = 4440)
Age	
Average age of disease manifestation, years	52 (20–90)
Under 50 y.o., people (%)	1332 (30)
51 y.o. and older, people (%)	3108 (70)
Family cancer history	
Yes, people (%)	533 (12)
No, people (%)	3907 (88)
Diagnosis	
PMMN (BC/BC or BC/OC), people (%)	313 (7)
BC, people (%)	4127 (93)
Molecular subtype of tumor	
ER(+) and/or PR(+)Her2(-), people (%)	2930 (66)
ER(+) and/or PR(+)Her2(+), people (%)	888 (20)
ER(-)PR(-)Her2(+), people (%)	222 (5)
ER(-)PR(-)Her2(-), people (%)	400 (9)
Histological type of tumor	
Infiltrating ductal carcinoma, people (%)	3330 (75)
Invasive lobular carcinoma, people (%)	577 (13)
Other, people (%)	533 (12)

Note: PMMN — primary multiple malignant neoplasms.

BRCA1 and *BRCA2* gene mutations, with the difference insignificant ($p > 0.05$).

Taking into account the available information on the features of *BRCA*-associated breast cancer, we analyzed some clinical characteristics of the patients that carried *BRCA1* and *BRCA2* gene mutations, and studied morphological features of their tumor samples (Table 4). In 94% of patients with *BRCA1*-associated breast cancer and in all patients with *BRCA2*-associated breast cancer, we detected at least one hereditary disease sign (age under 50, cancer in family history, primary multiple tumors, triple negative molecular subtype of the tumor). Six percent of the patients exhibited no clinical signs of a hereditary disease.

Comparison of the groups of patients with identified *BRCA1* and *BRCA2* gene mutations showed that in the *BRCA1*-associated BC group, the average disease manifestation age was 42 years (20–82 years), and in the *BRCA2*-associated BC group the onset of the disease was registered at 44, on average (25–79 years old). Moreover, 87% of the *BRCA2*-associated BC group patients had the cancer diagnosed when they were under 50, and in the *BRCA1*-associated BC group this figure was 81%.

Over half of gene mutation carriers (63% with abnormal BRCA1 and 74% with mutations in *BRCA2*) mentioned having blood relatives with BC/OC. In both *BRCA1*-associated and *BRCA2*-associated BC groups the frequency of detection of primary multiple malignant neoplasms was rather high (22% and 30% of cases, respectively) (Table 4).

The examination revealed that the majority of both *BRCA1*- (91%) and *BRCA2*-associated tumors (61%) were infiltrating ductal carcinomas (Table 4). However, upon comparison of the groups it was found that the carriers of *BRCA1* gene mutations had the said type of cancer in 91% of cases, while those with mutations in *BRCA2* — only in 61% (p = 0.0003). For *BRCA2*-associated tumors, on the contrary, there was a predominance of invasive lobular breast cancer (30%) compared with *BRCA1*-associated tumors (5%) (p = 0.0005).

The current classification of molecular subtypes of BC relies on the IHC-enabled detection of expression levels of estrogen (ER), progesterone (PR) and epidermal growth factor (Her2) receptors. These indicators, scored in points, allow classifying the cancer as one of the molecular subtypes, which, in turn, largely determines the disease therapy and prognosis. In the context of this study, we detected triple negative breast cancer

Table 2. Frequency of occurrence of *BRCA1* and *BRCA2* gene mutations most common in the population (BC patients)

Gene	Mutation name (BIC classification)	Number of mutation carriers in the examined group, people	Mutation frequency, %	Number of mutation carriers in the CSHD group, people	Mutation frequency, %
BRCA1	5382insC	127	2.9	118	11.5
BRCA1	4153delA	5	0.1	4	0.4
BRCA1	300T>G	10	0.2	10	1.0
BRCA1	2080delA	8	0.2	8	0.8
BRCA1	185delAG	10	0.2	9	0.9
BRCA1	3819delGTAAA	8	0.2	8	0.8
BRCA1	3875delGTCT	–	–	–	–
BRCA2	6174delT	1	0.02	1	0.1
Total		169	3.8	158	15.4

Table 3. Characteristics and frequency of rare pathogenic *BRCA1* and *BRCA2* sequence variants, CSHD BC patients group

Gene	Genetic variant name (HGVS classification)	Identification number (dbSNP)	Variant characteristic	Number of patients, people
BRCA1	c.4327C>T (p.Arg1443Ter)	rs41293455	nonsense mutation	1
BRCA1	c.4689C>G (p.Tyr1563Ter)	rs80357433	nonsense mutation	2
BRCA1	c.5531-1G>A	rs80358048	splicing site mutation	1
BRCA1	c.3607C>T (p.Arg1203Ter)	rs62625308	nonsense mutation	3
BRCA1	c.5224C>T (p.Gln1721Ter)	rs878854957	nonsense mutation	2
BRCA1	c.4258C>T (p.Gln1420Ter)	rs80357305	nonsense mutation	1
BRCA1	c.1687C>T (p.Gln563Ter)	rs80356898	nonsense mutation	1
BRCA1	c.4165_4166delAG (p.Ser1389Terfs)	rs80357572	frameshift deletion	1
BRCA1	c.3257T>G (p.Leu1086Ter)	rs80357006	nonsense mutation	1
BRCA1	c.5152+1G>T	rs80358094	splicing site mutation	1
BRCA1	c.1510delC (p.Arg504Valfs)	rs80357908	frameshift deletion	1
BRCA1	c.83_84delTG (p.Leu28Argfs)	rs80357728	frameshift deletion	1
BRCA1	c.5314C>T (p.Arg1772Ter)	rs80357123	nonsense mutation	1
BRCA1	c.763G>T (p.Glu255Ter)	rs80357009	nonsense mutation	1
BRCA2	8002A>T (p.Arg2668Ter)	rs276174900	nonsense mutation	1
BRCA2	6070C>T (p.Gln2024Ter)	rs80358844	nonsense mutation	1
BRCA2	c.6997_6998insT (p.Pro2334Thrfs)	rs754611265	frameshift deletion	1
BRCA2	c.3748_3749insA (p.Thr1251Asnfs)	rs397507683	frameshift deletion	1
BRCA2	c.5718_5719delCT (p.Leu1908Argfs)	rs80359530	frameshift deletion	1
BRCA2	c.1301_1304delAAAG (p.Lys437Ilefs)	rs80359277	frameshift deletion	2
BRCA2	c.9117G>A (p.Pro3039=)	rs28897756	splicing site mutation	1
BRCA2	c.9089_9090insA (p.Thr3033Asnfs)	rs397507419	frameshift deletion	2
BRCA2	c.632-1G>A	rs81002820	splicing site mutation	1
BRCA2	c.4111C>T (p.Gln1371Ter)	rs80358659	nonsense mutation	1
BRCA2	c.7254_7255delAG (p.Arg2418Serfs)	rs80359644	frameshift deletion	1
BRCA2	c.3881T>A (p.Leu1294Ter)	rs80358632	nonsense mutation	1
BRCA2	c.8909G>A (p.Trp2970Ter)	–	nonsense mutation	1
BRCA2	c.8168A>G (p.Asp2723Gly)	rs41293513	nonsense mutation	1
BRCA2	c.5633delA (p.Asn1878ThrfsTer31)	–	frameshift deletion	1
BRCA2	c.7007G>A (p.Arg2336His)	rs28897743	missense mutation	1
BRCA2	c.658_659delGT (p.Val220Ilefs)	rs80359604	frameshift deletion	1
BRCA2	c.3283C>T (p.Gln1095Ter)	rs397507662	nonsense mutation	2
BRCA2	c.8437G>T (p.Gly2813Ter)	–	nonsense mutation	1

(TNBC) in 29% of cases (54 patients) in the *BRCA1*-associated BC group, while for the *BRCA2*-associated BC group the same figure was only 4% (1 patient). We have also established that almost all *BRCA2*-associated tumors (96%) were of the luminal subtype and were characterized by the expression of estrogen (ER) and progesterone (PR) receptors (Table 4).

DISCUSSION

The results of this study are consistent with the data of previously published works. We confirmed that in the population of the Russian Federation, *BRCA1* and *BRCA2* gene mutations are rather frequent, with the most common of them being 5382insC in *BRCA1*, which is found an order of magnitude more often than other mutations in these genes [2, 3, 8]. This fact confirms the assumption that this sequence variant is of Slavic origin [2].

Among the rare pathogenic mutations detected with NGS, the most common sequence variant was the c.3607C>T mutation in the *BRCA1* gene. This genetic variant was described previously; it is associated with a high risk of development of both BC and OC [11, 12].

The analysis of international and Russian publications and databases showed that only a few of the identified rare sequence variants were covered in the Russian studies. The c.3607C>T mutation in the *BRCA1* gene was described in a BC patient from St. Petersburg whose family history included cancer patients [13]. The *BRCA1* gene mutations c.5224C>T and c.5314C>T were found in the Tatar population in patients with hereditary BC and OC [14]. Mutations c.4689C>G, c.5152+1G>T in *BRCA1* and mutations c.6997_6998insT, c.7254_7255delAG and c.658_659delGT in *BRCA2* were detected in residents of Siberia and the Far East with hereditary BC and OC [15]. The remaining variants, detected with the help of NGS, were described in foreign publications and databases only.

The results of this study confirm that BC patients with mutations in the *BRCA1* and *BRCA2* genes often exhibit CSHD, including: disease manifestation at any age under 50,

Table 4. Comparison of *BRCA1*- and *BRCA2*-associated BC, main clinical and morphological characteristics

Characteristic	*BRCA1*-associated BC (*n* = 187)	*BRCA2*-associated BC (*n* = 23)
Age		
Average age of disease manifestation, years	42 (20–82)	44 (25–79)
Under 50 y.o., people (%)	152 (81)	20 (87)
51 y.o. and older, people (%)	35 (19)	3 (13)
Family cancer history		
Yes, people (%)	118 (63)	17 (74)
No, people (%)	69 (37)	6 (26)
Diagnosis		
PMMN (BC/BC or BC/OC), people (%)	41 (22)	7 (30)
BC, people (%)	146 (78)	16 (70)
Molecular subtype of tumor		
ER(+) and/or PR(+)Her2(-), people (%)	122 (65)	22 (96)*
ER(+) and/or PR(+)Her2(+), people (%)	9 (5)	0
ER(-)PR(-)Her2(+), people (%)	2 (1)	0
ER(-)PR(-)Her2(-), people (%)	54 (29)	1 (4)*
Histological type of tumor		
Infiltrating ductal carcinoma, people (%)	171 (91)	14 (61)*
Invasive lobular carcinoma, people (%)	9 (5)	7 (30)*
Other, people (%)	7 (4)	2 (9)
Presence of clinical signs of hereditary BC		
With clinical signs of the disease, people (%)	176 (94)	23 (100)
Without clinical signs of the disease, people (%)	11 (6)	0

Note: * — significant differences with the *BRCA1*-associated BC group ($p < 0.05$); PMMN — primary multiple malignant neoplasms.

multiple primary tumors (BC and/or OC), cancer in the family history (BC and/or OC in first- and/or second-degree relatives), triple negative molecular subtype of the tumor. The absence of CSHD in 6% of patients with mutations in the *BRCA1* may be associated with their unawareness of cancer cases in the family history or development of such mutations *de novo*.

In conformity with the previously published papers, we found that the average age of cancer onset in the *BRCA2*-associated BC group is 44, which is older than the average onset age registered in the *BRCA1*-associated BC group (42). According to the results of the combined study that merged the analysis of pathomorphological characteristics of tumors and clinical data of 3797 carriers *BRCA1* gene mutations and 2392 patients with abnormal *BRCA2* genes, the median age of disease manifestation for the *BRCA1*-associated BC group was 40, for the *BRCA2*-associated BC group — 43 [16].

The data obtained in this study confirm that the majority of *BRCA*-associated tumors are infiltrating ductal carcinomas, but among the *BRCA2*-associated tumors, invasive lobular breast cancer predominates, compared with *BRCA1*-associated tumors [16].

We have shown that in carriers of the *BRCA1* gene mutations (compared to BC patients with this gene undamaged), the tumor is most often characterized by the absence of expression of the estrogen (ER), progesterone (PR) and epidermal growth factor (Her2) receptors, which makes it TNBC [16, 17]. Overall, TNBC was diagnosed in 29% of cases in the *BRCA1*-associated BC group, which is significantly different from the frequency of TNBC recorded in the *BRCA2*-associated BC group. In context of this study, almost all *BRCA2*-associated tumors (96%) belonged to the luminal subtype and were characterized by expression of estrogen (ER) and progesterone (PR) receptors, which is also characteristic of sporadic BC [18].

CONCLUSION

Thus, among the residents of the Russian Federation, the range of pathogenic variants of *BRCA*-associated breast cancer is wide, and it stretches beyond the mutations considered by the "standard" diagnostic panels designed for primary screening. The results of this study highlight the need for analysis of the entire coding regions of *BRCA1* and *BRCA2* genes, which would allow increasing efficiency of detection of germline mutations in BC patients at least twofold. Due to the certain clinical and morphological features of *BRCA*-associated breast cancer, such analysis should be prescribed, first of all, for patients in whom the disease manifested at the age under 50 years, whose blood relatives have tumors in their histories (BC and OC), and who have primary multiple malignant neoplasms (BC and BC and/or OC) and triple negative molecular subtype of the tumor.

References

1. Souhami RL, Tobajas Dzh. Rak i ego lechenie. M.: Binom. Laboratorija znanij, 2014; 440 s. Russian.
2. Imyanitov EN. Nasledstvennyj rak molochnoj zhelezy. Prakticheskaja Onkologija. 2010; 11 (4): 258–66. Russian.
3. Bit-Sava EM. Molekuljarno-biologicheskoe obosnovanie lechenija BRCA1/SNEK2/BLM-associirovannogo i sporadicheskogo raka molochnoj zhelezy [dissertacija]. S-P., 2015; 237 s. Russian.
4. Gudmundsdottir K, Ashworth A. The roles of BRCA1 and BRCA2

and associated proteins in the maintenance of genomic stability. Oncogene. 2006; 25 (43): 5864–74.
5. Antoniou A, Pharoah PDP, Narod S, Risch HA, Eyfjord JE, Hopperet JL, et al. Average risks of breast and ovarian cancer associated with BRCA1 or BRCA2 mutations detected in case series unselected for family history: a combined analysis of 22 studies. Am J Hum Genet. 2003; 72: 1117–30.
6. Mavaddat N, Peock S, Frost D, Ellis S, Platte R, Fineberg E, et al. Cancer risks for BRCA1 and BRCA2 mutation carriers: results from prospective analysis of EMBRACE. J Natl Cancer Inst. 2013; 105: 812–22.
7. Daly MB, Pilarski R, Berry M, Buys SS, Farmer M, Friedman S, et al. NCCN Guidelines Insights: Genetic/Familial High-Risk Assessment: Breast and Ovarian, Version 2.2017. J Natl Compr Canc Netw. 2017; 15 (1): 9–20.
8. Bateneva EI. Novaja diagnosticheskaja panel' dlja vyjavlenija nasledstvennoj predraspolozhennosti k razvitiju raka molochnoj zhelezy i raka jaichnikov [dissertacija]. M., 2015; 125 c. Russian.
9. Novikova EI, Snigireva GP, Solodkij VA. Redkie mutacii v genah BRCA1 i BRCA2 u rossijskih bol'nyh rakom molochnoj zhelezy. Medicinskaja genetika. 2017; 16 (9): 25–30. Russian.
10. Richards S, Aziz N, Bale S, Bick D, Das S, Gastier-Foster J, et al. Standards and guidelines for the interpretation of sequence variants: a joint consensus recommendation of the American College of Medical Genetics and Genomics and the Association for Molecular Pathology. Genet Med. 2015; 17 (5): 405–24.
11. Friedman LS, Ostermeyer EA, Szabo CI, Dowd P, Lynch ED, Rowell SE, et al. Confirmation of BRCA1 by analysis of germline mutations linked to breast and ovarian cancer in ten families. Nat Genet. 1994; 8: 399–404.
12. Manguoglu AE, Lüleci G, Ozçelik T, Colak T, Schayek H, Akaydinet M, et al. Germline mutations in the BRCA1 and BRCA2 genes in Turkish breast/ovarian cancer patients. 2003; 21 (4): 444–5.
13. Grudinina NA, Golubkov VI, Tihomirova OS, i dr. Preobladanie shiroko rasprostranennyh mutacij v gene BRCA1 u bol'nyh semejnymi formami raka molochnoj zhelezy Sankt-Peterburga. Genetika. 2005; 41: 405–10. Russian.
14. Brovkina OI, Gordiev MG, Enikeev RF, Druzhkov MO, Shigapova LH, Shagimardanova EI, i dr. Geny sistemy reparacii: populjacionnye razlichija nasledstvennyh tipov raka jaichnikov i molochnoj zhelezy, vyjavljaemye metodom sekvenirovanija novogo pokolenija. Opuholi zhenskoj reproduktivnoj sistemy. 2017; 3 (13): 61–67. Russian.
15. Kechin AA. Razrabotka i primenenie metoda opredelenija mutacij v genah BRCA1 i BRCA2 u bol'nyh rakom molochnoj zhelezy i rakom jaichnikov [dissertacija]. N., 2018; 118 c. Russian.
16. Mavaddat N, Barrowdale D, Andrulis IL, Domchek SM, Eccles D, Nevanlinna H, et al. Pathology of breast and ovarian cancers among BRCA1 and BRCA2 mutation carriers: results from the Consortium of Investigators of Modifiers of BRCA1/2 (CIMBA). Cancer Epidemiol Biomarkers Prev. 2012; 21 (1): 134–47.
17. Ljubchenko LN, Bateneva EI, Abramov IS, Emelyanova MA, Budik YuA, Tjuljandina AS, i dr. Nasledstvennyj rak molochnoj zhelezy i jaichnikov. Zlokachestvennye opuholi. 2013; (2): 53–61.
18. Lakhani SR, Van De Vijver MJ, Jocelyne Jacquemier J, Anderson TJ, Osin PP, McGuffoget L, et al. The pathology of familial breast cancer: predictive value of immunohistochemical markers estrogen receptor, progesterone receptor, HER-2, and p53 in patients with mutations in BRCA1 and BRCA2. J Clin Oncol. 2002. 20 (9): 2310–8.

Литература

1. Соухами Р. Л., Тобайас Дж. Рак и его лечение. М.: Бином. Лаборатория знаний, 2014; 440 с.
2. Имянитов Е. Н. Наследственный рак молочной железы. Практическая Онкология. 2010; 11 (4): 258–66.
3. Бит-Сава Е. М. Молекулярно-биологическое обоснование лечения BRCA1/CHEK2/BLM-ассоциированного и спорадического рака молочной железы [диссертация]. С-П., 2015; 237 с.
4. Gudmundsdottir K, Ashworth A. The roles of BRCA1 and BRCA2 and associated proteins in the maintenance of genomic stability. Oncogene. 2006; 25 (43): 5864–74.
5. Antoniou A, Pharoah PDP, Narod S, Risch HA, Eyfjord JE, Hopperet JL, et al. Average risks of breast and ovarian cancer associated with BRCA1 or BRCA2 mutations detected in case series unselected for family history: a combined analysis of 22 studies. Am J Hum Genet. 2003; 72: 1117–30.
6. Mavaddat N, Peock S, Frost D, Ellis S, Platte R, Fineberg E, et al. Cancer risks for BRCA1 and BRCA2 mutation carriers: results from prospective analysis of EMBRACE. J Natl Cancer Inst. 2013; 105: 812–22.
7. Daly MB, Pilarski R, Berry M, Buys SS, Farmer M, Friedman S, et al. NCCN Guidelines Insights: Genetic/Familial High-Risk Assessment: Breast and Ovarian, Version 2.2017. J Natl Compr Canc Netw. 2017; 15 (1): 9–20.
8. Батенева Е. И. Новая диагностическая панель для выявления наследственной предрасположенности к развитию рака молочной железы и рака яичников [диссертация]. М., 2015; 125 с.
9. Новикова Е. И., Снигирева Г. П., Солодкий В. А. Редкие мутации в генах BRCA1 и BRCA2 у российских больных раком молочной железы. Медицинская генетика. 2017; 16 (9): 25–30.
10. Richards S, Aziz N, Bale S, Bick D, Das S, Gastier-Foster J, et al. Standards and guidelines for the interpretation of sequence variants: a joint consensus recommendation of the American College of Medical Genetics and Genomics and the Association for Molecular Pathology. Genet Med. 2015; 17 (5): 405–24.
11. Friedman LS, Ostermeyer EA, Szabo CI, Dowd P, Lynch ED, Rowell SE, et al. Confirmation of BRCA1 by analysis of germline mutations linked to breast and ovarian cancer in ten families. Nat Genet. 1994; 8: 399–404.
12. Manguoglu AE, Lüleci G, Ozçelik T, Colak T, Schayek H, Akaydinet M, et al. Germline mutations in the BRCA1 and BRCA2 genes in Turkish breast/ovarian cancer patients. 2003; 21 (4): 444–5.
13. Грудинина Н. А., Голубков В. И., Тихомирова О. С. и др. Преобладание широко распространенных мутаций в гене BRCA1 у больных семейными формами рака молочной железы Санкт-Петербурга. Генетика. 2005; 41: 405–10.
14. Бровкина О. И., Гордиев М. Г., Еникеев Р. Ф., Дружков М. О., Шигапова Л. Х., Шагимарданова Е. И. и др. Гены системы репарации: популяционные различия наследственных типов рака яичников и молочной железы, выявляемые методом секвенирования нового поколения. Опухоли женской репродуктивной системы. 2017; 3 (13): 61–67.
15. Кечин А. А. Разработка и применение метода определения мутаций в генах BRCA1 и BRCA2 у больных раком молочной железы и раком яичников [диссертация]. Н., 2018; 118 с.
16. Mavaddat N, Barrowdale D, Andrulis IL, Domchek SM, Eccles D, Nevanlinna H, et al. Pathology of breast and ovarian cancers among BRCA1 and BRCA2 mutation carriers: results from the Consortium of Investigators of Modifiers of BRCA1/2 (CIMBA). Cancer Epidemiol Biomarkers Prev. 2012; 21 (1): 134–47.
17. Любченко Л. Н., Батенева Е. И., Абрамов И. С., Емельянова М. А., Будик Ю. А., Тюляндина А. С. и др. Наследственный рак молочной железы и яичников. Злокачественные опухоли. 2013; (2): 53–61.
18. Lakhani SR, Van De Vijver MJ, Jocelyne Jacquemier J, Anderson TJ, Osin PP, McGuffoget L, et al. The pathology of familial breast cancer: predictive value of immunohistochemical markers estrogen receptor, progesterone receptor, HER-2, and p53 in patients with mutations in BRCA1 and BRCA2. J Clin Oncol. 2002. 20 (9): 2310–8.

ANALYSIS OF 13 *TP53* AND *WRAP53* POLYMORPHISM FREQUENCIES IN RUSSIAN POPULATIONS

Olkova MV[1,2] ✉, Petrushenko VS[2], Ponomarev GYu[2]

[1] Research Centre of Medical Genetics (RCMG), Moscow, Russia

[2] Vavilov Institute of General Genetics, Moscow, Russia

In the last decade the search for and annotation of human genome polymorphisms associated with phenotype have become particularly important concerning the opportunity of their use in medical and population genetics, pharmacogenomics and evolutionary biology. The study was aimed to calculate the frequencies and analyze the prevalence of 13 germline polymorphisms of two genes, *TP53* encoding the genome-keeper p53 protein and *WRAP53* involved in regulation of p53 production, in 28 Russian populations. We obtained data on 9 exonic *TP53* variants (rs587781663, rs17882252, rs150293825, rs112431538, rs149633775, rs144340710, rs1042522, rs1800371, rs201753350), one intronic polymorphism (rs17881850), and three variants of *WRAP53* (rs17880282, rs2287499, rs34067256). In the majority of populations the sample size was over 50 people (except five populations with 30–49 surveyed people). The alternative alleles' population frequencies for studies genetic variants in most Russian populations were close to appropriate allele frequencies in European and Asian populations of similar origin taken from global databases. The exceptions were six populations ("Central Caucasus", "Dagestan", "northern Russians", "southeastern Russians", "Tatars" and "Transcaucasia") with increased alternative alleles' population frequencies. All listed populations except the population of "southeastern Russians" are characterized by polymorphisms with high allele frequencies not satisfying the Hardy–Weinberg principle.

Keywords: p53, TP53, WRAP53, tumor marker, polymorphism, population frequency, genetic epidemiology

Acknowledgement: we would like to express our appreciation to Oleg Balanovsky, head of the Genome Geography Laboratory of the Vavilov Institute of General Genetics for study management and manuscript editing, to all DNA donors and Biobank of North Eurasia for provided collection of samples, as well as to the Center for Precision Genome Editing and Genetic Technologies for Biomedicine of the Pirogov Russian National Research Medical University (Moscow, Russia) for the opportunity to use the molecular biology technologies.

Funding: the study was carried out as part of the public contract between the Ministry of Science and Higher Education of the Russian Federation and the Research Centre of Medical Genetics (phenotyping of samples, database construction, data analysis).

Author contribution: Olkova MV — study design, statistical analysis, manuscript writing; Petrushenko VS — bioinformatics analysis, Ponomarev GYu — experiments.

Compliance with ethical standards: the study was carried out in accordance with the World Medical Association Declaration of Helsinki. All samples were obtained from Biobank of North Eurasia. The informed consent was obtained from all donors.

✉ **Correspondence should be addressed:** Marina V. Olkova
Gubkina 3, Moscow, 119991; genetics@inbox.ru

Received: 26.11.2020 **Accepted:** 12.12.2020 **Published online:** 12.01.2021

DOI: 10.24075/brsmu.2021.001

АНАЛИЗ ЧАСТОТ 13 ПОЛИМОРФИЗМОВ В ГЕНАХ *TP53* И *WRAP53* В РОССИЙСКИХ ПОПУЛЯЦИЯХ

М. В. Олькова[1,2] ✉, В. С. Петрушенко[2], Г. Ю. Пономарев[2]

[1] Медико-генетический научный центр имени академика Н. П. Бочкова, Москва, Россия

[2] Институт общей генетики имени Н. И. Вавилова РАН, Москва, Россия

В последнее десятилетие поиск и аннотация ассоциированных с фенотипом геномных полиморфизмов человека, а также изучение их популяционных частот стали особенно актуальными в связи с возможностью их применения в медицинской и популяционной генетике, фармакогеномике и эволюционной биологии. Целью исследования было рассчитать частоту и проанализировать распространенность в 28 российских популяциях 13 герминальных полиморфизмов двух генов — *TP53,* матрицы «хранителя генома» белка p53 и гена *WRAP53*, влияющего на производство белка p53. Были получены данные для 9 экзонных вариантов гена *TP53* (rs587781663, rs17882252, rs150293825, rs112431538, rs149633775, rs144340710, rs1042522, rs1800371, rs201753350), одного интронного полиморфизма (rs17881850), а также трех вариантов гена *WRAP53* (rs17880282, rs2287499, rs34067256). Для большинства популяций выборка была представлена числом более 50 человек (за исключением пяти популяций, в которых было обследовано от 30 до 49 человек). Популяционные частоты альтернативных аллелей изученных генных вариантов в большинстве российских популяций оказались близки к значениям частот этих аллелей в соответствующей их происхождению европейской или азиатской популяции из мировых баз данных. Исключение составили шесть популяций («Центральный Кавказ», «Дагестан», «северные русские», «юго-восточные русские», «татары» и «Закавказье»), в которых популяционные частоты альтернативных аллелей для большинства маркеров оказались повышенными. Для всех вышеперечисленных популяций, кроме «юго-восточных русских», характерно несоответствие аллелей полиморфизмов с повышенными частотами равновесию Харди–Вайнберга.

Ключевые слова: p53, TP53, WRAP53, онкомаркер, полиморфизм, популяционная частота, генетическая эпидемиология

Благодарности: О. П. Балановскому, заведующему лабораторией геномной географии Института общей генетики им. Н. И. Вавилова, за руководство исследованием и правку статьи, всем донорам ДНК и АНО «Биобанк Северной Евразии» за предоставленную коллекцию образцов, а также Центру высокоточного редактирования и генетических технологий для биомедицины РНИМУ им. Н. И. Пирогова (Москва, Россия) за возможность использования молекулярно-генетических технологий.

Финансирование: исследование выполнено в рамках Государственного задания Министерства науки и высшего образования РФ для Медико-генетического научного центра им. академика Н. П. Бочкова (работы по фенотипированию образцов, созданию базы данных, анализу данных).

Вклад авторов: М. В. Олькова — дизайн, статистический анализ, написание текста статьи; В. С. Петрушенко — биоинформатический анализ, Г. Ю. Пономарев — экспериментальные работы.

Соблюдение этических стандартов: исследование проведено в соответствии с требованиями Хельсинкской декларации Всемирной медицинской ассоциации. Все образцы для исследования получены из «Биобанка Северной Евразии». От всех доноров получено добровольное информированное согласие.

✉ **Для корреспонденции:** Марина Викторовна Олькова
ул. Губкина, д. 3, г. Москва, 119991; genetics@inbox.ru

Статья получена: 26.11.2020 **Статья принята к печати:** 12.12.2020 **Опубликована онлайн:** 12.01.2021

DOI: 10.24075/vrgmu.2021.001

TP53 gene is responsible for synthesis of one of the most notorious tumor suppressors, the p53 protein, which plays a vital part in maintaining genetic stability of the cell and cancer prevention. After activation due to cell damage, p53 triggers a number of cellular responses aimed at cell recovery and survival, or, in case the recovery is impossible, at programmed cell death. Such diverse pleiotropic tissue effects of p53 are due to total effect of co-expressed p53 isoforms. To date, at least 12 p53 isoforms have been reported, which are produced through alternative initiation of translation, the alternative promoter usage and alternative splicing [1]. All p53 isoforms share the common DNA-binding domain, but contain distinct transactivation and inhibitory domain, enabling the differential regulation of gene expression [2].

The *TP53* gene shows an autosomal dominant pattern of inheritance; it is associated with the risk of Li–Fraumeni syndrome and other hereditary cancer syndromes. The altered sensitivity to certain medications in people with a number of TP53 gene polymorphisms has been confirmed (Table 1).

The region of *WRAP53* gene with at least three alternative promoters is located in the region 13.1 of the short arm of chromosome 17 partially overlapping the 5'-region of the TP53 gene, which is located on the chain oppositely oriented to *WRAP53* in a head-to-head orientation [3]. The *WRAP53* gene plays a dual role. First, it encodes the antisense RNA (WRAP53α), which regulates the levels of p53 mRNA through interaction with the first exon of *TP53*, and is also involved in stimulation of p53 protein production due to its impact on the 5'- untranslated region of p53 mRNA [4, 5]. Second, *WRAP53* is responsible for WRAP53β protein (also called WDR79 and TCAB1) synthesis; WRAP53β belongs to WD40 protein family. This protein contributes to maintaining the integrity and normal function of the Cajal bodies essential for maturation of the splicing machinery and telomere maintenance [6–8]. WRAP53β also promotes accumulation of the repair factor 53BP1 at DNA double-strand breaks, thus stimulating the DNA repair [9]. The WRAP53β protein possibly possesses oncogenic properties, as evidenced by the WRAP53β overexpression in various cancer cell lines compared to normal cells [7, 8]. It should be noted that the involvement of this protein in carcinogenesis currently remains questionable: there is a theory that overexpression may be caused by the involvement of WRAP53β in DNA multiple double-strand break repair in case of cancer development in certain tissue [7].

The *WRAP53* gene mutations show the autosomal recessive pattern of inheritance. The homozygous mutations of this gene may result in dyskeratosis congenita and Li–Fraumeni syndrome.

The clinical significance of genes *TP53* and *WRAP53*, as well as high prevalence of their germline pathogenic variants in various cancer types [10], explain the need for studying the frequencies of these genes in populations of different countries. The frequencies of polymorphisms of these genes have already been studied in some European countries and the United States: the details on frequencies of both clinically significant polimorphisms and markers with uncertain significance may be found on the web-sites of such projects as ClinVar [11] of the National Center for Biotechnology Information of the USA, Ensembl (joint scientific project of the European Bioinformatics Institute and Sanger Institute) [12], and Genome Aggregation Database (gnomAD) [13]. In Russia, "Genokarta", the web-site of genetic encyclopedia created by researchers from the Novosibirsk State University is being actively developed [14]. Our study aimed at exploring distribution and frequencies of 13 polymorphisms of *TP53* and *WRAP53* genes in Russian populations is directed to expand the scientific knowledge in this area with regard to populations living in our country.

METHODS

DNA sampling

DNA samples were provided by Biobank of North Eurasia [15]. DNA was extracted from blood and saliva using the standard phenol-chloroform extraction method. The study included 1,785 DNA samples of volunteers who belonged to 28 Russian populations, which, based on their places of residence, covered the main regions of Russia (Table 2). Inclusion criteria: volunteers belonging to certain ethnic group (based on the self-identified ethnicity in four or more generations). Exclusion criteria: samples failing to meet criteria of belonging to certain ethnic group. Since the study was aimed at investigation of autosomal markers, the gender distribution was not taken into account during DNA sampling.

The size of each population was 30–87 people. The composition of studied populations is presented in Table 2. It should be taken into account that the studied genes *TP53* and *WRAP53* were autosomal, therefore, the actual number of studied alleles was twice as much: 60–174 alleles for each population.

Selection of polymorphisms

The list of *TP53* and *WRAP53* polymorphisms was established based on genetic variants with proven clinical significance submitted to ClinVar database (except the TP53 intronic variant, rs17881850). The intronic variant rs17881850 was included in the study in order to compare the allele frequencies of neutral polymorphism with the allele frequencies of genetic variants with confirmed clinical significance. Unfortunately, after genotyping much of polymorphisms included in original list had to be excluded from analysis, i. e. the population frequencies were calculated only using markers genotyped successfully in all populations.

Genotyping

All individuals were genotyped for nine *TP53* exon polymorphisms (rs587781663, rs17882252, rs150293825, rs112431538, rs149633775, rs144340710, rs1042522, rs1800371, rs201753350) and one intronic variant (rs17881850), as well as for three *WRAP53* polymorphisms (rs17880282, rs2287499, rs34067256). Genotyping was carried out using the Illumina (Illumina Inc.; USA) genomic analysis microarray technology. The standard 0.15 GenCall score cutoff value was used to discard the poorly typed samples.

Basic data on studied polymorphisms

Full information on studied polymorphisms was obtained from the web-site of the National Center for Biotechnology Information of the USA [16], in particular from the ClinVar archive [17] and Genome Aggregation Database (gnomAD) [18]. The position of polymorphism in the human genome was specified based on the version GRCh38.p12 of human reference Genome Assembly (Table 1).

Since the information about some polymorphisms available from public domains was incomplete, all markers were also studied by functional analysis through hidden Markov models designed for prediction of missense protein variants using the

Table 1. Basic data on studied markers; data obtained from ClinVar (NCBI)

Gene	Marker	GRCh38.p12	Gene region	Reference nucleotide	Alternative nucleotide	Polymorphism type	Amino acid substitution	Clinical significance of polymorphism (ClinVar)	FATHMM analysis results	Marker validation	Predisposition to disease
TP53	rs17881850	chr17:7669739	Intron 10	G	A	Intronic	No	No information	No calculation	No	No
	rs587781663	chr17: 7670627	Exon 10	C	T	Missense	Gly361Glu	No information	No calculation	Validated	Li–Fraumeni syndrome and other hereditary cancer syndromes
	rs17882252	chr17: 7670694	Exon 10	C	T	Missense	Glu339Lys	Likely benign/uncertain significance	CANCER	Validated. Conflicting data	
	rs150293825	chr17:7670695	Exon 10	G	A	Silent	Phe338=	Benign/likely benign	CANCER	Validated. No conflicting data	
	rs112431538	chr17:7673767	Exon 10	C	T	Missense	Glu285Lys	Pathogenic/ likely pathogenic	CANCER	Approved by FDA experts	
	rs149633775	chr17:7673773	Exon 7	G	A	Missense	Arg283Cys	Uncertain significance	CANCER	Проверен экспертами FDA	
	rs144340710	chr17:7674259	Exon 6	T	C	Missense	Asn235Ser	Benign	CANCER	Approved by FDA experts	
	rs1042522	chr17:7676154	Exon 3	G	C	Missense	Pro72Arg	Benign	CANCER	Included in expert panel of Pharmacogenomics Knowledgebase (PharmGKB)	
	rs1800371	chr17:7676230	Exon 3	G	A	Missense	Pro47Ser	Benign	CANCER	Approved by FDA experts	
	rs201753350	chr17:7676387	Exon 2	C	T	Missense	Val31Ile	Benign/likely benign/ conflicting data	CANCER	Validated. Conflicting data	
WRAP53	rs17880282	chr17:7688679	Exon 2	C	T	Missense	Pro11Ser	Benign/likely benign	PASSENGER/ OTHER	Validated. No conflicting data	Li–Fraumeni syndrome, dyskeratosis congenita
	rs2287499	chr17:7688850	Exon 2	C	G	Missense	Arg68Gly	Benign	PASSENGER/ OTHER	Validated. No conflicting data	
	rs34067256	chr17:7689055	Exon 2	C	G	Missense	Pro136Arg	Benign/likely benign	PASSENGER/ OTHER	Validated. No conflicting data	

Table 2. *TP53* and *WRAP53* polymorphism frequencies in studied Russian populations and reference worlds' populations

Population	Численность	rs17881850	rs587781663	rs17882252	rs150293825	rs112431538	rs149633775	rs144340710	rs1042522	rs1800371	rs201753350	rs17880282	rs2287499	rs34067256
Altaians	77	0.026	0.000	0.007	0.000	0.000	0.000	0.000	0.766	0.000	0.000	0.006	0.156	0.000
Bashkirs	43	0.000	0.012	0.000	0.000	0.000	0.000	0.000	0.720	0.000	0.000	0.000	0.116	0.000
Belarusians and Russians of the Northwest	30	0.017	0.000	0.000	0.000	0.000	0.000	0.017	0.650	0.000	0.000	0.000	0.117	0.033
Buryats, Khamnigans, Yakuts	57	0.000	0.000	0.000	0.000	0.000	0.000	0.000	0.772	0.000	0.000	0.000	0.158	0.000
Central Caucasus	64	0.071	0.048	0.063	0.047	0.032	0.032	0.000	0.697	0.032	0.032	0.047	0.125	0.016
Chukchis and Koryaks	67	0.000	0.000	0.000	0.000	0.000	0.000	0.000	0.657	0.000	0.000	0.000	0.313	0.000
Dagestan	79	0.025	0.013	0.019	0.013	0.013	0.013	0.000	0.643	0.019	0.025	0.013	0.165	0.025
Far East (peoples of the Amur region)	84	0.000	0.000	0.000	0.000	0.006	0.000	0.000	0.690	0.000	0.000	0.012	0.208	0.000
Karelians and Vepsians	59	0.000	0.000	0.000	0.000	0.000	0.000	0.000	0.717	0.000	0.000	0.000	0.113	0.000
Kazakhs, Karakalpaks, Uighurs, Nogays	44	0.025	0.000	0.008	0.000	0.000	0.000	0.000	0.797	0.000	0.000	0.000	0.042	0.000
Khanty, Mansi, Nenets	53	0.034	0.011	0.000	0.000	0.000	0.000	0.000	0.727	0.011	0.000	0.000	0.216	0.000
Komi and Udmurts	84	0.006	0.006	0.006	0.000	0.012	0.000	0.000	0.645	0.006	0.000	0.006	0.232	0.000
Mari and Chuvash	53	0.000	0.000	0.000	0.000	0.000	0.000	0.000	0.651	0.000	0.000	0.000	0.264	0.009
Khalkha Mongols	49	0.010	0.000	0.000	0.000	0.000	0.000	0.000	0.688	0.000	0.000	0.000	0.198	0.020
Mongols (other groups) and Kalmyks	78	0.000	0.000	0.000	0.000	0.000	0.000	0.000	0.654	0.000	0.000	0.000	0.231	0.000
Mordvins	40	0.013	0.000	0.000	0.000	0.000	0.000	0.000	0.700	0.000	0.000	0.000	0.125	0.000
Northern Russians	83	0.060	0.025	0.018	0.018	0.018	0.024	0.006	0.756	0.024	0.018	0.030	0.120	0.012
Russians of the Southeast of Central Russia	51	0.010	0.000	0.000	0.000	0.000	0.010	0.039	0.622	0.020	0.000	0.029	0.127	0.059
Russians of the Southwest of Central Russia	50	0.020	0.000	0.000	0.000	0.000	0.000	0.010	0.796	0.000	0.000	0.000	0.140	0.010
Russians of the north of the Arkhangelsk region	70	0.029	0.000	0.000	0.000	0.000	0.000	0.000	0.766	0.000	0.000	0.000	0.093	0.000
Siberian Tatars	68	0.007	0.000	0.015	0.015	0.007	0.000	0.000	0.664	0.009	0.000	0.007	0.184	0.000
Tajiks, Pamiris, Yaghnobi people	72	0.014	0.000	0.000	0.000	0.000	0.000	0.000	0.681	0.007	0.000	0.000	0.208	0.000
Tatars	52	0.102	0.160	0.143	0.140	0.130	0.120	0.031	0.717	0.127	0.100	0.135	0.225	0.039
Transcaucasia	77	0.059	0.034	0.040	0.032	0.020	0.019	0.000	0.669	0.027	0.026	0.026	0.125	0.007
Tuvans and Tofalars	55	0.009	0.000	0.000	0.000	0.000	0.000	0.000	0.764	0.000	0.000	0.000	0.236	0.000
Ukranians	79	0.019	0.000	0.026	0.000	0.000	0.000	0.000	0.753	0.000	0.000	0.000	0.152	0.000
Uzbeks, Turkmens, Kyrgyz	80	0.006	0.000	0.000	0.000	0.000	0.000	0.000	0.700	0.000	0.000	0.000	0.156	0.000
Western Caucasus	87	0.012	0.006	0.000	0.006	0.000	0.000	0.000	0.622	0.000	0.000	0.000	0.149	0.011
Europe	Data from NCBI. gnomAD	0.013	0.000	0.000	0.0005	0.00001	0.0003	0.0004	0.717	0.00	0.00001	0.0006	0.120	0.0001
Africa		0.004	0.000	0.000	0.000	0.000	0.000	0.000	0.571	0.013	0.000	0.076	0.422	0.000
Asia		0.000	0.000	0.000	0.000	0.000	0.000	0.000	0.600	0.000	0.010	0.000	0.250	0.030

fathmm web-site [19]. To minimize the number of false positives, a conservative threshold of –3.0 was chosen for analysis. The data obtained were included in Table. 1.

Mathematical and statistical methods

Calculation of population alternative allele frequencies for studied polymorphisms, calculation of χ^2 criterion and *p*-value for assessment of Hardy–Weinberg genotype frequencies, as well as assessment of alternative allele frequency distribution normality in studied populations were performed with RStudio R, version 4.0.2 (RStudio; USA) and Microsoft Excel (Microsoft Corp.; USA). The differences were considered significant at $p < 0.01$.

Multidimensional scaling

Two-dimensional representation of spatial distribution of populations based on the alternative allele frequencies calculated for studied markers *TP53* and *WRAP53* was obtained with STATISTICA10 software package (StatSoft; USA) via multidimensional scaling using the Nei's genetic distances calculated with the DJ genetic software (RCMG; Russia).

RESULTS

Calculation of alternative allele frequencies for studied markers in Russian populations

Based on the genotyping of 28 Russian populations, we calculated alternative allele frequencies for nine exon TP53 polymorphisms (exon 2 — rs201753350; exon 3 — rs1042522, rs1800371; exon 6 — rs144340710; exon 7 — rs112431538, rs149633775; exon 10 — rs587781663, rs17882252, rs150293825), one intronic *TP53* variant (rs17881850), as well as for three polymorphisms of exon 2 of *WRAP53* gene (rs17880282, rs2287499, rs34067256). The calculated population alternative allele frequencies for the listed markers are presented in Table 2.

Alternative allele frequencies and Hardy–Weinberg equilibrium

To test the studied markers *TP53* and *WRAP53* for Hardy–Weinberg equilibrium in the population, χ^2 criterion was calculated based on the existing allele ratio and the calculated in accordance with the Hardy–Weinberg principle marker population frequencies. Table 3 was compiled in order to visualize the relationship between the alternative allele frequencies and the Hardy–Weinberg equilibrium. In five of 28 studied populations (“Central Caucasus”, “Dagestan”, “northern Russians”, “Tatars” and “Transcaucasia”) the combination of high (compared to the listed in Table 2 reference frequencies for the world’s populations of appropriate origin) alternative allele frequencies and their non-equilibrium pattern in the population (orange cells) were observed for most markers. This suggests that the external factors (for example, accidental inbreeding) may affect the pattern of studied alleles in the discussed population. Genotyping errors may also affect the results.

In the population of “southeastern Russians” alternative alleles for many markers were identified; the frequencies of those were higher compared to reference European population, however, the alleles showed no deviation from the Hardy–Weinberg equilibrium.

In some populations (“Komi and Udmurts”, “Siberian Tatars”, “Western Caucasus”), the diversity of identified markers was higher compared to reference populations of appropriate origin, however, their frequencies were low (close to reference values) and satisfied the Hardy–Weinberg principle. Among studied markers, two markers (rs1042522, located in exon 3 of *TP53,* and rs2287499, located in exon 2 of *WRAP53*) were characterized by high frequencies and satisfied the Hardy–Weinberg principle in all populations.

Assessment of normality for distribution of alternative allele frequencies in the populations

Since in theory the neutral alleles are not affected by natural selection, and their population frequencies may follow a normal distribution, we have assessed the normality of the marker frequency distribution in the population using the Shapiro-Wilk test. The test results have made it possible to confirm the null-hypothesis for two markers: rs1042522 ($W = 0.95$, $p = 0.18$) and rs2287499 ($W = 0.97$, $p = 0.46$). For other markers, the normal distribution has not been confirmed.

Analysis of marker population frequencies by multidimensional scaling (MDS)

In our study, multidimensional scaling was the most effective method for the studied populations’ positioning in the low-dimensional space allowing us to evaluate the genetic distances between populations. MDS was performed for 29 populations (Tatar and African populations were excluded due to sharp contrast between their marker frequencies and the data for the main population pool) (see Figure). For the MDS performed the stress value was 0.068, and the alienation coefficient was 0.058.

The populations were pre-labeled as belonging to one of three groups: Asian, European and Caucasian. The populations grouped based on their origin (see Figure) allowed us to determine three appropriate clusters: Asian, European and Caucasian. In the Asian and European clusters having the overlap area of a significant size, the populations are closer to each other based on polymorphism frequencies, and in the Caucasian cluster, the large frequencies’ variability between populations is observed.

The boundaries of Asian cluster are quite clear. The only exception is the joint population which includes Kazakhs, Karakalpaks, Uighurs and Nogais; the position of this population outside the cluster is due to higher level of some markers showing the equilibrium pattern compared to other Asian populations (Table 3).

European cluster has a more compact shape with high population density around the central reference European population, the marker frequencies for which have been obtained from public sources. The following three European populations appear to be far beyond the cluster: “northern Russians", "southeastern Russians" and the joint population of Mari and Chuvash. The population of “northern Russians” is the only European population showing higher frequencies of many markers deviating from equilibrium, which are absent in other European population (Table 3). Compared to the “northern Russians" population, the population of "southeastern Russians" characterized by high frequencies of some polymorphisms unusual for European populations, the majority of which are in Hardy–Weinberg equilibrium (Table 3), is extended beyond European cluster in the opposite direction on the plot. The "Mari and Chuvash" population is deep inside the Asian cluster, which may be due to anthropological composition

Table 3. Overlapping of marker population frequencies and assessment of Hardy–Weinberg equilibrium

Population	*TP53*										*WRAP53*		
	rs17881850	rs587781663	rs17882252	rs150293825	rs112431538	rs149633775	rs144340710	rs1042522	rs1800371	rs201753350	rs17880282	rs2287499	rs34067256
Altaians	0.026	0	0.007	0	0	0	0	0.766	0	0	0.006	0.156	0
Bashkirs	0	0.01	0	0	0	0	0	0.720	0	0	0	0.116	0
Belarusians and Russians of the Northwest	0.017	0	0	0	0	0	0.017	0.650	0	0	0	0.117	0.033
Buryats, Khamnigans, Yakuts	0	0	0	0	0	0	0	0.772	0	0	0	0.158	0
Central Caucasus	0.071	0.048	0.063	0.047	0.032	0.032	0	0.697	0.032	0.032	0.047	0.125	0.016
Chukchis and Koryaks	0	0	0	0	0	0	0	0.657	0	0	0	0.313	0
Dagestan	0.025	0.013	0.019	0.013	0.013	0.013	0	0.643	0.019	0.025	0.013	0.165	0.025
Far East (peoples of the Amur region)	0	0	0	0	0.006	0	0	0.690	0	0	0.012	0.208	0
Karelians and Vepsians	0.025	0	0.008	0	0	0	0	0.797	0	0	0	0.042	0
Kazakhs, Karakalpaks, Uighurs, Nogays	0.034	0.011	0	0	0	0	0	0.727	0.011	0	0	0.216	0
Khanty, Mansi, Nenets	0	0	0	0	0	0	0	0.717	0	0	0	0.113	0
Komi and Udmurts	0.006	0.006	0.006	0	0.012	0	0	0.645	0.006	0	0.006	0.232	0
Mari and Chuvash	0	0	0	0	0	0	0	0.651	0	0	0	0.264	0.01
Khalkha Mongols	0.010	0	0	0	0	0	0	0.688	0	0	0	0.198	0.02
Mongols (other groups) and Kalmyks	0	0	0	0	0	0	0	0.654	0	0	0	0.231	0
Mordvins	0.013	0	0	0	0	0	0	0.700	0	0	0	0.125	0
Northern Russians	0.060	0.025	0.018	0.018	0.018	0.024	0.01	0.756	0.024	0.018	0.030	0.120	0.012
Russians of the Southeast of Central Russia	0.010	0	0	0	0	0.010	0.039	0.622	0.02	0	0.029	0.127	0.059
Russians of the Southwest of Central Russia	0.020	0	0	0	0	0	0.01	0.796	0	0	0	0.140	0.010
Russians of the north of the Arkhangelsk region	0.029	0	0	0	0	0	0	0.766	0	0	0	0.093	0
Siberian Tatars	0.007	0	0.015	0.015	0.007	0	0	0.664	0.009	0	0.007	0.184	0
Tajiks, Pamiris, Yaghnobi people	0.014	0	0	0	0	0	0	0.681	0.007	0	0	0.208	0
Tatars	0.102	0.160	0.143	0.140	0.130	0.120	0.031	0.717	0.127	0.100	0.135	0.225	0.039
Transcaucasia	0.059	0.034	0.040	0.032	0.020	0.019	0	0.669	0.027	0.026	0.026	0.125	0.007
Tuvans and Tofalars	0.009	0	0	0	0	0	0	0.764	0	0	0	0.236	0
Ukranians	0.019	0	0.026	0	0	0	0	0.753	0	0	0	0.152	0
Uzbeks, Turkmens, Kyrgyz	0.006	0	0	0	0	0	0	0.700	0	0	0	0.156	0
Western Caucasus	0.012	0.006	0	0.006	0	0	0	0.622	0	0	0	0.149	0.011

Note: Hardy–Weinberg equilibrium is assessed based on the χ^2 *p*-value ($p < 0.01$); *orange cells* — null-hypothesis for alternative allele is rejected based on the χ^2 test, *green cells* — null-hypothesis is not rejected.

Алт	Altaians
Баш	Bashkirs
Бел/РСЗ	Belarusians and Russians of the Northwest
Бур/Хмн/	Buryats, Khamnigans, Yakuts
ЦентК	Central Caucasus
Ч/Кор	Chukchis and Koryaks
Даг	Dagestan
ДВ	Far East (peoples of the Amur region)
Кар/В	Karelians and Vepsians
Кз/Кр/Уй	Kazakhs, Karakalpaks, Uighurs, Nogays
Х/М/Н	Khanty, Mansi, Nenets
Км/Удм	Komi and Udmurts
Мр/Чв	Mari and Chuvash
Мн-хл	Khalkha Mongols
Мн-нехл/	Mongols (other groups) and Kalmyks
Мрд	Mordvins
РС	Northern Russians
РЮВ	Russians of the Southeast of Central Russia
РЮЗ	Russians of the Southwest of Central Russia
РДС	Russians of the north of the Arkhangelsk region
СТ	Siberian Tatars
Тдж/Пм/Я	Tajiks, Pamiris, Yaghnobi people
ЗК	Transcaucasia
Тув/Тоф	Tuvans and Tofalars
Ук	Ukranians
Уз/Тур/К	Uzbeks, Turkmens, Kyrgyz
ЗапК	Western Caucasus
Евр	Europe
Аз	Asia

Fig. Multidimensional scaling plot based on Nei's genetic distance matrix for 29 populations (Tatar and African populations were excluded from analysis due to excessively large frequency differences with the rest of populations); stress value is 0.068, and the alienation coefficient is 0.058. The populations are divided into three groups: Asian (*red triangle*), European (*green triangle*) and Caucasian (*blue sign*). The appropriate clusters have been distinguished: *orange* — Asian populations, *green* — European populations, *blue* — Caucasian populations.

of the Chuvash that includes both Caucasian individuals and a significant proportion of Mongoloid individuals together with mixed forms.

All populations of Caucasian cluster, except for the "Western Caucasus" population falling in the overlap area with Asian cluster and being in the close proximity to European cluster, are characterized by high frequencies of all analyzed polymorphisms and their non-equilibrium patterns (Table 3), which brings them close to "northern Russians" based on the discussed parameters (see Figure).

DISCUSSION

The study of *TP53* and *WRAP53* gene polymorphisms in 28 populations covering all major regions of Russia made it possible to assess the frequency and distribution of selected markers in various Russian regions and populations.

Assessment of alternative allele frequencies for the studied markers in Russian populations revealed two major trends:

– two of 13 studied markers (rs1042522, located in exon 3 of *TP53*, and rs2287499, located in exon 2 of *WRAP53*) are characterized by high frequencies in all populations, normal distribution of marker population frequencies, and Hardy–Weinberg proportions of alleles;

– in five populations ("Central Caucasus", "Dagestan", "northern Russians", "Tatars" and "Transcaucasia"), the frequencies of most markers (except the mentioned above rs1042522 and rs2287499, as well as the benign rs144340710 located in exon 6 of TP53) appeared to be high, and the alleles of these markers showed non-equilibrium patterns. In the Tatar population the abundance, frequencies and distribution of the studied polymorphisms' alternative alleles were significantly higher compared to reference global values; they also significantly exceeded the frequencies and abundance of these polymorphisms in the major pool of Russian populations (Table 2). This matter is subject to further research.

Two prevalent equilibrium markers, rs1042522 of *TP53* gene and rs2287499 of *WRAP53* gene, are listed in the ClinVar data base as benign markers. It means that their frequency is too high for markers to be pathogenic mutations; markers are found in hetero- and homozygous state in individuals without severe disease for that gene; markers show no disease association in appropriately sized case-control studies [20]. The fact that the alternative allele of rs1042522 polymorphism being a part of p53 DNA-binding domain [21] shows high frequency in all populations compared to reference genome may indicate the reference genome carrying a random minor allele. This assumption is indirectly supported by the reported increased functional ability to induce apoptosis and prevent cancer development in alternative Arg72 variant of p53 protein compared to reference Pro72 variant [22].

Despite rs1042522 and rs2287499 are listed in scientific databases as benign markers, literature contains a large amount of data on their involvement in carcinogenesis. In particular, it has been reported that heterozygous variant Arg/Pro of p53 Pro72Arg polymorphism (Table 1) is associated with high risk of melanoma compared to heterozygous variant Pro/Pro [23]; another paper reports association of the marker Pro/Pro genotype with increased risk of nonsmall cell lung cancer in patients from Moscow Region [21].

There are many literary sources on survival of cancer patients, homo- and heterozygous for Pro72Arg, however, the reported data is controversial. There is evidence of increased median survival time in cervical cancer patients carrying Arg/Pro genotype when compared with patients with Arg/Arg and Pro/Pro genotypes [24], however, the extensive research carried out by Danish specialists [25] has shown no association of the mentioned above polymorphism with lower mortality after cancer and lower cancer incidence in the general population.

However, rs1042522 is better known as a marker included in the expert panel of Pharmacogenomics Knowledgebase, which is associated with altered body response to some antineoplastic drugs [26]. There is evidence of the p53 Pro allele association with toxicity due to chemotherapy [27], as well as evidence of lower response rate to fluorouracil-based chemotherapy in gastric cancer patients carrying the Pro/Pro genotype compared to patients carrying the Arg/Arg genotype [28].

The clinical significance of rs2287499 marker of gene *WRAP53* is much less well understood, however, there is evidence of moderate linkage disequilibrium between studied markers rs1042522 and rs2287499. The haplotype combination CA/GC is associated with increased risk of breast cancer, and the haplotype combination GA/CC, by contrast, is assumed to be a protective factor against breast cancer [29].

The abundance and frequencies of other polymorphisms in Russian populations vary significantly, however the calculated frequencies of most polymorphisms correspond to reference marker frequencies for Asian and European populations in accordance with the origin of surveyed Russian populations. Exceptions are five listed above populations with high frequencies of the discussed markers. The clinical significance of some studied polymorphisms (for example, the intronic variant rs17881850) remains poorly understood. However, recent evidence suggests that intronic *TP53* gene polymorphisms may also have some clinical significance [30].

CONCLUSION

The study allowed us to obtain data on germline *TP53* (10 markers of five exons and one intron) and *WRAP53* (three markers of exon 2) polymorphism frequencies for 28 Russian populations. In the majority of populations the calculated polymorphism frequencies are close to values obtained for reference global population (Asian or European) of appropriate origin. Six populations ("Central Caucasus", "Dagestan", "northern Russians", "south-eastern Russians", "Tatars" and "Transcaucasia") are characterized by increased marker frequencies compared to reference values; in all listed populations except the population of "southeastern Russians" the marker alleles with high frequencies do not satisfy the Hardy–Weinberg principle. The Tatar population is characterized by high frequencies of polymorphisms' allelic disequilibrium, which demonstrates the need for more detailed investigation of those in this population in order to reveal the cause of such differences.

References

1. Joruiz SM, Bourdon JC. P53 isoforms: Key regulators of the cell fate decision. Cold Spring Harbor Perspectives in Medicine. 2016; 6: 8.
2. Surget S, Khoury MP, Bourdon JC. Uncovering the role of p53 splice variants in human malignancy: a clinical perspective. OncoTargets and Therapy. 2013; 7: 57–68.
3. Rassoolzadeh H. Unwrapping the role of WRAP53β in DNA damage response [Internet]. [Solna]; 2016. Available from: http://ceder.graphics.
4. Mahmoudi S, Henriksson S, Corcoran M, Méndez-Vidal C, Wiman KG, Farnebo M. Wrap53, a natural p53 antisense transcript required for p53 induction upon DNA damage. Molecular Cell. 2009; 33 (4): 462–71.
5. Farnebo M. Wrap53, a novel regulator of p53. Cell Cycle. 2009; 8 (15): 2343–6. DOI: 10.4161/cc.8.15.9223.
6. Henriksson S, Farnebo M. On the road with WRAP53β: guardian of Cajal bodies and genome integrity. Front Genet. 2015; 6: 91. doi: 10.3389/fgene.2015.00091.
7. Bergstrand S, O'Brien EM, Farnebo M. The Cajal body protein WRAP53β prepares the scene for repair of DNA double-strand breaks by regulating local ubiquitination. Front Mol Biosci. 2019; 6: 51. Published 2019 Jul 4. DOI:10.3389/fmolb.2019.00051.
8. Mahmoudi S. WRAP53 unwrapped; roles in nuclear architecture and cancer. 2011.
9. Coucoravas C, Dhanjal S, Henriksson S, Böhm S, Farnebo M. Phosphorylation of the Cajal body protein WRAP53β by ATM promotes its involvement in the DNA damage response. RNA Biol. 2017; 14(6): 804–13. DOI:10.1080/15476286.2016.1243647.
10. Rogoża-Janiszewska E, Malińska K, Górski B, Scott RJ, Cybulski C, Kluźniak W, et al. Prevalence of germline TP53 variants among early-onset breast cancer patients from Polish population. Breast Cancer. 2020.
11. rs2287499 RefSNP Report - dbSNP - NCBI [Internet]. Available from: https://www.ncbi.nlm.nih.gov/snp/rs2287499#frequency_tab.
12. rs2287499 (SNP) — Population genetics — Homo_sapiens — Ensembl genome browser 101 [Internet]. Available from: http://www.ensembl.org/Homo_sapiens/Variation/Population?db=core;r=17:7688350-7689350;v=rs2287499;vdb=variation;vf=87573072
13. rs2287499 | gnomAD v2.1.1 | gnomAD [Internet]. Available from: https://gnomad.broadinstitute.org/variant/rs2287499?dataset=gnomad_r2_1.
14. rs2287499 C>G | Genokarta — geneticheskaja enciklopedija [Internet]. Available from: https://genokarta.ru/snps/rs2287499_CG.
15. Balanovskaya EV, Zhabagin MK, Agdzhoyan AT, Chukhryaeva MI, Markina NV, Balaganskaya OA et al. Populyaczionnye biobanki: princzipy organizaczii i perspektivy primeneniya v genogeografii i personalizirovannoj mediczine. Genetika. 2016; 52 (12): 1371–87.
16. National Center for Biotechnology Information [Internet]. Available from: https://www.ncbi.nlm.nih.gov/.
17. What is ClinVar? [Internet]. Available from: https://www.ncbi.nlm.nih.gov/clinvar/intro/.
18. gnomAD [Internet]. Available from: https://gnomad.broadinstitute.org/.
19. fathmm — Home [Internet]. Available from: http://fathmm.biocompute.org.uk/.
20. Pesaran T, Karam R, Huether R, Li S, Farber-Katz S, Chamberlin A, et al. Beyond DNA: an integrated and functional approach for classifying germline variants in breast cancer genes. Int J Breast Cancer. 2016; 2016: 2469523. DOI: 10.1155/2016/2469523.
21. Zavarykina T, Byrdennyy A, Loginov V, Atkarskaya M, Zhizhina G. A84: Polymorphic markers Arg72Pro and Gln157Lys of TP53 gene in nonsmall cell lung cancer. European Journal of Cancer Supplements [Internet]. 2015; 13 (1): 69. Available from: https://linkinghub.elsevier.com/retrieve/pii/S1359634915001238.
22. Zheltuhin AO, Chumakov PM. Povsednevnye i induciruemye funkcii gena p53. 2010; 50: 447–516.
23. Geng P, Liao Y, Ruan Z, Liang H. Increased risk of cutaneous melanoma associated with p53 Arg72pro polymorphism. PLoS ONE [Internet]. 2015; 10 (3): e0118112. Available from: https://dx.plos.org/10.1371/journal.pone.0118112.
24. Coelho A, Nogueira A, Soares S, Assis J, Pereira D, Bravo I, et al. TP53 Arg72Pro polymorphism is associated with increased overall survival but not response to therapy in Portuguese/Caucasian patients with advanced cervical cancer. Oncology Letters [Internet]. 2018; 15 (5): 8165–71. Available from: http://www.spandidos-publications.com/10.3892/ol.2018.8354/abstract.
25. Kodal JB, Vedel-Krogh S, Kobylecki CJ, Nordestgaard BG, Bojesen SE. TP53 Arg72Pro, mortality after cancer, and all-cause mortality in 105,200 individuals. Scientific Reports. 2017; 7 (1).
26. rs1042522 - Clinical Annotations [Internet]. Available from: https://www.pharmgkb.org/variant/PA166155173/clinicalAnnotation.
27. Henríquez-Hernández LA, Murias-Rosales A, González-Hernández A, de León AC, Díaz-Chico N, Fernández-Pérez L. Distribution of TYMS, MTHFR, p53 and MDR1 gene polymorphisms in patients with breast cancer treated with neoadjuvant chemotherapy. Cancer Epidemiology. 2010; 34 (5): 634–8. DOI: 10.1016/j.canep.2010.06.013.
28. Huang ZH, Hua D, Li LH, Zhu J De. Prognostic role of p53 codon 72 polymorphism in gastric cancer patients treated with fluorouracil-based adjuvant chemotherapy. J Cancer Res Clin Oncol. 2008; 134 (10): 1129–34. DOI: 10.1007/s00432-008-0380-8.
29. Pouladi N, Abdolahi S, Farajzadeh D, Feizi MAH. Haplotype and linkage disequilibrium of TP53-WRAP53 locus in Iranian-Azeri women with breast cancer. Roemer K, editor. PLOS ONE [Internet]. 2019; 14 (8): e0220727. Available from: https://dx.plos.org/10.1371/journal.pone.0220727.
30. Voropaeva EN, Pospeloya TI, Voevoda MI, Mabimovv N. Changes in non-coding sequences of the tp53 gene in diffuse large b-cell lymphoma. Gematologiya i Transfusiologiya. 2018; 63 (3): 239–49.

Литература

1. Joruiz SM, Bourdon JC. P53 isoforms: Key regulators of the cell fate decision. Cold Spring Harbor Perspectives in Medicine. 2016; 6: 8.
2. Surget S, Khoury MP, Bourdon JC. Uncovering the role of p53 splice variants in human malignancy: a clinical perspective. OncoTargets and Therapy. 2013; 7: 57–68.
3. Rassoolzadeh H. Unwrapping the role of WRAP53β in DNA damage response [Internet]. [Solna]; 2016. Available from: http://ceder.graphics.
4. Mahmoudi S, Henriksson S, Corcoran M, Méndez-Vidal C, Wiman KG, Farnebo M. Wrap53, a natural p53 antisense transcript required for p53 induction upon DNA damage. Molecular Cell. 2009; 33 (4): 462–71.
5. Farnebo M. Wrap53, a novel regulator of p53. Cell Cycle. 2009; 8 (15): 2343–6. DOI: 10.4161/cc.8.15.9223.
6. Henriksson S, Farnebo M. On the road with WRAP53β: guardian of Cajal bodies and genome integrity. Front Genet. 2015; 6: 91. doi: 10.3389/fgene.2015.00091.
7. Bergstrand S, O'Brien EM, Farnebo M. The Cajal body protein WRAP53β prepares the scene for repair of DNA double-strand breaks by regulating local ubiquitination. Front Mol Biosci. 2019; 6: 51. Published 2019 Jul 4. DOI:10.3389/fmolb.2019.00051.
8. Mahmoudi S. WRAP53 unwrapped; roles in nuclear architecture and cancer. 2011.
9. Coucoravas C, Dhanjal S, Henriksson S, Böhm S, Farnebo M. Phosphorylation of the Cajal body protein WRAP53β by ATM promotes its involvement in the DNA damage response. RNA Biol. 2017; 14(6): 804–13. DOI:10.1080/15476286.2016.1243647.
10. Rogoża-Janiszewska E, Malińska K, Górski B, Scott RJ, Cybulski C, Kluźniak W, et al. Prevalence of germline TP53 variants among early-onset breast cancer patients from Polish population. Breast Cancer. 2020.

11. rs2287499 RefSNP Report - dbSNP - NCBI [Internet]. Available from: https://www.ncbi.nlm.nih.gov/snp/rs2287499#frequency_tab.
12. rs2287499 (SNP) — Population genetics — Homo_sapiens — Ensembl genome browser 101 [Internet]. Available from: http://www.ensembl.org/Homo_sapiens/Variation/Population?db=core;r=17:7688350-7689350;v=rs2287499;vdb=variation;vf=87573072
13. rs2287499 | gnomAD v2.1.1 | gnomAD [Internet]. Available from: https://gnomad.broadinstitute.org/variant/rs2287499?dataset=gnomad_r2_1
14. rs2287499 C>G | Генокарта — генетическая энциклопедия [Internet]. Available from: https://genokarta.ru/snps/rs2287499_CG.
15. Балановская Е. В., Жабагин М. К., Агджоян А. Т., Чухряева М. И., Маркина Н. В., Балаганская О. А. и др. Популяционные биобанки: принципы организации и перспективы применения в геногеографии и персонализированной медицине. Генетика. 2016; 52 (12): 1371–87.
16. National Center for Biotechnology Information [Internet]. Available from: https://www.ncbi.nlm.nih.gov/.
17. What is ClinVar? [Internet]. Available from: https://www.ncbi.nlm.nih.gov/clinvar/intro/.
18. gnomAD [Internet]. Available from: https://gnomad.broadinstitute.org/.
19. fathmm — Home [Internet]. Available from: http://fathmm.biocompute.org.uk/.
20. Pesaran T, Karam R, Huether R, Li S, Farber-Katz S, Chamberlin A, et al. Beyond DNA: an integrated and functional approach for classifying germline variants in breast cancer genes. Int J Breast Cancer. 2016; 2016: 2469523. DOI: 10.1155/2016/2469523.
21. Zavarykina T, Byrdennyy A, Loginov V, Atkarskaya M, Zhizhina G. A84: Polymorphic markers Arg72Pro and Gln157Lys of TP53 gene in nonsmall cell lung cancer. European Journal of Cancer Supplements [Internet]. 2015; 13 (1): 69. Available from: https://linkinghub.elsevier.com/retrieve/pii/S1359634915001238.
22. Желтухин А. О., Чумаков П. М. Повседневные и индуцируемые функции гена p53. 2010; 50: 447–516.
23. Geng P, Liao Y, Ruan Z, Liang H. Increased risk of cutaneous melanoma associated with p53 Arg72pro polymorphism. PLoS ONE [Internet]. 2015; 10 (3): e0118112. Available from: https://dx.plos.org/10.1371/journal.pone.0118112.
24. Coelho A, Nogueira A, Soares S, Assis J, Pereira D, Bravo I, et al. TP53 Arg72Pro polymorphism is associated with increased overall survival but not response to therapy in Portuguese/Caucasian patients with advanced cervical cancer. Oncology Letters [Internet]. 2018; 15 (5): 8165–71. Available from: http://www.spandidos-publications.com/10.3892/ol.2018.8354/abstract.
25. Kodal JB, Vedel-Krogh S, Kobylecki CJ, Nordestgaard BG, Bojesen SE. TP53 Arg72Pro, mortality after cancer, and all-cause mortality in 105,200 individuals. Scientific Reports. 2017; 7 (1).
26. rs1042522 - Clinical Annotations [Internet]. Available from: https://www.pharmgkb.org/variant/PA166155173/clinicalAnnotation.
27. Henríquez-Hernández LA, Murias-Rosales A, González-Hernández A, de León AC, Díaz-Chico N, Fernández-Pérez L. Distribution of TYMS, MTHFR, p53 and MDR1 gene polymorphisms in patients with breast cancer treated with neoadjuvant chemotherapy. Cancer Epidemiology. 2010; 34 (5): 634–8. DOI: 10.1016/j.canep.2010.06.013.
28. Huang ZH, Hua D, Li LH, Zhu J De. Prognostic role of p53 codon 72 polymorphism in gastric cancer patients treated with fluorouracil-based adjuvant chemotherapy. J Cancer Res Clin Oncol. 2008; 134 (10): 1129–34. DOI: 10.1007/s00432-008-0380-8.
29. Pouladi N, Abdolahi S, Farajzadeh D, Feizi MAH. Haplotype and linkage disequilibrium of TP53-WRAP53 locus in Iranian-Azeri women with breast cancer. Roemer K, editor. PLOS ONE [Internet]. 2019; 14 (8): e0220727. Available from: https://dx.plos.org/10.1371/journal.pone.0220727.
30. Voropaeva EN, Pospeloya TI, Voevoda MI, Mabimovv N. Changes in non-coding sequences of the tp53 gene in diffuse large b-cell lymphoma. Gematologiya i Transfusiologiya. 2018; 63 (3): 239–49.

MORPHOFUNCTIONAL CHARACTERISTICS OF CUTANEOUS CONNECTIVE TISSUE SCARS IN WOMEN WITH PAST HISTORY OF CHILDBIRTH AFTER CESARIAN DELIVERY

Mishina ES[1]✉, Zatolokina MA[1], Mnikhovich MV[2], Kharchenko VV[1]

[1] Kursk State Medical University, Kursk, Russia

[2] Research Institute of Human Morphology, Moscow, Russia

The inevitable outcome of skin injuries caused by a variety of external factors is the formation of a connective tissue scar. A scar can deform when exposed to stretching, pressure or repeat surgeries and undergo structural changes leading to its dehiscence. Scar dehiscence is a common problem seen in women with a past history of cesarean delivery. There have been comprehensive studies of uterine scars formed after the C-section, but the morphology of cutaneous C-section scars has not yet been investigated. The aim of this study was to look into the morphology of connective tissue scars in multiparas with a past history of cesarean delivery. Specimens of cutaneous scars were collected from 30 women after the C-section. Within one age group, fiber thickness was directly proportional to the number of previous deliveries. Comparison of different age groups with the same number of previous deliveries revealed the thinning of collagen fibers and the increased density of type III collagen fibers. The most pronounced changes were observed in women with a history of 3 or more deliveries. We hypothesize that a connective tissue scar undergoes structural transformation, becomes thinner, and its fibers dissociate due to repeated skin stretching, which might indirectly suggest the dehiscence of the postoperative scar.

Keywords: connective tissue scar, skin, collagen fibers, regeneration, stretching, cesarean section

Author contribution: Mishina ES — study design; collection and processing of specimens; data analysis; manuscript preparation; Zatolokina MA, Mnikhovich MV, Kharchenko VV — study concept; manuscript editing. The final version of the manuscript was approved by all the authors.

Compliance with ethical standards: the study was approved by the Regional Ethics Committee of Kursk State Medical University (Protocol № 4 dated June 10, 2019). The study complied with the ethical standards for medical research studies involving humans. Informed consent was obtained from all study participants.

✉ **Correspondence should be addressed:** Ekaterina S. Mishina
Karla Marxa, 3, Kursk, 305041; katusha100390@list.ru

Received: 11.12.2020 **Accepted:** 12.01.2021 **Published online:** 22.01.2021

DOI: 10.24075/brsmu.2021.002

МОРФОФУНКЦИОНАЛЬНЫЕ ОСОБЕННОСТИ СОЕДИНИТЕЛЬНОТКАННОГО РУБЦА НА КОЖЕ У ПОВТОРНОРОДЯЩИХ ЖЕНЩИН ПОСЛЕ ОПЕРАТИВНОГО РОДОРАЗРЕШЕНИЯ

Е. С. Мишина[1]✉, М. А. Затолокина[1], М. В. Мнихович[2], В. В. Харченко[1]

[1] Курский государственный медицинский университет, Курск, Россия

[2] Научно-исследовательский институт морфологии человека, Москва, Россия

Нарушение целостности кожного покрова под действием различных факторов неизбежно приводит к образованию соединительнотканного рубца. Под воздействием динамических факторов (растяжение, давление, повторно проведенные операции) рубец подвергается деформации, вследствие чего возможна дезорганизация его структурных компонентов и последующая его несостоятельность. Наиболее частой проблемой такого плана является несостоятельность рубцов у повторнородящих женщин, в анамнезе которых имеется хирургическое родоразрешение путем кесарева сечения. В литературе представлены результаты комплексного изучения рубцов на матке после операции кесарева сечения, в то время как морфологическое исследование кожного рубца у этих же беременных не проводилось. Целью работы было изучить морфофункциональные особенности соединительнотканного рубца на коже у повторнородящих женщин после оперативного родоразрешения. Исследовали фрагмент кожного рубца у 30 женщин после кесарева сечения. У женщин в одной возрастной группе утолщение волокон было прямопропорционально числу родов. При сравнении разных возрастных групп с одинаковым числом родов наблюдали истончение коллагеновых волокон, а также увеличение плотности волокон коллагена 3-го типа. Наиболее выраженные изменения выявлены у женщин с тремя и более родоразрешениями. Можно предположить, что под влиянием кратности растяжений кожи происходит структурная перестройка соединительнотканного рубца в виде истончения и дезорганизации волокнистых структур, что может косвенно говорить о несостоятельности послеоперационного рубца.

Ключевые слова: соединительнотканный рубец, кожа, коллагеновые волокна, регенерация, растяжение, кесарево сечение

Вклад авторов: Е. С. Мишина — дизайн исследования, сбор и обработка материалов, анализ полученных данных, написание текста; М. А. Затолокина, М. В. Мнихович, В. В. Харченко — концепция и редактирование текста; все авторы прочли и одобрили финальную версию статьи.

Соблюдение этических стандартов: исследование одобрено региональным этическим комитетом Курского государственного медицинского университета (протокол № 4 от 10 июня 2019 г.), выполнено с соблюдением этических принципов проведения научных медицинских исследований с участием человека; все участники подписали добровольное информированное согласие на участие в исследовании.

✉ **Для корреспонденции:** Екатерина Сергеевна Мишина
ул. Карла Маркса, д. 3, г. Курск, 305041; katusha100390@list.ru

Статья получена: 11.12.2020 **Статья принята к печати:** 12.01.2021 **Опубликована онлайн:** 22.01.2021

DOI: 10.24075/vrgmu.2021.002

The inevitable outcome of skin injuries caused by a variety of exposures is the formation of a connective tissue scar [1–3]. Some scars, including hypertrophic scars and keloids, can be esthetically displeasing; immature scars are prone to more serious complications. Differences in scar tissue organization and morphology are determined not only by the type of injury but also by the duration and frequency of injurious exposure [4–10]. This might explain the phenomena of wound dehiscence, postoperative hernias and other negative outcomes [11, 12]. As indications for cesarean delivery are expanding, more women of childbearing age are acquiring uterine scars, which, in turn, necessitate cesarean delivery in future pregnancies [13]. In some cases, a C-section is combined with genitoplasty or abdominal wall reinforcement to avert scar dehiscence, the

most common complication of the C-section [14–17]. So, it would be clinically relevant to study cutaneous scar morphology and the reorganization of scar tissue in women with a past history of childbirth.

METHODS

Our study recruited 30 patients of Kursk Maternity Hospital. The following inclusion criteria were applied: the absence of obstetric or gynecologic pathology; delivery by cesarean section. Exclusion criteria: preterm labor; systemic connective tissue disorders. Fig.1 illustrates the distribution of the participants by age.

The mean age of the participants was 33.1 ± 3.93 years; the mean height was 164.3 ± 6.47 cm; the mean weight, 74.57 ± 3.13 kg; the mean BMI, 0.28 ± 0.05 kg/m^2. The total number of pregnancies specified in medical histories was 89. The total number of deliveries was 77. Twenty-three women (76.67%) had a past history of 2 cesarean deliveries; 6 women (20%) had undergone a total of 3 cesarian sections; 1 woman (3.33%) had a history of 4 cesarean deliveries. These figures include cesarean sections performed during the study.

The participants were grouped by age and the number of deliveries. A total of 5 groups with 1 to 12 women in each group)were formed (Table 1).

Specimens of scar tissue with the adjacent flaps of normal skin sized 3 × 6 cm were collected from all study participants after the C-section. For light microscopy, the specimens were fixed in 10% neutral buffered formalin. The specimens were embedded in paraffin and sliced on a microtome following the standard protocol. Sections of 5–7 μm were stained with hematoxylin-eosin and Mallory's trichrome stain. The presence of collagen fibers in the specimens was verified by means of immunohistochemical staining (IHC) with anti-collagen type I and III monoclonal rabbit antibodies (Novocastra; Germany). Staining was performed in an automated LEICA BOND MAX IHC stainer (Leica; Germany). Digital photos geometrically and optically calibrated in ImageJ 14,7a (National Institutes of Health; USA) were further used to measure fiber thickness, the areas of collagen fibers (for each collagen type) and interfiber space in 30 fields of view (×10). The scar density coefficient was calculated using the previously proposed formula:

$K = (S_{c.f.}, \%)/(S_{i.s.}, \%)$,

where K is the scar density coefficient;

$S_{c.f.}$ is the area of collagen fibers;

$S_{i.s.}$ is the area of interfiber space.

Then, the cellular makeup of the sampled scar tissue was analyzed. Based on karyological features (×40), we identified fibroblast cell lineages and proinflammatory cells. Immunophenotyping tests were not performed. Cell count was done per 100 cells in several (at least 10) non-overlapping fields of view. Then, mean values were calculated. Statistical analysis was carried out in Statistika 10.0 (Stat Soft; Russia). The normality of data distribution was tested using the Kolmogorov-Smirnov and the Shapiro–Wilk tests. The significance of differences was assessed using the Mann–Whitney *U* test for independent samples. Differences were considered significant at $p \leq 0.05$.

RESULTS

Fiber analysis revealed that all the studied connective tissue structures were composed of mature granulation tissue. In groups I and III (see Table 1), the fibers lied closest to each other and were organized in one direction. In all groups, the fibers were fairly thick, with dense intrafibrillar structures. However, the major fibers in groups II and V (see Table 1) were composed of multiple thin branching fibers. Cross-sectionally, all fibers were mostly round. The morphometric analysis revealed that collagen fibers in the studied fibrous tissue differed significantly in their thickness between the groups. The thickest fibers were observed in the specimens obtained from women of young reproductive age with a past history of 3 deliveries. The thickness of collagen fibers was 1.2 lower in women of the same age with a past history of 2 deliveries (7.8 ± 0.11 μm). In women of late reproductive age, the thickness of collagen fibers was directly proportional to the number of previous deliveries, decreasing from 6.1 ± 0.12 to 4.7 ± 0.1 μm for women with a history of fewer deliveries.

The analysis of the ratio of collagen fibers area to the area of interfiber space in postoperative scars revealed that connective tissue fibers were more densely arranged in women with a past history of 2 deliveries at young reproductive age. The lowest ratio was observed in women with a history of 3 to 4 deliveries. These morphometric characteristics are shown in Fig. 2.

The IHC study of scar fragments revealed a decrease in collagen content in patients with a history of 2 and 3 deliveries at late reproductive age. Type I collagen was the most prevalent in the scar tissue of younger women (Table 2).

The dynamics of inflammation and tissue repair was analyzed by means of cell count in the scar tissue. The analysis revealed that collagen synthesis was the dominant process in the scar tissue of all study participants at the end of gestation. However, the fact that immature fibroblast lineage cells dominated the cellular composition of scars in women of late reproductive age led us to hypothesize that collagen synthesis was still ongoing. The dynamics of scar tissue cellular composition is illustrated in Fig. 3.

DISCUSSION

With regard to the dynamics of cutaneous scar tissue structure, the roughness and thickness of collagen fibers were directly

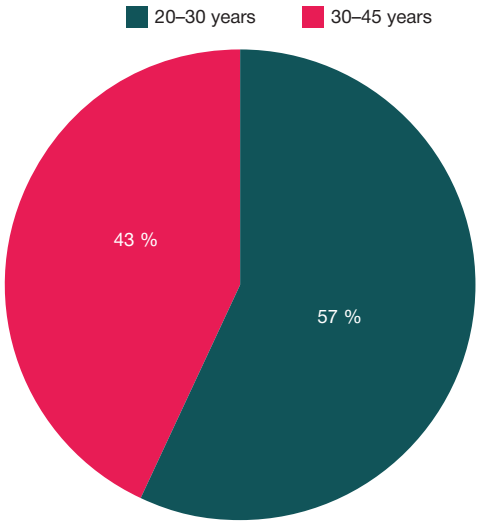

Fig. 1. The distribution of the participants by age

Table 1. The distribution of the participants by age and the number of cesarean deliveries

Age	Number of deliveries		
	2	3	4
20–30 years	Group I	Group III	
31–40 years	Group II	Group IV	Group V

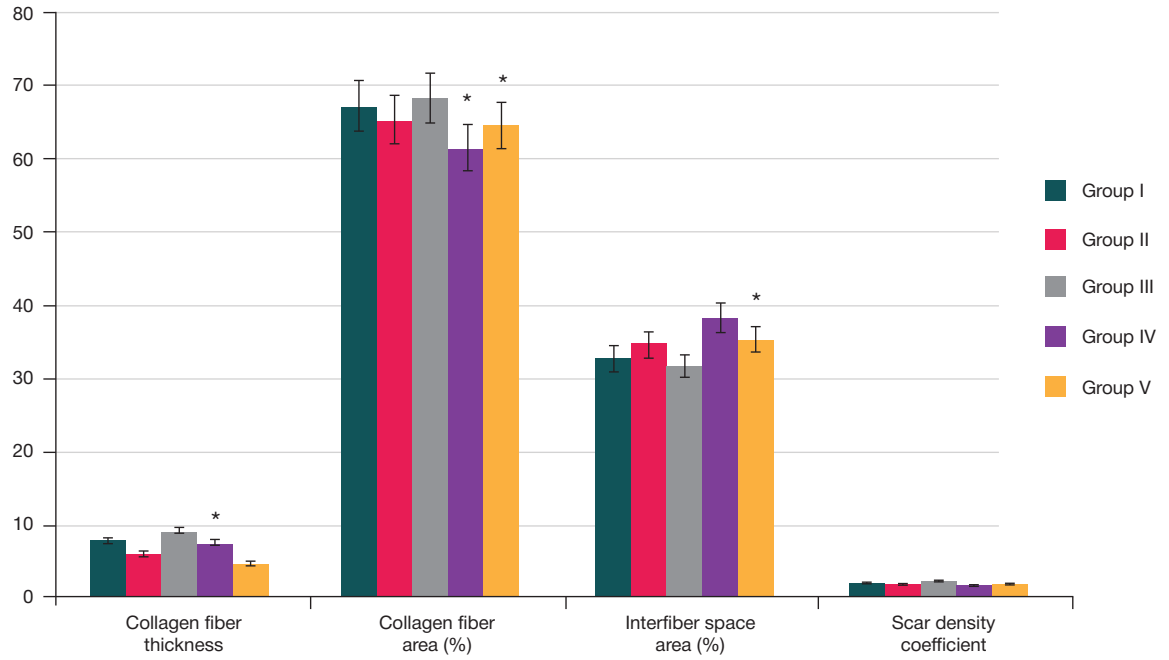

Fig. 2. The dynamics of morphometric characteristics of fibrous tissue. * — differences are statistically significant relative to the previous group ($p \leq 0.05$)

Table 2. The distribution of collagen types in the scar tissue between different groups of patients

Group	Type I collagen density	Type II collagen density	Type 1 to 3 collagen ratio
I	23.4 ± 1.1*	20.7 ± 1.2	1.1 ± 0.32
II	19.6 ± 0.76	18.9 ± 1.3	1.03 ± 0.1
III	23.4 ± 1.1	25.9 ± 1.2*	0.9 ± 0.07
IV	14.9 ± 1.3*	10.7 ± 0.4*	1.4 ± 0.05
V	17.9 ± 1.3	16.6 ± 0.5	1.07 ± 0.05

Note: * — differences are statistically significant relative to the previous group ($p \leq 0.05$).

proportional to the number of previous deliveries (groups I and III). The densest scars with the narrowest interfiber space were observed in young women with a history of 3 deliveries. Comparison of different age groups with the same number of past deliveries revealed collagen fiber thinning. These structural changes were the most pronounced in groups IV and V, i.e. in women with a past history of 3 or more deliveries. One of the main characteristics of a mature scar is its thickness and

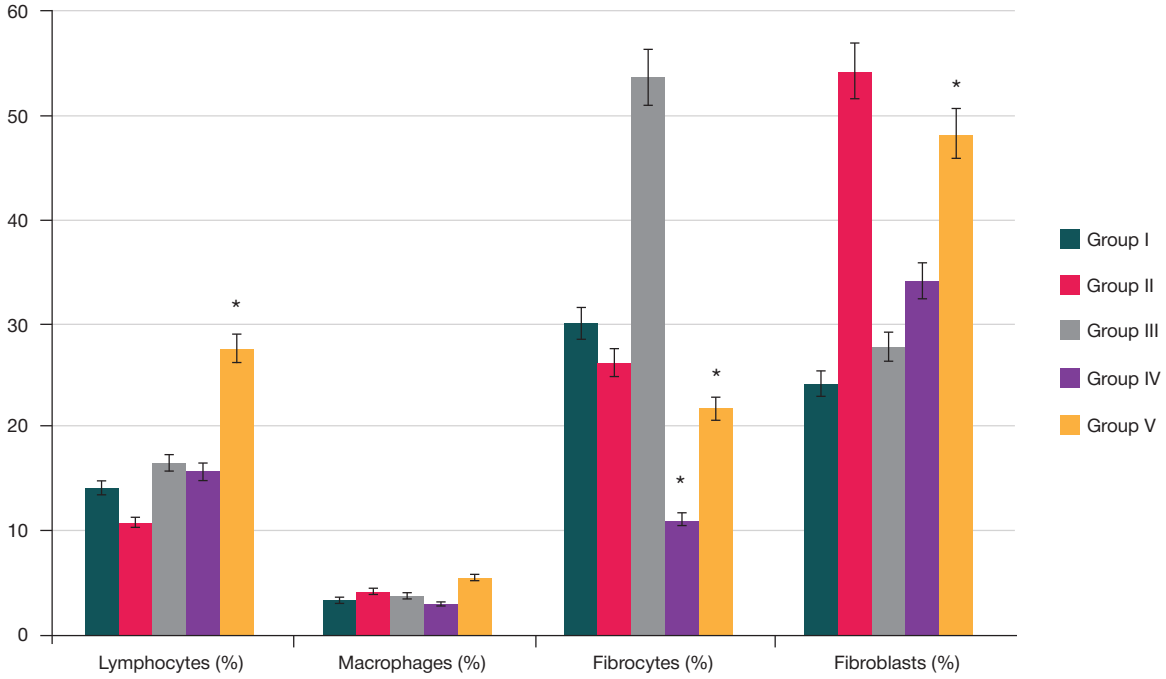

Fig. 3. The dynamics of scar tissue cellular composition. * — differences are statistically significant relative to the previous group ($p \leq 0.05$)

structural heterogeneity [18]. The scar density coefficient calculated in the study reflects fiber thickness and the size of the interfiber space. The greater is the scar density coefficient, the thicker is the scar and the less pronounced is the interstitial edema, which can expand the interfiber space. The obtained data are indirectly suggestive of scar tissue dehiscence after the third delivery in young patients. The analysis of collagen types distribution demonstrated that the greatest number of fibrous structures made up of type III collagen was observed in young women; in older women, scar tissue was mainly composed of type I collagen. These data are consistent with the data on the mechanisms of collagen synthesis in uterine scars. Immunohistochemically, connective tissue is characterized by moderate expression of type III collagen [19]. Cellular mechanisms play a significant role in the formation of a mature scar. One of the most important criteria of a mature scar is the completion of the inflammation phase, i.e. a decline in lymphocyte and granulocyte counts [20]. The analysis of scar tissue cellular composition demonstrated that the morphology of the examined scars was consistent with mature granulation tissue dominated by fibroblast lineage cells.

CONCLUSION

Low inflammation levels, the cessation of collagen synthesis and the prevalence of fibroblast lineage cells are prerequisites for a sound scar. Microscopically, a sound scar is characterized by dense bundles of collagen fibers separated by small interfiber spaces. Repeated stretching causes fibrous structures to become thinner and dissociate. This morphological picture can be an indirect indication for abdominal wall and suture reinforcement with synthetic materials.

References

1. Duhanin AS, Malkin PA, Shimanovskij NL. Vnutrikletochnyj ph kak rannij differencial'nyj marker gljukokortikoid-inducirovannogo apoptoza fibroblastov kozhi. Vestnik rossijskogo gosudarstvennogo medicinskogo universiteta. 2013; 1: 54–57. Russian.
2. Lyahoveckij BI, Glazkova LK, Peretolchina TF. Kozhnye priznaki nedifferencirovannoj displazii soedinitel'noj tkani. Sovremennye problemy dermatovenerologii, immunologii i vrachebnoj kosmetologii. 2012; 1 (20): 30–35. Russian.
3. Shishkina VV, Atjakshin DA. Tuchnye kletki i fibrillogenez kollagena v uslovijah nevesomosti. Zhurnal anatomii i gistopatologii. 2019; 8 (3): 79–88. Russian.
4. Mishina ES, Zatolokina MA, Sergeeva SYu. Izuchenie faktorov dinamicheskogo strukturirovanija kollagenovyh volokon v jeksperimente. Morfologija. 2019; 11 (2): 199. Russian.
5. Omelyanenko NP, Sluckij LI. Soedinitel'naja tkan' (gistofiziologija i biohimija). M.: Izvestija, 2009; 1: 380. Russian.
6. Fetisov SO, Alekseeva NT, Nikityuk DB, Serezhenko NP, Atyakshin DA. Modelirovanie kak metod ocenki specificheskih morfofunkcional'nyh patternov pri regeneracii. Zhurnal anatomii i gistopatologii. 2015; 4 (4): 49–55. Russian.
7. Rittie L, editor. Fibrosis: methods and protocols. Humana Press, 2017; 530 p.
8. Ghazanfari S, Khademhosseini A, Smit TH. Mechanisms of lamellar collagen formation in connective tissues. Biomaterials. 2016; 97: 74–84.
9. Harris JR, Lewis RJ. The collagen type I segment long spacing (SLS) and fibrillar forms: Formation by ATP and sulphonated diazo dyes. Micron. 2016; 86: 36–47.
10. Lu Y, Zhou Q, Lu JW, Wang WS, Sun K. Involvement of STAT3 in the synergistic induction of 11β-HSD1 by SAA1 and cortisol in human amnion fibroblasts. Am J Reprod Immunol. 2019 Aug; 82 (2): e13150. DOI: 10.1111/aji.13150.
11. Grigoreva YuV, Suvorova GN, Bormotov AV, Chemidronov SN. K voprosu o roli kollagena III tipa v shejke matki krys pri beremennosti i rodah. Zhurnal anatomii i gistopatologii. 2015; 4 (3): 29–39. Russian.
12. Mnihovich MV, Sokolov DA, Zagrebin VL. Ot anatomii i gistologii k klinicheskoj patologii. Zhurnal anatomii i gistopatologii. 2017; 3: 29–30. Russian.
13. Ji Won Kwon, Won-Jae Lee, Si-Bog Park. Generalized joint hypermobility in healthy female koreans: prevalence and age-related differences. Ann Rehabil Med. 2013; 37 (6): 832–8.
14. Vasin RV, Filimonov VB, Mnihovich MV, Kaprin AD. Morfologicheskaja struktura i immunogistohimicheskij analiz stenok vlagalishha u zhenshhin s prolapsom genitalij. Urologija. 2019; 6: 12–20. Russian.
15. Gasparov AC, Dubinskaya ED, Babicheva IA, Lapteva NB. Rol' displazii soedinitel'noj tkani v akushersko-ginekologicheskoj praktike. Kazanskij medicinskij zhurnal. 2014; 95 (6): 897–904. Russian.
16. Shevlyuk NN, Gatiatullin IZ, Stadnikov AA. Osobennosti reparativnyh gistogenezov pri ispol'zovanii bioplasticheskih materialov. Zhurnal anatomii i gistopatologii. 2020; 9 (1): 86–93. Russian.
17. Moalli PA, Shand SH, Zyczynski HM. Remodeling of vaginal connective tissue in patients with prolapse. Obstet Gynecol. 2005; 106: 953–63.
18. Ajlamazyan YeK, Kulakov VI, Radzinskij VE, Saveleva GM, redaktory. Akusherstvo, nacional'noe rukovodstvo. M., 2007; 1197 s. Russian.
19. Kazaryan RM, Apresyan SV, Orazmuradov AA, Knyazev SA. Geneticheskie i morfologicheskie osobennosti rubca na matke posle kesareva sechenija. Vestnik Rossijskogo universiteta druzhby narodov. Serija: Medicina. 2008; 1: 12–17. Russian.
20. Telegina IV, Pavlov RV, Selkov SA. Osobennosti formirovanija rubca na matke posle kesareva sechenija v zavisimosti ot haraktera rodorazreshenija. Zhurnal akusherstva i zhenskih boleznej. 2013; 4 (62): 61–66. Russian.

Литература

1. Духанин А. С., Малкин П. А., Шимановский Н. Л. Внутриклеточный ph как ранний дифференциальный маркер глюкокортикоид-индуцированного апоптоза фибробластов кожи. Вестник российского государственного медицинского университета. 2013; 1: 54–57.
2. Ляховецкий Б. И., Глазкова Л. К., Перетолчина Т. Ф. Кожные признаки недифференцированной дисплазии соединительной ткани. Современные проблемы дерматовенерологии, иммунологии и врачебной косметологии. 2012; 1 (20): 30–35.
3. Шишкина В. В., Атякшин Д. А. Тучные клетки и фибриллогенез коллагена в условиях невесомости. Журнал анатомии и гистопатологии. 2019; 8 (3): 79–88.
4. Мишина Е. С., Затолокина М. А., Сергеева С. Ю. Изучение факторов динамического структурирования коллагеновых волокон в эксперименте. Морфология. 2019; 11 (2): 199.
5. Омельяненко Н. П., Слуцкий Л. И. Соединительная ткань (гистофизиология и биохимия). М.: Известия, 2009; 1: 380.
6. Фетисов С. О., Алексеева Н. Т., Никитюк Д. Б., Сереженко Н. П., Атякшин Д. А. Моделирование как метод оценки специфических морфофункциональных паттернов при регенерации. Журнал

анатомии и гистопатологии. 2015; 4 (4): 49–55.
7. Rittie L, editor. Fibrosis: methods and protocols. Humana Press, 2017; 530 p.
8. Ghazanfari S, Khademhosseini A, Smit TH. Mechanisms of lamellar collagen formation in connective tissues. Biomaterials. 2016; 97: 74–84.
9. Harris JR, Lewis RJ. The collagen type I segment long spacing (SLS) and fibrillar forms: Formation by ATP and sulphonated diazo dyes. Micron. 2016; 86: 36–47.
10. Lu Y, Zhou Q, Lu JW, Wang WS, Sun K. Involvement of STAT3 in the synergistic induction of 11β-HSD1 by SAA1 and cortisol in human amnion fibroblasts. Am J Reprod Immunol. 2019 Aug; 82 (2): e13150. DOI: 10.1111/aji.13150.
11. Григорьева Ю. В., Суворова Г. Н., Бормотов А. В., Чемидронов С. Н. К вопросу о роли коллагена III типа в шейке матки крыс при беременности и родах. Журнал анатомии и гистопатологии. 2015; 4 (3): 29–39.
12. Мнихович М. В., Соколов Д. А., Загребин В. Л. От анатомии и гистологии к клинической патологии. Журнал анатомии и гистопатологии. 2017; 3: 29–30.
13. Ji Won Kwon, Won-Jae Lee, Si-Bog Park. Generalized joint hypermobility in healthy female koreans: prevalence and age-related differences. Ann Rehabil Med. 2013; 37 (6): 832–8.
14. Васин Р. В., Филимонов В. Б., Мнихович М. В., Каприн А. Д. Морфологическая структура и иммуногистохимический анализ стенок влагалища у женщин с пролапсом гениталий. Урология. 2019; 6: 12–20.
15. Гаспаров А. С., Дубинская Е. Д., Бабичева И. А., Лаптева Н. В. Роль дисплазии соединительной ткани в акушерско-гинекологической практике. Казанский медицинский журнал. 2014; 95 (6): 897–904.
16. Шевлюк Н. Н., Гатиатуллин И. З., Стадников А. А. Особенности репаративных гистогенезов при использовании биопластических материалов. Журнал анатомии и гистопатологии. 2020; 9 (1): 86–93.
17. Moalli PA, Shand SH, Zyczynski HM. Remodeling of vaginal connective tissue in patients with prolapse. Obstet Gynecol. 2005; 106: 953–63.
18. Айламазян Э. К., Кулаков В. И., Радзинский В. Е., Савельева Г. М., редакторы. Акушерство, национальное руководство. М., 2007; 1197 с.
19. Казарян Р. М., Апресян С. В., Оразмурадов А. А., Князев С. А. Генетические и морфологические особенности рубца на матке после кесарева сечения. Вестник Российского университета дружбы народов. Серия: Медицина. 2008; 1: 12–17.
20. Телегина И. В., Павлов Р. В., Сельков С. А. Особенности формирования рубца на матке после кесарева сечения в зависимости от характера родоразрешения. Журнал акушерства и женских болезней. 2013; 4 (62): 61–66.

ELEMENTAL COMPOSITION OF BLOOD OF INFERTILE PATIENTS PARTICIPATING IN ASSISTED REPRODUCTION PROGRAMS

Syrkasheva AG ✉, Frankevich VE, Dolgushina NV

Kulakov National Medical Research Center for Obstetrics, Gynecology and Perinatology, Moscow, Russia

The association between levels of trace elements, endocrine diseases and reproductive impairments is actively investigated currently. In this connection, it seems relevant to study elemental status (elemental composition of blood and amounts of elements therein) of infertile patients enlisted in programs employing assisted reproductive technologies (ART). This study aimed to analyze trace elements in blood of infertile patients, relationship between the level of such trace elements and parameters of the ART programs they are in. The study included 30 infertile patients aged 18–39 years. Relying on inductively coupled plasma mass spectrometry, we identified concentrations of 31 chemical element in blood of the participants. Two elements out of 31 (antimony and beryllium) were not found in any blood sample; 10 elements (titanium, chromium, cobalt, nickel, arsenic, mercury, barium, gold, vanadium) were detected in some blood samples, the remaining 19 elements were found in all samples. Age of the patients correlated negatively with the level of silicon (r = –0.384; p = 0.036) and positively with the level of molybdenum (r = 0.384; p = 0.036). The level of anti-mullerian hormone was in a significant negative correlation with the level of lithium (r = –0.367; p = 0.046). The level of free thyroxine was in a significant negative correlation with the level of boron (r = –0.402; p = 0.028) and a positively correlated with the levels of iron (r = 0.410; p = 0.024) and silver (r = 0.432; p = 0.017). Considering the embryological cycle, we noted a positive correlation between the level of silicon and the number of blastocysts obtained (r = 0.387; p = 0.034). There was no statistical relationship registered between elemental composition of blood the frequency of pregnancy in ART cycles.

Keywords: assisted reproductive technologies, embryos, pregnancy, heavy metals, mass spectrometry, trace elements, blood elemental status, AMH

Author contribution: Syrkasheva AG — conducting the clinical stage of the study, statistical processing of data, article authoring; Frankevich VE — conducting mass spectrometric studies; Dolgushina NV — article authoring, final review.

Compliance with ethical standards: the study was approved by the ethics committee of the V.I. Kulakov National Medical Research Center for Obstetrics, Gynecology and Perinatology (Minutes #10 of October 20, 2016).

✉ **Correspondence should be addressed:** Anastasia G. Syrkasheva
Akademika Oparina, 4, Moscow, 117997; a_syrkasheva@oparina4.ru

Received: 10.02.2021 **Accepted:** 24.02.2021 **Published online:** 28.02.2021

DOI: 10.24075/brsmu.2021.010

ЭЛЕМЕНТНЫЙ СОСТАВ КРОВИ ПАЦИЕНТОК С БЕСПЛОДИЕМ В ПРОГРАММАХ ВСПОМОГАТЕЛЬНЫХ РЕПРОДУКТИВНЫХ ТЕХНОЛОГИЙ

А. Г. Сыркашева ✉, В. Е. Франкевич, Н. В. Долгушина

Национальный медицинский исследовательский центр акушерства, гинекологии и перинатологии имени В. И. Кулакова, Москва, Россия

В связи с активным изучением ассоциаций между уровнями микроэлементов, эндокринными заболеваниями и нарушением репродуктивной функции представляется актуальным изучение элементного статуса у пациенток с бесплодием в программах вспомогательных репродуктивных технологий (ВРТ). Целью работы было проанализировать у пациенток с бесплодием содержание микроэлементов, связь между уровнем микроэлементов в их крови и параметрами программ ВРТ. В исследование включено 30 пациенток с бесплодием в возрасте 18–39 лет. Определяли концентрации 31 химического элемента в крови пациенток методом масс-спектрометрии с индуктивно-связанной плазмой. Два элемента из 31 (сурьма и бериллий) не были обнаружены ни в одном образце крови, 10 элементов (титан, хром, кобальт, никель, мышьяк, ртуть, барий, золото, ванадий) выявлены в части образцов крови, оставшиеся 19 элементов — во всех образцах. Возраст пациенток находился в отрицательной корреляционной связи с уровнем кремния (r = –0,384; p = 0,036) и в положительной — с уровнем молибдена (r = 0,384; p = 0,036). Уровень антимюллерова гормона находился в значимой отрицательной корреляционной связи с уровнем лития (r = –0,367; p = 0,046). Уровень свободного тироксина находился в значимой отрицательной корреляционной связи с уровнем бора (r = –0,402; p = 0,028) и положительной корреляционной связи с уровнем железа (r = 0,410; p = 0,024) и серебра (r = 0,432; p = 0,017). При оценке эмбриологического этапа отмечена положительная корреляционная связь между уровнем кремния и числом полученных бластоцист (r = 0,387; p = 0,034). Не выявлено статистической зависимости между элементным составом крови и частотой наступления беременности в циклах ВРТ.

Ключевые слова: вспомогательные репродуктивные технологии, эмбрионы, беременность, тяжелые металлы, масс-спектрометрия, микроэлементы, элементный состав крови, АМГ

Вклад авторов: А. Г. Сыркашева — проведение клинического этапа исследования, статистическая обработка данных, написание текста статьи; В. Е. Франкевич — проведение масс-спектрометрических исследований, Н. В. Долгушина — написание текста статьи, финальное рецензирование.

Соблюдение этических стандартов: исследование одобрено этическим комитетом НМИЦ АГП им. В. И. Кулакова (протокол № 10 от 20 октября 2016 г.).

✉ **Для корреспонденции:** Анастасия Григорьевна Сыркашева
ул. Академика Опарина, г. Москва, 4117485; a_syrkasheva@oparina4.ru

Статья получена: 10.02.2021 **Статья принята к печати:** 24.02.2021 **Опубликована онлайн:** 28.02.2021

DOI: 10.24075/vrgmu.2021.010

The term "trace elements" appeared in the middle of the 20th century. According to the definition from the Medical Encyclopedic Dictionary, trace elements are chemical elements contained in body tissues at the concentrations of 1:100,000 or below. There are essential (necessary) trace elements, which are bioelements vitally important for sustaining life. They are integral components of the human body. There are also conditionally essential trace elements, for which there is a growing body of evidence backing their role in supporting normal functioning of the body. Finally, there are toxic or potentially toxic trace elements, those that the body holds in small amounts only, with their role and possible negative effects not well understood currently [1].

The world scientific community has grown interested in trace elements when researchers began investigating specific diseases that have a direct connection with certain elements. The most prominent examples of such diseases are the Minamata disease (mercury poisoning) and Itai-Itai (cadmium poisoning).

Elemental status is also well known to play a role in development of other diseases, as is the case with iron deficiency and anemia, iodine deficiency and thyroid pathology, zinc deficiency and skin diseases and nervous system disorders.

However, this area of medicine remains one of the least studied. Firstly, this is due to the low concentrations of various trace elements in the human body: detecting and quantifying them requires application of complex and expensive methods. Secondly, there are no data on the metabolism of rare trace elements in the body: samples of human blood and/or hair are mainly used to study them. Thirdly, changes in the composition of trace elements are well studied only in the context of specific diseases. Currently, researchers actively develop this area. For example, there are studies aimed at uncovering the relationship between changes in the composition of trace elements and endocrine system diseases [2, 3].

In 1984, the International Society for Trace Element Research in Humans was founded. Its goals are to consolidate and distribute data on the biological role of trace elements in various pathological processes in human beings.

Investigating the role of trace elements in reproductive disorders is a difficult yet rewarding task. Patients participating in programs relying on assisted reproductive technologies (ART) are an interesting group to study. Firstly, they are young women without chronic somatic diseases and with good medical examination results (the examination mandatory before joining an ART program). Secondly, this group allows studying the embryological parameters, such as quality of oocytes and embryos, frequency of oocyte fertilization. Therefore, we decided to select this category of patients for the present study.

This study aimed to analyze the content of trace elements in infertile patients, investigate the relationship between the level of trace elements in their blood and the parameters of ART programs designed for them.

METHODS

The study included 30 patients who applied for ART infertility treatment 2017 to 2018. The inclusion criteria were: no contraindications for ART; normal karyotype of both spouses; absence of severe male factor (100% teratozoospermia, absolute asthenozoospermia, all types of azoospermia); age 18 through 39 years; body mass index (BMI) 19–25 kg/m^2. All the participating patients have been residents of Moscow for the last 5 years. The exclusion criteria were: use of donor gametes, surrogacy; obtaining three or less oocytes on the day of transvaginal ovarian puncture.

All the couples included in the study were examined as necessary before enrolling in an ART program [3].

Ovarian stimulation followed the protocol with gonadotropin releasing hormone antagonists [4]. For transvaginal ovarian puncture and oocyte aspiration, we relied on the standard technique [4].

Venous blood was sampled for examination on the day of transvaginal puncture; the samples, once taken, were cryopreserved at –70 °C. Inductively coupled plasma mass spectrometry enabled quantification of essential and toxic trace elements in the patients' blood. The laboratory that studied the samples had no access to the clinical particulars of the participants. We identified concentrations of the following trace elements: lithium (Li), boron (B), sodium (Na), magnesium (Mg), aluminum (Al), silicon (Si), potassium (K), calcium (Ca), titanium (Ti), chromium (Cr), manganese (Mn), iron (Fe), cobalt (Co), nickel (Ni), copper (Cu), zinc (Zn), arsenic (As), selenium (Se), molybdenum (Mo), cadmium (Cd), antimony (Sb), mercury (Hg), lead (Pb), barium (Ba), gold (Au), vanadium (V), silver (Ag), beryllium (Be), bismuth (Bi), tungsten (W), gallium (Ga) (31 elements).

The oocytes were fertilized in vitro, following the "classical" *in vitro* fertilization (IVF) technique, or through intracytoplasmic sperm injection (ICSI). The embryos were cultivated and transfered using methods accepted in clinical practice [4].

Fourteen days after transfer to the uterine cavity, we measured the concentration of β-hCG in the patient's blood. In case of registration of the embryo's heartbeat 5 weeks after the transfer, we announced clinical pregnancy.

SPSS 22 (IBM; USA) software package enabled statistical analysis. Normally distributed data were presented as mean (standard deviation). In comparison of category variables, our statistical analysis relied on the χ^2 test, in comparison of medians — on the Mann–Whitney test. Abnormally distributed data were presented as median (interquartile range). Pearson criterion was factored into the correlation analysis.

The differences between statistical values were considered significant at $p < 0.05$.

RESULTS

We analyzed concentrations of 31 chemical element in blood of 30 patients. Two elements (antimony and beryllium) were not found in any blood sample; 10 elements (titanium, chromium, cobalt, nickel, arsenic, mercury, barium, gold, vanadium) were detected in some blood samples, the remaining 19 elements were found in all samples. Table 1 presents the chemical elements distribution data.

Age of the patients correlated negatively with the level of silicon ($r = –0.384$; $p = 0.036$) and positively with the level of molybdenum ($r = 0.384$; $p = 0.036$). Body weight and BMI were not connected to the patients' elemental status.

In smoking patients ($n = 5$), the median calcium level was significantly ($p = 0.02$) lower than in non-smokers ($n = 25$): 98.2 mg/l versus 102.4 mg/l.

Assessing the obstetric history, we noted that the number of pregnancies positively correlated with the patient's levels of sodium ($r = 0.455$; $p = 0.012$) and chromium ($r = 0.484$; $p = 0.007$).

Studying gynecological histories of the patients, we found no connection between the level of trace/macroelements and recorded gynecological diseases (endometriosis, myoma, inflammatory diseases of the pelvic organs), primary or secondary infertility and duration thereof.

Analyzing laboratory indicators of the patients, we discovered a relationship the level of trace elements, anti-mullerian hormone (AMH) and free thyroxine ($T4_{free}$). The level of AMH was in a significant negative correlation with the level of lithium ($r = –0.367$; $p = 0.046$). The level of free thyroxine correlated negatively (significant correlation) with the level of boron ($r = –0.402$; $p = 0.028$) and positively with the levels of iron ($r = 0.410$; $p = 0.024$) and silver ($r = 0.432$; $p = 0.017$) (Table 2).

Evaluation of features of the ovarian stimulation protocol revealed a relationship between the total dose of gonadotropins, the duration of stimulation, the levels of aluminum, zinc, selenium and barium (Table 3).

Analysis of the parameters of oogenesis and early embryogenesis allowed discovering a positive correlation

Table 1. Concentrations of essential and toxic trace elements in patients

Element	Detection frequency	Median	Interquartile range	Minimum/maximum
Lithium (Li), μg/l	100%	18.17	1.01–34.43	10.22–29.83
Boron (B), μg/l	100%	141.6	84.0–165.7	68.6–206.5
Sodium (Na), mg/l	100%	3213.5	3070.0–3459.0	2946.0–3567.0
Magnesium (Mg), mg/l	100%	20.0	18.8–21.4	13.3–25.9
Aluminum (Al), μg/l	100%	60.145	51.55–85.03	24.19–126.45
Silicon (Si), μg/l	100%	493.200	179.9–636.9	38.5–892.1
Potassium (K), mg/l	100%	165.5	152.0–190.0	136.0–210.0
Calcium (Ca), mg/l	100%	100.550	95.2–106.0	92.3–109.5
Titanium (Ti), μg/l	93.3% (n = 28)	2.745	1.88–3.56	0–4.95
Chromium (Cr), μg/l	26.7% (n = 8)	0	0–1.41	0–0.40
Manganese (Mn), μg/l	80.0% (n = 24)	0.76	0.63–0.93	0–1.59
Iron (Fe), μg/l	100%	1377.5	965.0–1754.0	401.0–2568.0
Cobalt (Co), μg/l	76.7% (n = 23)	0.197	0.113–0.339	0–0.412
Nickel (Ni), μg/l	36.7% (n = 11)	0	0–0.61	0–6.18
Copper (Cu), μg/l	100%	1401.5	1121.0–1740.0	788.0–2427.0
Zinc (Zn), μg/l	100%	873.0	781.0–960.0	593.0–1150.0
Arsenic (As), μg/l	96.7% (n = 29)	0.41	0.23–0.80	0–3.20
Selenium (Se), μg/l	100%	85.3	76.5–95.6	55.0–119.5
Molybdenum (Mo), μg/l	100%	0.705	0.640–0.860	0.400–1.150
Cadmium (Cd), μg/l	100%	0.275	0.20–0.38	0.1–2.42
Antimony (Sb), μg/l	0	–	–	–
Mercury (Hg), μg/l	96.7% (n = 29)	0.19	0.14–0.41	0–0.70
Lead (Pb), μg/l	100%	8.970	7.43–12.98	4.80–17.86
Barium (Ba), μg/l	40.0% (n = 12)	0	0–0.55	0–2.28
Gold (Au), μg/l	96.7% (n = 29)	0.034	0.019–0.072	0–0.099
Vanadium (V), μg/l	3.3% (n = 1)	0	0–0	0–0.278
Silver (Ag), μg/l	100%	0.270	0.160–0.760	0.030–3.410
Beryllium (Be), μg/l	0	–	–	–
Bismuth (Bi), μg/l	100%	2.068	0.935–2.839	0.107–3.408
Tungsten (W), μg/l	100%	0.034	0.028–0.045	0.0015–0.050
Gallium (Ga), μg/l	100%	0.007	0.005–0.009	0.001–0.010

between the number of blastocysts obtained and the level of silicon (r = 0.387; p = 0.034). No other significant differences between levels of trace elements and parameters of oogenesis/early embryogenesis were detected.

Clinical pregnancy was registered in 15 cases (50%). The level of trace elements did not differ significantly in patients with different ART program outcomes (p > 0.05).

DISCUSSION

The number of studies demonstrating relationship between a person's elemental status and peculiarities of various diseases in this person has been growing in the recent years [2, 5, 6]. In a healthy body, homeostatic mechanisms keep the levels of trace elements within physiological range. However, against the background of changing external conditions (as a rule — changes in diet and the surrounding environment, ecology), the balance of trace elements may be broken, which leads to a deficiency or, conversely, an excess of certain substances [3]. Such conditions are difficult to diagnose, mainly due to the lack of a characteristic clinical picture associated with them and problematic access to laboratories capable of analyzing elemental composition of the human body. The discussion about the ideal matrix for trace element analysis (blood/urine/hair) is ongoing [1, 7]. It should also be remembered that it is still unclear what roles many of the trace elements play in the human body, same as the processes of metabolism of trace elements. Elemental status of a person may depend on sex, age and other less obvious attributes [8]. All these factors make research in this area extremely promising.

In this study, we evaluated elemental status of blood of infertile patients who applied for ART programs. One of the inclusion criteria required residency in a region of Russia favorable from the point of view of the trace element balance [9]. Selection of patients with certain clinical characteristics reduces the likelihood of influence of known factors (obesity, endocrine diseases, ecologically unfavorable region of residence) on the elemental status.

The study revealed a relationship between elemental composition of the patients' blood and their clinical characteristics, but uncovered no connection between the women's elemental status and ART program outcomes.

Age of the patients was negatively associated with the level of silicon, while correlating positively with the level of molybdenum. Molybdenum is an essential trace element; silicon can be called an element "probably necessary" for functioning of a human body. Silicon is concentrated in connective tissue: arterial walls, tendons, skin. It is assumed that the content of silicon

Table 2. Correlation between hormonal parameters and elemental composition of the patients' blood

	AMH	$T4_{free}$	Lithium	Boron	Iron	Silver
AMH	1	*r* = 0.130	*r* = –0.367	*r* = –0.055	*r* = 0.040	*r* = 0.253
		h = 0.495	*p* = 0.046	*p* = 0.773	*p* = 0.835	*p* = 0.177
$T4_{free}$	*r* = 0.130	1	*r* = 0.183	*r* = –0.402	*r* = 0.410	*r* = 0.432
	h = 0.495		*p* = 0.334	*p* = 0.028	*p* = 0.024	*p* = 0.017
Lithium	*r* = –0.367	*r* = 0.183	1	*r* = 0.104	*r* = 0.258	*r* = –0.281
	p = 0.046	*p* = 0.334		*p* = 0.583	*p* = 0.168	*p* = 0.133
Boron	*r* = –0.055	*r* = –0.402	*r* = 0.104	1	*r* = –0.074	*r* = –0.329
	p = 0.773	*p* = 0.028	*p* = 0.583		*p* = 0.698	*p* = 0.076
Iron	*r* = 0.040	*r* = 0.410	*r* = 0.258	*r* = –0.074	1	*r* = –0.59
	p = 0.835	*p* = 0.024	*p* = 0.168	*p* = 0.698		*p* = 0.758
Silver	*r* = 0.253	*r* = 0.432	*r* = –0.281	*r* = –0.329	*r* = –0.59	1
	p = 0.177	*p* = 0.017	*p* = 0.133	*p* = 0.076	*p* = 0.758	

in the human body changes with age, but the mechanisms behind this change have not been described exhaustively [10]. Molybdenum plays a controversial role in the human body. It is a component of various enzymes. Molybdenum preparations are traditionally used to treat Wilson's disease; in addition, there are reported cases when it was used successfully to treat Crohn's disease [11]. Researchers have shown angiogenesis suppressing properties of molybdenum preparations in the context of pre-clinical anticancer drug studies [12]. At the same time, at elevated concentrations, this metal is toxic. High level of molybdenum in the blood translates into higher risk of arterial hypertension and other cardiovascular diseases [13]. Further research is needed to assess the negative effects of molybdenum on human health.

Osteoporosis and osteopenia are the background conditions for studies analyzing the effect of smoking on calcium metabolism [14]. In our study, smoking patients had reduced calcium levels compared with nonsmokers. Calcium is an important element for a human body; during pregnancy and lactation, the need for this element increases significantly. The data obtained can be used in counseling patients, recommending smoking cessation during pregnancy planning.

The analysis of laboratory indicators showed a negative correlation between levels of lithium and AMH. AMH is most widely used descriptor of ovarian reserve. Lithium preparations have long been used to treat psychiatric conditions (mainly manic depressive disorders). In some cases, it is necessary to continue taking lithium preparations during pregnancy, which is why researchers pay special attention to evaluation of their negative impact on the reproductive and endocrine systems [15]. A group of Iranian researchers demonstrated a decrease in the expression of genes for steroidogenesis in rat ovaries [16]. The connection between lithium and human ovarian reserve values requires further study.

The level of free thyroxine is connected with the levels of iron, boron and silver. At the same time, there was no connection registered between the levels of thyroid-stimulating hormone and trace elements. Various authors have reported negative relationship between boron and the level of thyroid hormones in animals [17, 18]. In laboratory animals, boron preparations were associated with development of hypothyroidism. Boron regulates the activity of parathyroid hormone, which may explain the link between boron and trace element levels.

Analyzing the ovarian stimulation protocol, we discovered a connection between the levels of aluminum and zinc and the total dose of gonadotropins, as well as a relationship between selenium, barium and the duration of ovarian stimulation. No other studies published report such correlations. Overall, the number of days of stimulation correlates with the duration of the patient cycle's follicular phase, which, in turn, is associated with the ovarian reserve. Duration of the cycle may be influenced by the increased levels of selenium, which is a coenzyme of glutathione peroxidase, an antioxidant enzyme. At the same time, growing level of selenium may be a compensatory response to the increasing concentration of barium, a toxic heavy metal, since selenium plays a key role in detoxification of heavy metals.

Table 3. Features of the superovulation stimulation protocol and elemental composition of the patients' blood

	Number of days of stimulation	Total dose of gonadotropins	Aluminum	Zinc	Selenium	Barium
Number of days of stimulation	1	*r* = 0.318	*r* = 0.209	*r* = 0.296	*r* = 0.409	*r* = 0.562
		p = 0.087	*p* = 0.268	*p* = 0.113	*p* = 0.025	*p* = 0.001
Total dose of gonadotropins	*r* = 0.318	1	*r* = 0.588	*r* = 0.469	*r* = 0.246	*r* = 0.029
	p = 0.087		*p* = 0.001	*p* = 0.009	*p* = 0.190	*p* = 0.881
Aluminum	*r* = 0.209	*r* = 0.562	1	*r* = 0.354	*r* = 0.006	*r* = –0.153
	p = 0.268	*p* = 0.001		*p* = 0.055	*p* = 0.977	*p* = 0.420
Zinc	*r* = 0.296	*r* = 0.469	*r* = 0.354	1	*r* = 0.351	*r* = 0.175
	p = 0.113	*p* = 0.009	*p* = 0.055		*p* = 0.057	*p* = 0.355
Selenium	*r* = 0.409	*r* = 0.246	*r* = 0.006	*r* = 0.351	1	*r* = 0.492
	p = 0.025	*p* = 0.190	*p* = 0.977	*p* = 0.057		*p* = 0.006
Barium	*r* = 0.562	*r* = 0.029	*r* = –0.153	*r* = 0.175	*r* = 0.492	1
	p = 0.001	*p* = 0.881	*p* = 0.420	*p* = 0.355	*p* = 0.006	

We have identified a positive link between total gonadotropin dose and zinc and aluminum levels, with a weak positive association between these elements. Zinc is a component of at least 200 different enzymes, and perhaps some of them play a role in the synthesis of steroid hormones and their receptors. The toxic effect aluminum has on oogenesis in rodents was demonstrated by biologists from Brazil. They assume aluminum directly damages ovarian tissues and inhibits antioxidant enzymes [19].

Considering the embryological cycle, we noted a positive correlation between the level of silicon and the number of blastocysts obtained, while the relationship between silicon and the number of oocytes was not registered. Silicon is necessary for formation of bone and connective tissue, but its role in the processes of embryogenesis is currently unknown.

CONCLUSIONS

We have studied elemental status of infertile patients in ART programs. Most of the trace elements have detectable concentrations in the blood of the patients. We revealed a link between the content of trace elements and patient's age, laboratory indicators (AMH and $T4_{free}$ levels), ovarian stimulation cycle parameters. The effect elemental status of patients has on the outcomes (efficacy) of ART programs requires further research.

References

1. Skalnyj AV, Rudakov IA. Biojelementologija — novyj termin ili novoe nauchnoe napravlenie? Vestnik OGU. 2005; 2: 4–8. Russian.
2. Talebi S, Ghaedi E, Sadeghi E, Mohammadi H, Hadi A, Clark CCT, et al. Trace Element Status and Hypothyroidism: A Systematic Review and Meta-analysis. Biol Trace Elem Res. 2020; 197 (1): 1–14.
3. Sanjeevi N, Freeland-Graves J, Beretvas SN, Sachdev PK. Trace element status in type 2 diabetes: A meta-analysis. J Clin Diagn Res. 2018; 12 (5): OE01–8.
4. Syrkasheva AG, Dolgushina NV, Makarova NP, Kovalskaya EV, Agarsheva MA. Ishody programm vspomogatel'nyh reproduktivnyh tehnologij u pacientok s dismorfizmami oocitov. Akusherstvo i ginekologija. 2015; 7: 56–62. Russian.
5. Sağlam HS, Altundağ H, Atik YT, Dündar MŞ, Adsan Ö. Trace elements levels in the serum, urine, and semen of patients with infertility. Turkish J Med Sci. 2015; 45 (2): 443–8.
6. Zemrani B, Bines JE. Recent insights into trace element deficiencies: causes, recognition and correction. Curr Opin Gastroenterol. 2020; 36 (2): 110–7.
7. Takeuchi H, Taki Y, Nouchi R, Yokoyama R, Kotozaki Y, Nakagawa S, et al. Association of iron levels in hair with brain structures and functions in young adults. J trace Elem Med Biol Organ Soc Miner Trace Elem. 2020; 58: 126436.
8. Laue HE, Moroishi Y, Jackson BP, Palys TJ, Madan JC, Karagas MR. Nutrient-toxic element mixtures and the early postnatal gut microbiome in a United States longitudinal birth cohort. Environ Int. 2020; 138: 105613.
9. Skalnyj AV, Kiselev MF, redaktory. Jelementnyj status naselenija Rossii. SPb.: Medkniga «JeLBI-SPb», 2014; 544 s. Russian.
10. Vapirov VV, Feoktistov VM, Venskovich AA, Vapirova NV. K voprosu o povedenii kremnija v prirode i ego biologicheskoj roli. Uchenye zapiski Petrozavodskogo gosudarstvennogo universiteta. 2017; 2 (163): 95–102. Russian.
11. Novotny JA, Peterson CA. Molybdenum. Adv Nutr. 2018; 9 (3): 272–3.
12. Llamas A, Chamizo-Ampudia A, Tejada-Jimenez M, Galvan A, Fernandez E. The molybdenum cofactor enzyme mARC: Moonlighting or promiscuous enzyme? Biofactors. 2017; 43 (4): 486–94.
13. Shiue I. Higher urinary heavy metal, phthalate, and arsenic but not parabens concentrations in people with high blood pressure, U.S. NHANES, 2011–2012. Int J Environ Res Public Health. 2014; 11 (6): 5989–99.
14. Breitling LP. Smoking as an effect modifier of the association of calcium intake with bone mineral density. J Clin Endocrinol Metab. 2015; 100 (2): 626–35.
15. Neri C, De Luca C, D'oria L, Licameli A, Nucci M, Pellegrino M, et al. Managing fertile women under lithium treatment: the challenge of a Teratology Information Service. Minerva Ginecol. 2018; 70 (3): 261–7.
16. Mirakhori F, Zeynali B, Tafreshi AP, Shirmohammadian A. Lithium induces follicular atresia in rat ovary through a GSK-3β/β-catenin dependent mechanism. Mol Reprod Dev. 2013; 80 (4): 286–96.
17. Luca E, Fici L, Ronchi A, Marandino F, Rossi ED, Caristo ME, et al. Intake of Boron, Cadmium, and Molybdenum enhances rat thyroid cell transformation. J Exp Clin Cancer Res. 2017; 36 (1): 73.
18. Popova EV, Tinkov AA, Ajsuvakova OP, Skalnaya MG, Skalny AV. Boron — A potential goiterogen? Med Hypotheses. 2017; 104: 63–7.
19. da Silva Lima D, da Silva Gomes L, de Sousa Figueredo E, de Godoi MM, Silva EM, da Silva Neri HF, et al. Aluminum exposure promotes histopathological and pro-oxidant damage to the prostate and gonads of male and female adult gerbils. Exp Mol Pathol. 2020; 116: 104486.

Литература

1. Скальный А. В., Рудаков И. А. Биоэлементология — новый термин или новое научное направление? Вестник ОГУ. 2005; 2: 4–8.
2. Talebi S, Ghaedi E, Sadeghi E, Mohammadi H, Hadi A, Clark CCT, et al. Trace Element Status and Hypothyroidism: A Systematic Review and Meta-analysis. Biol Trace Elem Res. 2020; 197 (1): 1–14.
3. Sanjeevi N, Freeland-Graves J, Beretvas SN, Sachdev PK. Trace element status in type 2 diabetes: A meta-analysis. J Clin Diagn Res. 2018; 12 (5): OE01–8.
4. Сыркашева А. Г., Долгушина Н. В., Макарова Н. П., Ковальская Е. В., Агаршева М. А. Исходы программ вспомогательных репродуктивных технологий у пациенток с дисморфизмами ооцитов. Акушерство и гинекология. 2015; 7: 56–62.
5. Sağlam HS, Altundağ H, Atik YT, Dündar MŞ, Adsan Ö. Trace elements levels in the serum, urine, and semen of patients with infertility. Turkish J Med Sci. 2015; 45 (2): 443–8.
6. Zemrani B, Bines JE. Recent insights into trace element deficiencies: causes, recognition and correction. Curr Opin Gastroenterol. 2020; 36 (2): 110–7.
7. Takeuchi H, Taki Y, Nouchi R, Yokoyama R, Kotozaki Y, Nakagawa S, et al. Association of iron levels in hair with brain structures and functions in young adults. J trace Elem Med Biol Organ Soc Miner Trace Elem. 2020; 58: 126436.
8. Laue HE, Moroishi Y, Jackson BP, Palys TJ, Madan JC, Karagas MR. Nutrient-toxic element mixtures and the early postnatal gut microbiome in a United States longitudinal birth cohort. Environ Int. 2020; 138: 105613.
9. Скальный А. В., Киселев М. Ф., редакторы. Элементный статус населения России. СПб.: Медкнига «ЭЛБИ-СПб», 2014; 544 с.

10. Вапиров В. В., Феоктистов В. М., Венскович А. А., Вапирова Н. В. К вопросу о поведении кремния в природе и его биологической роли. Ученые записки Петрозаводского государственного университета. 2017; 2 (163): 95–102.
11. Novotny JA, Peterson CA. Molybdenum. Adv Nutr. 2018; 9 (3): 272–3.
12. Llamas A, Chamizo-Ampudia A, Tejada-Jimenez M, Galvan A, Fernandez E. The molybdenum cofactor enzyme mARC: Moonlighting or promiscuous enzyme? Biofactors. 2017; 43 (4): 486–94.
13. Shiue I. Higher urinary heavy metal, phthalate, and arsenic but not parabens concentrations in people with high blood pressure, U.S. NHANES, 2011–2012. Int J Environ Res Public Health. 2014; 11 (6): 5989–99.
14. Breitling LP. Smoking as an effect modifier of the association of calcium intake with bone mineral density. J Clin Endocrinol Metab. 2015; 100 (2): 626–35.
15. Neri C, De Luca C, D'oria L, Licameli A, Nucci M, Pellegrino M, et al. Managing fertile women under lithium treatment: the challenge of a Teratology Information Service. Minerva Ginecol. 2018; 70 (3): 261–7.
16. Mirakhori F, Zeynali B, Tafreshi AP, Shirmohammadian A. Lithium induces follicular atresia in rat ovary through a GSK-3β/β-catenin dependent mechanism. Mol Reprod Dev. 2013; 80 (4): 286–96.
17. Luca E, Fici L, Ronchi A, Marandino F, Rossi ED, Caristo ME, et al. Intake of Boron, Cadmium, and Molybdenum enhances rat thyroid cell transformation. J Exp Clin Cancer Res. 2017; 36 (1): 73.
18. Popova EV, Tinkov AA, Ajsuvakova OP, Skalnaya MG, Skalny AV. Boron — A potential goiterogen? Med Hypotheses. 2017; 104: 63–7.
19. da Silva Lima D, da Silva Gomes L, de Sousa Figueredo E, de Godoi MM, Silva EM, da Silva Neri HF, et al. Aluminum exposure promotes histopathological and pro-oxidant damage to the prostate and gonads of male and female adult gerbils. Exp Mol Pathol. 2020; 116: 104486.

OCULOMOTOR RESPONSE TO IMAGES IN PRIMARY SCHOOL CHILDREN WITH MILD INTELLECTUAL DISABILITY

Nikishina VB[1], Prirodova OF[1], Petrash EA[1] ✉, Sevrukova IA[2]

[1] Pirogov Russian National Research Medical University, Moscow, Russia

[2] Kursk State Medical University, Kursk, Russia

Oculomotor activity (eye movements) is an essential component of visual data acquisition, analysis and use. The aim of this study was to determine the characteristics of oculomotor response to static images in primary school children with mild intellectual disability (ID). Our sample included a total of 49 schoolers (23 children with mild ID and 26 typically developing children). Oculomotor activity was evaluated using a GP3 Gazepoint eye tracker. The participants were presented with 15 visual stimuli: 10 pictorial and 5 mixed (pictures + text) static color images. Children with mild ID generated significantly fewer fixations ($p = 0.038$) than typically developing children. So, learning materials containing both pictorial and textual images are ineffective because textual elements are completely ignored by children with mild ID. The total duration of gaze fixations was significantly longer ($p = 0.029$) in typically developing children than in children with mild ID. However, the average duration of a single gaze fixation was longer in children with mild ID. The identified features of oculomotor response can help to optimize the format of instructional materials for primary school children with mild ID.

Keywords: oculomotor response, intellectual disability, gaze fixation, latency, fixation duration

Author contribution: Nikishina VB and Prirodova OF proposed the concept, interpreted and summarized the obtained data; Petrash EA performed qualitative and quantitative analysis of the obtained data; interpreted and summarized the results; Sevrukova IA conducted the study and performed data acquisition

Compliance with ethical standards: the study was approved by the Ethics Committee of Kursk Medical State University (Protocol № 9 dated December 10, 2019). Written informed consent was obtained from the children's parents or legal representatives.

✉ **Correspondence should be addressed:** Ekaterina A. Petrash
Ostrovityanova, 1, Moscow, 117997; petrash@mail.ru

Received: 21.01.2021 **Accepted:** 15.02.2021 **Published online:** 26.02.2021

DOI: 10.24075/brsmu.2021.008

ГЛАЗОДВИГАТЕЛЬНЫЕ РЕАКЦИИ ПРИ ВОСПРИЯТИИ ИЗОБРАЖЕНИЙ МЛАДШИМИ ШКОЛЬНИКАМИ С ЛЕГКОЙ СТЕПЕНЬЮ УМСТВЕННОЙ ОТСТАЛОСТИ

В. Б. Никишина[1], О. Ф. Природова[1], Е. А. Петраш[1] ✉, И. А. Севрюкова[2]

[1] Российский национальный исследовательский медицинский университет имени Н. И. Пирогова, Москва, Россия

[2] Курский государственный медицинский университет, Курск, Россия

Окуломоторная активность (глазодвигательные реакции) может быть необходимым компонентом психических процессов, связанных с получением, преобразованием и использованием зрительной информации. Целью работы было определить, каковы особенности глазодвигательных реакций при восприятии статичных изображений у младших школьников с легкой степенью умственной отсталости (УО). Объем выборки составил 49 человек: 23 человека с легкой степенью УО, 26 человек с нормативным типом психического развития. Оценку глазодвигательных реакций осуществляли с использованием программно-аппаратного комплекса GP3 Gazepoint. Стимульный материал представлял собой 15 статичных цветных изображений: картинки, содержащие только изображения (10 картинок); картинки, содержащие одновременно изображения и текст (5 картинок). В ходе исследования установлено, что число фиксаций у детей с легкой степенью УО значимо меньше ($p = 0,038$) по сравнению с детьми с нормативным развитием. Одновременное размещение картинки и текстовой информации неэффективно, поскольку текстовая часть остается проигнорированной в полном объеме. Общая длительность фиксаций значимо выше ($p = 0,029$) у детей с нормативным развитием по сравнению с детьми с легкой степенью УО. При этом средняя длительность единичной фиксации при УО выше. В практическом аспекте выявленные особенности глазодвигательных реакций у детей младшего школьного возраста с легкой степенью УО позволяют оптимизировать форму предъявления информации в процессе обучения.

Ключевые слова: глазодвигательные реакции, умственная отсталость, зрительные фиксации, латентное время фиксации, длительность фиксации

Вклад авторов: В. Б. Никишина — формирование концепции исследования, интерпретация и обобщение полученного эмпирического материала; О. Ф. Природова — формирование концепции исследования, интерпретация и обобщение полученного эмпирического материала; Е. А. Петраш — количественная и качественная обработка полученного эмпирического материала, интерпретация и обобщение результатов исследования; И. А. Севрюкова — проведение исследования, сбор первичного эмпирического материала.

Соблюдение этических стандартов: исследование одобрено этическим комитетом Курского государственного медицинского университета (протокол № 9 от 10 декабря 2019 г.); родители или законные представители детей подписали добровольное информированное согласие на участие в исследовании.

✉ **Для корреспонденции:** Екатерина Анатольевна Петраш
ул. Островитянова, д. 1, г. Москва, 117997; petrash@mail.ru

Статья получена: 21.01.2021 **Статья принята к печати:** 15.02.2021 **Опубликована онлайн:** 26.02.2021

DOI: 10.24075/vrgmu.2021.008

In 2019, 0 to 14-year-old Russians with first-time diagnosed intellectual disability (ID) amounted to 4.8% of all pediatric patients with mental disorders [1]. This number has been showing a positive curvilinear trend over the past 10 years.

At primary school, intentional learning is the leading type of activity, i.e. the main driver of a child's mental development. Visual perception forms the basis for intellectual activity. Children with perceptual differentiation deficiency cannot recognize an object from its parts and are unable to discriminate between similar-looking objects [2].

In order to address educational challenges faced by the teachers and parents of children with developmental disorders, visual perception should be viewed as a function involving the encoding and analysis of object features, their multisensory convergence, object identification, and the assessment of object importance [3].

Intellectual disability coded as F70 by ICD-10 is a type of developmental disorder. It is characterized by incomplete brain development, increased exhaustibility of mental activity, slow cortical activity, and compromised anatomy and physiology of the visual system underlying cognitive impairments, including sensory and perceptual dysfunction [4–10].

Visual perception is the sum of processes involved in creating a visual impression of the environment based on visual input [3].

In primary school children with cognitive disorders the generality of perception is compromised. Minor details and small objects go unnoticed; only salient features are perceived. The structural elements of an object are not recognized [4]. Children with ID have a narrow scope of visual perception. Typically developing primary school children are capable of simultaneously perceiving 8 to 12 small objects, whereas their peers with ID can only perceive 4-6 objects at a time [10].

Size constancy (perception of distant objects) is much worse in children with ID than in their typically developing peers [8].

Children with ID cannot establish connections or identify a relationship between animate or inanimate objects in a genre scene [5]. This may be due to slow mental activity and sequential picture processing. The analysis of eye trajectory during picture viewing reveals that the glance is often drawn to the same, probably more informative elements of the picture; other elements receive much less attention [7].

Summing up, the following aspects of visual perception are compromised in primary school children with mild ID: integrity, concreteness, fidelity, wholeness, constancy, scope, generality, selectivity, rate, and differentiation. Ocular motor responses (oculomotor activity) are the critical components of mental processes implicated in visual data acquisition, processing and use.

Dyslexic children are reported to generate more saccades when reading a static text than their typically developing peers. Dyslexic children also generate more than 3 saccades during gaze fixation tasks. This might be explained by the immaturity of their cortical structures responsible for saccadic inhibition [11].

A study of oculomotor reactions revealed that children with autism spectrum disorders were fast to fixate on human faces when presented with a socially relevant stimulus; after that, however, their attention slackened. The more pronounced was developmental delay, the more the participants fixated on the central elements of the presented picture. This might be explained by the low average saccade velocity in autistic children [12].

It is reported that lower IQ is associated with slower response and less stable gaze fixations in children with various grades of ID [13].

A Russian study investigated oculomotor responses to texts in different age groups [14]. None of the studied eye movement parameters differed between older and younger dyslexic children. The immaturity of some brain structures might disrupt the formation of basic components of reading skills required for the successful analysis and understanding of written texts.

In contrast to typically developing children, their peers with mild ID need more time to read a text and make more fixations; fixation duration is longer, and the amplitude of saccades is reduced. This may be due to the impaired ability to perform phonemic analysis and understand letter/sound correspondences [15].

Preschoolers with mild ID make fewer and longer fixations when viewing static images due to limited visual perception [10] and its slow rate [4]. Incomplete or arrested development of brain structures can affect oculomotor response to images.

The aim of the study was to investigate the characteristics of oculomotor response to static images in primary school children with mild ID. The obtained data might be used to optimize the format of teaching materials for such children.

METHODS

Study participants

The study was carried out in 49 children aged 7–9 years who were in their first year at school (non-repeaters). The following inclusion criteria were applied: any sex; no visual impairment confirmed by an ophthalmologist. Exclusion criteria: chronic diseases.

The children were grouped by the type of mental development. The main group comprised 12 boys and 11 girls with mild ID (F70.0, MCI-10) and the average IQ of 63.57 ± 3.24, attending specialized schools for emotional and behavioral disorders (type VIII schools). The mean age of the children was 8.63 ± 0.57 years. The control group consisted of 26 typically developing children (11 boys and 15 girls; mean age: 8.12 ± 0.81 years) pronounced healthy by the expert panel.

Equipment: technical specifications, setup, calibration

Oculomotor response studied using a GP3 Gazepoint eye-tracking system (Gazepoint Research Inc.; Canada) that exploits a 60 Hz machine-vision camera to collect and analyze visual data. This eye tracker comes with Gazepoint Control and Gazepoint Analysis software for calibration, running experiments and data analysis.

Both eyes were tracked simultaneously

Technical specifications of the eye tracker: accuracy 0.5–1 degree of visual angle; 60 Hz update rate; 5- and 9-point calibration; open-standard API; 25 × 11 cm horizontal x vertical movement; ±15 cm range of depth movement; USB-powered.

Computer requirements: modern processor (i5-i7); memory: 2 Gb; OS: Windows XP / Vista / 7/8, 32/64 bit; 15.6-inch monitor; 1920 × 1080 screen resolution.

The following instructions were applied to create a project for each study participant: start Gazepoint Analysis → create a New project → select a folder to save the project → add a stimulus (a static image).

1. Areas of interest (AOI; images of individual objects simultaneously presented on the computer screen) were selected in the Analyze data mode. It is possible to select areas of interest on each presented image. The software collects statistics on the number of viewers who view the selected AOI; the average time to the first view (latency); the average time spent on viewing the selected AOI (fixation duration); the average percentage of the total time spent on AOI; the number of revisitors.

2. The Gazepoint Control window shows 4 types of settings: Calibrate, Gaze pointer, Select screen, and Switch Tracker Type.

The camera view in the middle of the screen helps to adjust the distance between the camera and the subject and right/left eye capture. Feedback information is provided in the bottom status bar, which shows frame time (16.6 ms; 60 Hz), the number of participants connected to the server and the ongoing data transmission.

The eye tracker must be placed directly below the computer screen. Direct and indirect light casting on the subject's face

must be avoided because it interferes with the recording of corneal reflexes. In our experiment, the distance between the camera and the subject's eyes was 65 cm.

For better accuracy, a calibration step must be performed. Calibration reveals possible differences between the eyes of the participant and the eye model. During calibration, the eye tracker analyzes light reflections from the subject's eyes. A bright marker will appear on the dark calibration screen, moving between 5 or 9 different positions. The participant is requested to look at each marker position. Then, a white point-of-gaze dot appears on the screen and the participant is again requested to look at each calibration point.

The following instruction was given during the calibration step: You will see white dots on the screen. You will need to look only at these dots.

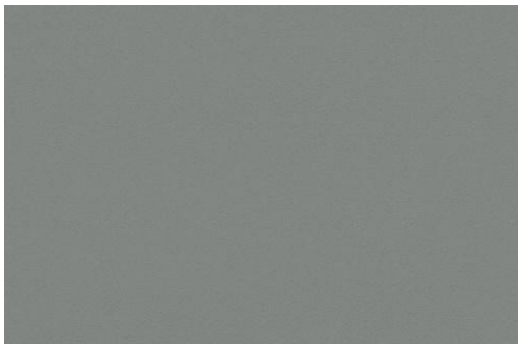

Interfering background image

Fig. 1. Example of a visual stimulus

3. During the data collection step, the following instruction was given to the participants: You will see images on the screen. You will need to look at the images very attentively without changing your posture.

Data collected during the experiment can be exported in various formats including static images, videos of gaze trajectories, heat maps and numerical *.csv data.

Visual stimuli

Visual stimuli were shortlisted by the panel of experts: teachers of primary schools for typically developing children and specialized type VIII schools for children with intellectual disabilities. Image selection criteria: image type (photos, diagrams, genre scenes, pictures of individual objects); image

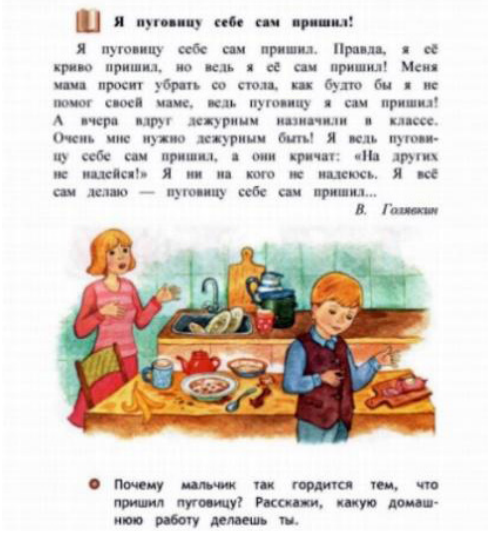

Я пуговицу себе сам пришил!

Я пуговицу себе сам пришил. Правда, я её криво пришил, но ведь я её сам пришил! Меня мама просит убрать со стола, как будто бы я не помог своей маме, ведь пуговицу я сам пришил! А вчера вдруг дежурным назначили в классе. Очень мне нужно дежурным быть! Я ведь пуговицу себе сам пришил, а они кричат: «На других не надейся!» Я ни на кого не надеюсь. Я всё сам делаю — пуговицу себе сам пришил...

В. Голявкин

Почему мальчик так гордится тем, что пришил пуговицу? Расскажи, какую домашнюю работу делаешь ты.

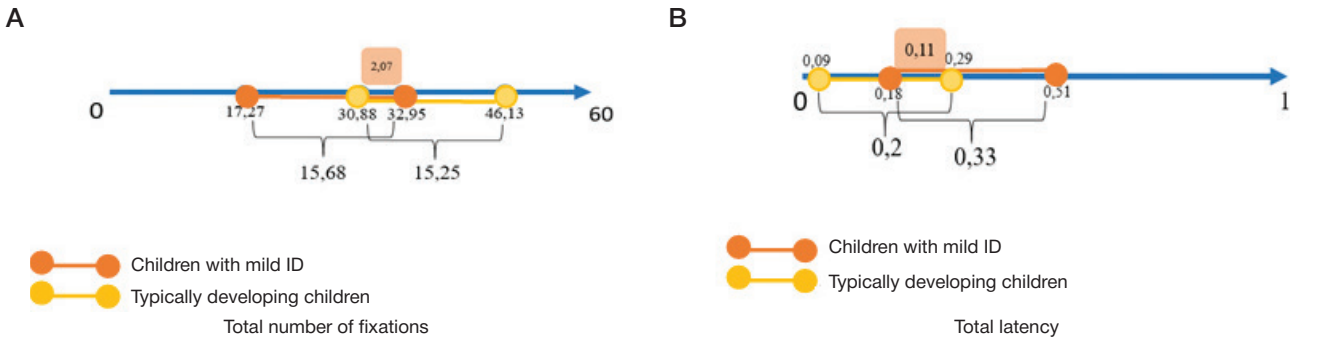

Fig. 2. The schematic representation of the overlap in the range of mean total number of fixations (**A**) and total latency (**B**) in children with ID and their typically developing peers

quality, sharpness and contrast. Criteria for final choice: bitmap images and static 2D color images (children with ID recognize basic colors but have difficulty differentiating between poorly saturated colors).

A total of 15 static color images were selected (Fig.1). Each presented image was followed by the gray background image.

The selected visual stimuli were divided into 3 groups: images depicting 6 objects (2 images showing individual objects and 3 genre scenes); images depicting 12 objects (2 images showing individual objects and 3 genre scenes); 5 images containing both pictorial and textual (task description or a legend) elements. In each experiment, images were presented in the same sequence: 1) images depicting 6 objects, 2) images depicting 12 objects, 3) images containing both pictorial and textual elements.

Resolution of the presented images: 1200 × 1373 for vertical images, 1920 × 1080 for horizontal images (consistent with the resolution of the computer screen; the aspect ratio was preserved). File format: jpg (JPEG). The children were presented with pictures from traditional school textbooks and textbooks for children with ID. Presentation time: 20 s. Background image presentation time: 3 s. Total presentation time: 7 min.

The following parameters of oculomotor response to AOI were analyzed: latency (average time to the first view); mean fixation duration (time spent looking at AOI); the average percentage of the total time spent on viewing AOI; the total number of fixations per image (the sum of gaze fixations on each AOI per image). Each parameter was evaluated for each presented images (a picture or a combination of a picture and text).

Statistical analysis was carried out using descriptive (mean values, standard deviations) and comparative statistics (nonparametric Mann–Whitney *U* test, Wilcoxon *T* test). Absolute values were compared between the groups.

RESULTS

The total number of fixations and total latency varied within both groups (children with ID and typically developing children (Fig. 2A, B).

The total number of fixations was significantly higher in the group of typically developing children than in their peers with mild ID ($p = 0.038$). At the same time, the overlap in the range of mean values for this parameter between the groups was minimal. The average number of fixations was 15.68 (17.27; 32.95) in the main group and 15.25 (30.88; 46.13) in the control group. Total latency was significantly higher ($p = 0.044$) in the group of children with mild ID than in the group of typically developing children. Average latency was 0.33 (0.18; 0,.51) in the main group and 0.2 (0.09; 0.29) in the control group.

These results reveal the following trend: children with mild ID fixate their gaze at fewer objects (points on the image) because they need significantly more time for fixation than typically developing children (Fig. 3).

In both groups, the number of fixations increased for pictures containing more objects (12 vs 6 objects depicted in the picture) (Table).

In both groups, the highest number of fixations was registered when children were presented with images containing 12 objects. For images containing 6 objects and

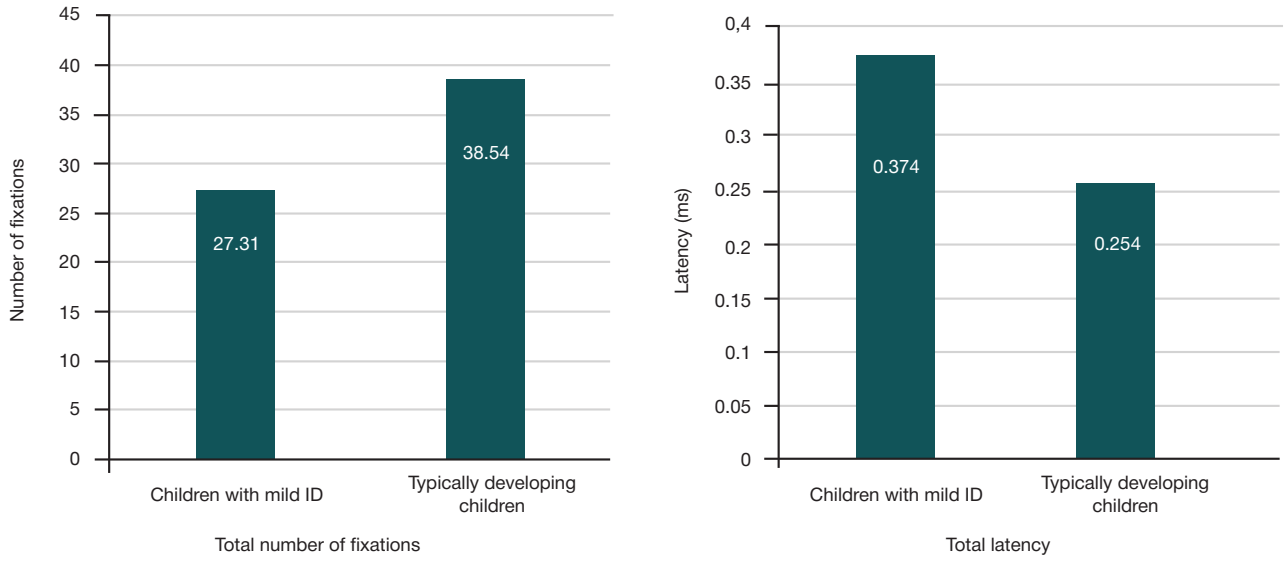

Fig. 3. A histogram showing mean values for the total number of fixations in children with mild ID and their typically developing peers

Table. Differences in the total number of fixations between the groups presented with images containing 6 and 12 objects (Wilcoxon sign-ranked test; $p < 0.05$)

	Number of objects: 6 (x ± σ)	Number of objects: 12 (x ± σ)	*p*
Children with mild ID	25.15 ± 4.49	30.22 ± 6.24	0.029*
Typically developing children	36.18 ± 9.12	41.39 ± 8.42	0.027*

Note: * — differences are statistically significant.

images containing both pictorial and textual elements, the average number of fixations did not differ significantly between the groups (Fig. 4).

The spatial distribution of gaze fixations on the image differed significantly between typically developing children and their peers with ID.

Fig. 5 shows heat maps revealing the distribution of the number of fixations over the presented stimuli. Fig. 5A shows heat maps for a child with mild ID (age: 8 years 7 months). Fig. 5B shows heat maps for a typically developing child (age: 8 years 1 month).

In the main group, the total number of fixations on images containing 6 unrelated individual objects and on genre scenes containing 6 objects was almost the same ($p = 0.75$). Similarly, the total number of fixations on images containing 12 unrelated individual objects and on genre scenes containing 12 objects did not differ significantly in the group of children with mild ID ($p = 0.73$). Typically developing children made more fixations ($p = 0.027$) on genre scenes containing 6 objects than on images containing 6 unrelated individual objects. In this group of children, the number of fixations increased significantly ($p = 0.029$) for genre scenes containing 12 objects, as compared with images containing 12 unrelated individual objects.

Children with mild ID ignored textual elements in mixed images and fixated on pictorial elements. Typically developing children tended to fixate their gaze predominantly on textual elements.

The fact that children with mild ID did not fixate their gaze on written text means that texts do not facilitate visual perception and are excluded from it.

Images containing 6 or 12 objects were divided into 2 groups: images of unrelated individual objects and genre scenes.

Children with mild ID tended to make fixations on the central elements of images containing unrelated individual objects (6 objects). Typically developing children made gaze fixations on the objects contained in the pictures and the space between the objects. This facilitates spatial perception, allowing the child to perceive the size of the viewed object relative to other objects. In children with mild ID, spatial perception is impaired, which might be associated with some aspects of volitional visual perception.

When viewing genre scenes, children with mild ID tended to fixate their gaze on the heads of the depicted objects (animals and birds) and on the faces of the depicted people (teachers and children), and made only single fixations on secondary objects. In typically developing children, fixations were distributed equally between primary and secondary objects.

The ratio of gaze fixations on the peripheral elements to the fixations on the central part of the presented image (6 objects) was uniform in both groups.

When viewing images containing 12 objects, children with mild ID made more fixations on primary objects depicted in the presented images, whereas secondary objects were almost completely ignored. The maximal number of fixations was observed for the central part of the presented image vs its peripheral elements. Peripheral elements were ignored regardless of their number and importance (primary and secondary objects). In typically developing children, the number of fixations was distributed equally between the central and peripheral elements of the image.

In both groups, fixations were concentrated on human faces in cases when humans were depicted in the presented pictures. Children with mild ID tended to make fixations on adult faces, whereas their normally developing peers fixated on children's faces.

Total latency was calculated as the sum of latencies for all AOI per image. Total latency shows time from the presentation of the first stimulus to the first registered fixation. Average total latency was higher in children with mild ID than in typically developing children ($p = 0.024$), i.e. children with mild ID needed more time to fixate the gaze when viewing static images (Fig. 6A).

Regardless of the number of objects in the picture (12 or 6), children with mild ID exhibited longer latency for both central and peripheral elements than their typically developing peers. Typically developing children were faster to fixate on the peripheral elements of the presented pictures. This suggests

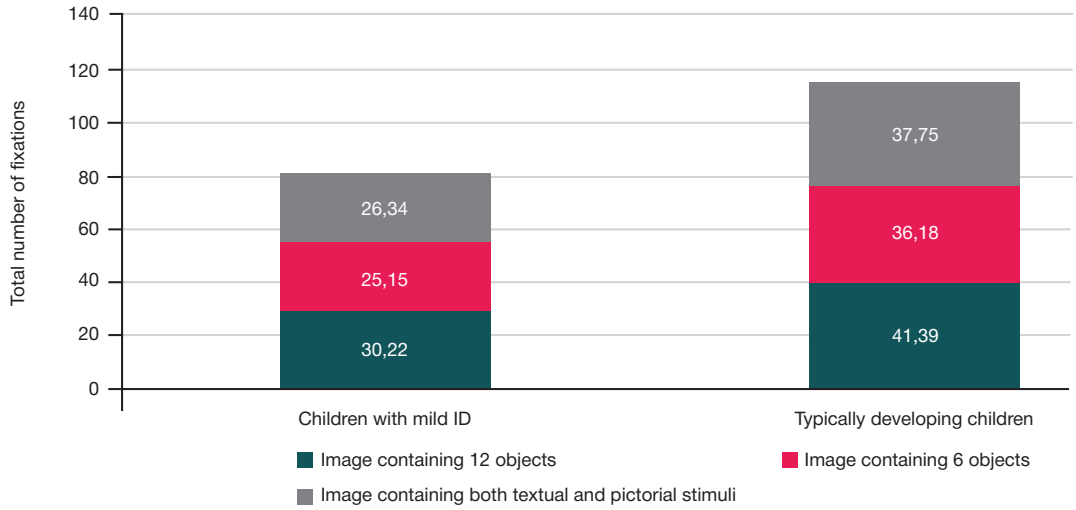

Fig. 4. Cumulative histograms showing average values for the total number of fixations in the groups presented with different types of visual stimulus

Genre scene (6 objects)

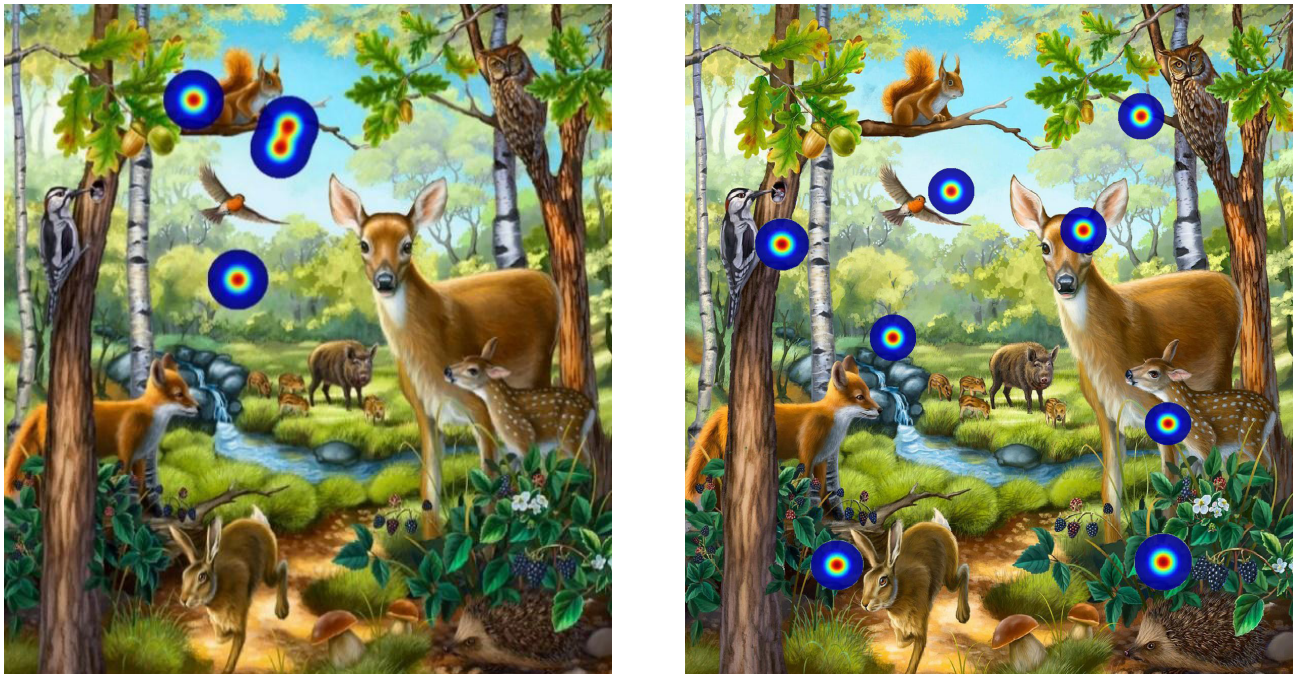

Genre scene (12 objects)

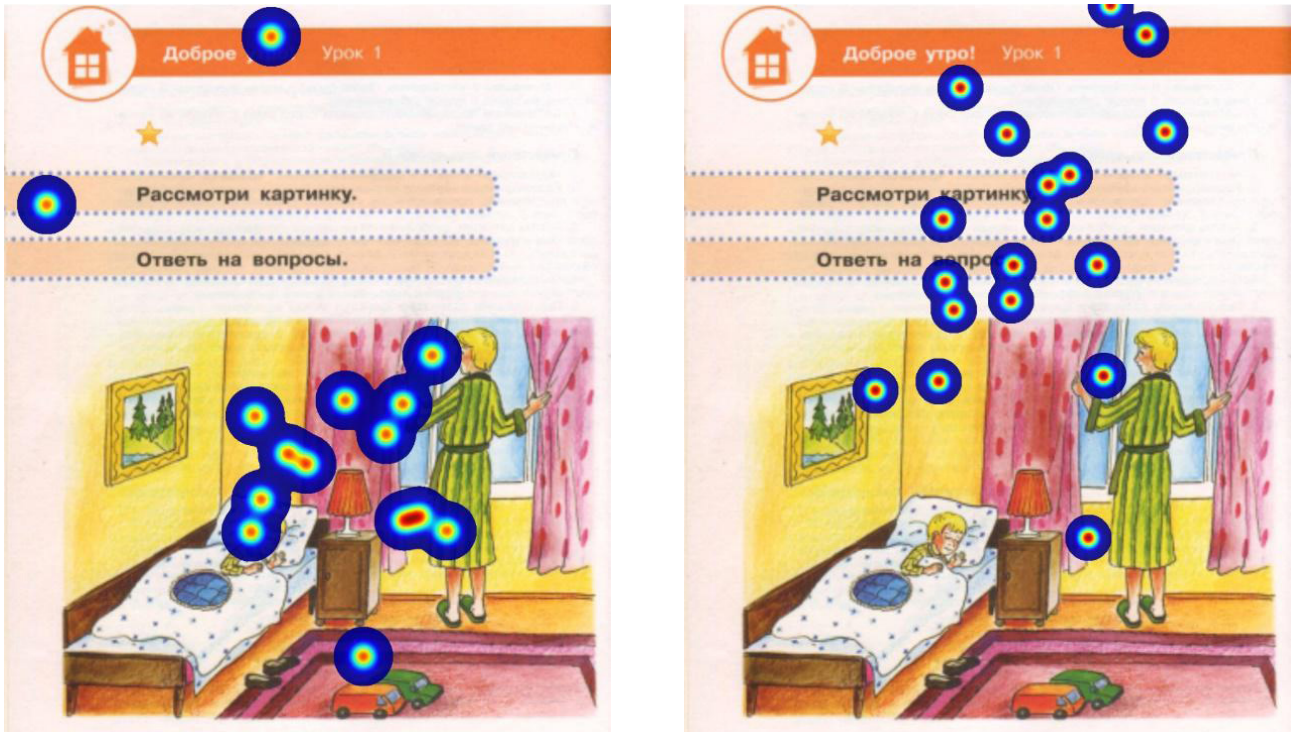

Image containing both textual and pictorial elements

Children with mild ID

Typically developing children

Fig. 5. Heat maps of gaze fixations on the elements of mixed images in the main and control groups

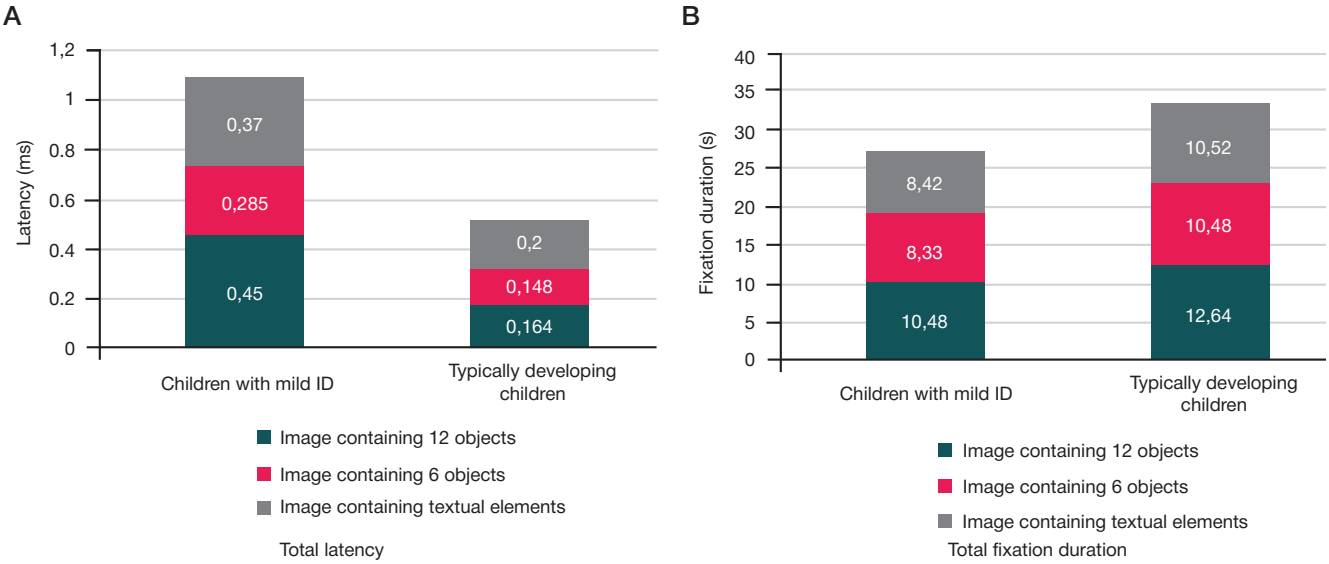

Fig. 6. Cumulative histograms showing average values for total latency (**A**) and fixation duration (**B**) in the groups presented with different types of visual stimulus

that faster fixations may be associated with faster attentional shifts in healthy children. In children with mild ID, the minimal time to a fixation on a central or peripheral element was observed for pictures containing 6 objects; so, it could be hypothesized that it is easier for such children to control their attention in the presence of fewer depicted objects.

The total duration of fixations was significantly longer in the control group ($p = 0.029$) than in the main group. The average duration of one fixation was 0.29 ± 0.08 ms for typically developing children and 0.33 ± 0.11 ms for children with mild ID. Thus, children with mild ID need more time to visually perceive a static image. Fewer and longer fixations made by children with mild ID are exhausting for active perception and reduce the scope of perception.

The analysis of the total duration of fixations following the presentation of different stimulus types (6 or 12 objects, text) suggests that the mean total duration of fixations is significantly longer ($p = 0.027$) in typically developing children than in children with mild ID (Fig. 6B). Children with mild ID spent 62.37 ± 8.31% of the total fixation time on viewing AOI, whereas for their typically developing peers this parameter equaled 68.42 ± 9.14%.

For children with mild ID, the total number of fixations was lower and total latency was longer.

DISCUSSION

While perceiving a static image containing multiple objects, the attention of children with mild ID is drawn to the central part of the image. This finding is consistent with the results of previous studies [10, 12]. When presented with images containing fewer objects, the attention of children with mild ID is distributed more uniformly. Such children make fewer fixations when presented with images containing both textual and pictorial elements; those fixations are concentrated on pictorial elements, whereas the text is completely ignored. This is associated with the informative value of pictorial elements [7].

On the whole, typically developing children make more fixations during the experiment. The number of gaze fixations on each object (AOI) is relatively stable regardless of the total number of objects depicted in the image (6 or 12). Fixations are uniformly distributed between the central and peripheral elements of images containing only pictorial elements. For mixed images, most fixations are concentrated on textual elements; only single fixations are registered for pictorial elements.

Children with mild ID exhibit longer latency than their typically developing peers. Children with ID need more time to perceive an image. The detected trend is consistent with the findings of other researchers who reported increased duration of gaze fixations in such children [15]. The total duration of gaze fixations in typically developing primary school students is longer than in children with mild ID. Considering that the number of fixations is greater in healthy children, the duration of a single fixation is shorter. So, the lower total number of fixations and shorter duration of fixations in children with mild ID might be explained by the fact that they need more time to perceive a static image.

CONCLUSION

The structural and dynamic characteristics of oculomotor response (the number of fixations, total fixation duration and latency) described in the study show that children with mild ID ignore textual elements on textbook pages containing a pictorial element and a task; their attention is focused on the periphery of an image if the image contains more than 6 objects.

These characteristics of oculomotor response of children with mild ID may help to optimize the form in which learning materials are presented. Attention is distributed uniformly between simultaneously presented objects if their number does not exceed 6. If more than 6 objects are simultaneously presented on a textbook page, some of them located on the periphery escape from the field of active perception. Learning materials containing both pictorial and textual elements are ineffective because the textual elements are completely ignored. Texts and pictures should be presented in sequence. This will help to optimize the process of active perception in children with mild ID. Increased latency and increased duration of a single fixation mean that image presentation should be extended in time.

References

1. Zdravoohranenie v Rossii. 2019: Stat. sb. / Rosstat. M., 2019; 170 s. Russian.
2. Petrova VG. Psihologija umstvenno otstalyh shkol'nikov. M.: Akademija, 2002; 160 s. Russian.
3. Luriya AR. Osnovy nejropsihologii. M.: Akademija, 2003; 384 s. Russian.
4. Berezhnaja SA. Osobennosti razvitija zritel'nogo vosprijatija u mladshih shkol'nikov s narusheniem intellektual'nogo razvitija. V sbornike: Materialy nauchno-prakticheskoj konferencii; Simferopol, 16 maja 2017 g. Simferopol: Arial, 2017; s. 32–34. Russian.
5. Evlahova ZA. Osobennosti vosprijatija sjuzhetno-hudozhestvennyh kartin uchashhimisja vspomogatel'noj shkoly. Uchebno-vospitatel'naja rabota v spec. shkolah. M., 1987; 205 s. Russian.
6. Zabramnaja SD. Nekotorye psihologo-pedagogicheskie poazateli razgranichenija stepenej umstvennoj otstalosti u detej na nachal'nom jetape shkol'nogo obuchenija. Korrekcionnaja pedagogika. 2008; 1: 5–13. Russian.
7. Isaev DN. Umstvennaja otstalost' u detej i podrostkov. SPb.: Rech', 2007; 389 s. Russian.
8. Petrova VG. Psihologija umstvenno otstalyh shkol'nikov. M.: Akademija, 2002; 160 s. Russian.
9. Rubinshtejn SYa. Psihologija umstvenno otstalogo shkol'nika. M.: Prosveshhenie, 1986; 192 s. Russian.
10. Solovev IM. Osobennosti poznavatel'noj dejatel'nosti uchashhihsja vspomogatel'noj shkoly. M., 2004; 378 s. Russian.
11. Tiadi A, Gérard C-L, Peyre H., Bui-Quoc E, et al. Immaturity of Visual Fixations in Dyslexic Children. Frontiers in Human Neuroscience. 2016; 10: 574–84.
12. Wang S, Jiang M, Duchesne XM, Laugeson EA, et al. Atypical Visual Saliency in Autism Spectrum Disorder Quantified through Model-Based Eye Tracking. Neuron. 2015; 88 (3): 604–16.
13. Boot FH, Pel JJ, Evenhuis HM, et al. Delayed visual orienting responses in children with developmental and/or intellectual disabilities. Journal of Intellectual Disability Research. 2012; 47: 57–58
14. Oganov SR. Nekotorye osobennosti razvitija chitatel'skoj dejatel'nosti u detej s disleksiej 9–13 let. V sbornike: Tezisy dokladov Vserossijskoj nauchno-prakticheskoj konferencii molodyh uchenyh s mezhdunarodnym uchastiem «Fundamental'nye issledovanija v pediatrii; Sankt-Peterburg, 31 oktjabrja 2019; SPb., 2019; s. 42–43. Russian.
15. Dinevich KV, Dunaevskaja YeB. Issledovanie zritel'nogo vosprijatija tekstov raznogo vizual'nogo formata u detej s umstvennoj otstalost'ju. Kompleksnye issledovanija detstva. 2019; 2: 114–120. Russian.

Литература

1. Здравоохранение в России. 2019: Стат. сб. / Росстат. М., 2019; 170 с.
2. Петрова В. Г. Психология умственно отсталых школьников. М.: Академия, 2002; 160 с.
3. Лурия А. Р. Основы нейропсихологии. М.: Академия, 2003; 384 с.
4. Бережная С. А. Особенности развития зрительного восприятия у младших школьников с нарушением интеллектуального развития. В сборнике: Материалы научно-практической конференции; Симферополь, 16 мая 2017 г. Симферополь: Ариал, 2017; с. 32–34.
5. Евлахова З. А. Особенности восприятия сюжетно-художественных картин учащимися вспомогательной школы. Учебно-воспитательная работа в спец. школах. М., 1987; 205 с.
6. Забрамная С. Д. Некоторые психолого-педагогические поазатели разграничения степеней умственной отсталости у детей на начальном этапе школьного обучения. Коррекционная педагогика. 2008; 1: 5–13
7. Исаев Д. Н. Умственная отсталость у детей и подростков. СПб.: Речь, 2007; 389 с.
8. Петрова В. Г. Психология умственно отсталых школьников. М.: Академия, 2002; 160 с.
9. Рубинштейн С. Я. Психология умственно отсталого школьника. М.: Просвещение, 1986; 192 с.
10. Соловьев И. М. Особенности познавательной деятельности учащихся вспомогательной школы. М., 2004; 378 с.
11. Tiadi A, Gérard C-L, Peyre H., Bui-Quoc E, et al. Immaturity of Visual Fixations in Dyslexic Children. Frontiers in Human Neuroscience. 2016; 10: 574–84.
12. Wang S, Jiang M, Duchesne XM, Laugeson EA, et al. Atypical Visual Saliency in Autism Spectrum Disorder Quantified through Model-Based Eye Tracking. Neuron. 2015; 88 (3): 604–16.
13. Boot FH, Pel JJ, Evenhuis HM, et al. Delayed visual orienting responses in children with developmental and/or intellectual disabilities. Journal of Intellectual Disability Research. 2012; 47: 57–58.
14. Оганов С. Р. Некоторые особенности развития читательской деятельности у детей с дислексией 9–13 лет. В сборнике: Тезисы докладов Всероссийской научно-практической конференции молодых ученых с международным участием «Фундаментальные исследования в педиатрии; Санкт-Петербург, 31 октября 2019; СПб., 2019; с. 42–43.
15. Диневич К. В., Дунаевская Э. Б. Исследование зрительного восприятия текстов разного визуального формата у детей с умственной отсталостью. Комплексные исследования детства. 2019; 2: 114–120.

BONE TURNOVER MARKERS IN PATIENTS WITH ISOLATED FEMORAL SHAFT FRACTURE UNDERGOING SYSTEMIC OZONE THERAPY

Osikov MV ✉, Davidova EV, Abramov KS

South Ural State Medical University, Chelyabinsk, Russia

Efferent physical therapy holds promise as an adjunct to the combination treatment of femoral fractures in young, working-age individuals. The aim of the study was to investigate the dynamics of bone turnover markers at different stages of femoral fracture consolidation in patients undergoing ozone therapy. The study enrolled 20 men (group 2, 47.8 ± 3.5 years) with a femoral shaft fracture (AO/ASIF 32A, 32B). The control group (group 1, 46.8 ± 3.7 years) comprised 10 healthy males. Subgroup 2a (n = 10) was assigned to receive standard therapy; subgroup 2b (n = 10) was assigned to receive standard therapy complemented by minor autohemotherapy (MAHT) at 20 mg/L ozone concentrations. On days 7, 30 and 90, fracture consolidation was assessed on the RUST scale and blood levels of C-terminal telopeptides of type I collagen (bCTx, pg/ml) and procollagen type I carboxy-terminal propeptide (PICP, ng/ml) were measured. On day 7, the total RUST score in subgroups 2a and 2b was 4 points; on day 30, it was 6.5 and 8.7 points, respectively, and on day 90, it reached 10 and 11.5 points, respectively. Bone mineral density was as high as 90% in the MAHT subgroup vs. 78% in subgroup 2a, indicating faster bone healing. On day 30, bCTx levels in subgroup 2b were higher than in subgroup 2a (2289.4 [2145.3; 2365.4] vs. 1894.6 [1745.3; 2098.2], respectively. On day 7, PICP was significantly elevated in subgroup 2b in comparison with subgroup 2a; its levels peaked on days 30 and 90 (day 30: 268.3 [231.2; 286.3] vs. 183.2 [174.6; 195.6]; day 90: 584.6 [512.3; 589.3] vs. 351.2 [312.3; 369.4]. Thus, MAHT produces a positive effect on the quality and intensity of bone healing in men with isolated closed femoral shaft fractures.

Keywords: closed isolated femoral shaft fracture, ozone therapy, bone remodeling

Author contribution: Osikov MV conceived the study, proposed its design, analyzed the obtained data, wrote and edited the manuscript; Davidova EV conceived the study, proposed its design, analyzed the obtained data, participated in writing the manuscript; Abramov KS collected clinical data, analyzed the results of the study, wrote and edited the manuscript. The authors equally contributed to the study and preparation of the manuscript, read and approved the final version of this article before publication.

Compliance with ethical standards: the study was approved by the Ethics Committee of the South Ural State Medical University, Chelyabinsk (Protocol № 4 dated May 22, 2020). Informed consent was obtained from all study participants.

✉ **Correspondence should be addressed:** Mikhail V. Osikov
Vorovskogo, 64, Chelyabinsk, 454092; prof.osikov@yandex.ru

Received: 29.12.2020 **Accepted:** 17.01.2021 **Published online:** 02.02.2021

DOI: 10.24075/brsmu.2021.003

МАРКЕРЫ РЕМОДЕЛИРОВАНИЯ КОСТНОЙ ТКАНИ ПРИ КОНСОЛИДАЦИИ ИЗОЛИРОВАННОГО ПЕРЕЛОМА БЕДРЕННОЙ КОСТИ В УСЛОВИЯХ СИСТЕМНОЙ ОЗОНОТЕРАПИИ

М. В. Осиков ✉, Е. В. Давыдова, К. С. Абрамов

Южно-Уральский государственный медицинский университет, Челябинск, Россия

В комплексном лечении переломов бедра у лиц молодого трудоспособного возраста перспективно использование эфферентной физической терапии. Целью работы было изучить маркеры ремоделирования костной ткани в динамике консолидации перелома бедренной кости в условиях озонотерапии. В исследование были включены 20 мужчин (группа 2, 47,8 ± 3,5 лет) с переломом диафиза бедренной кости (AO/ASIF 32A, 32B). Контрольную группу (группа 1, 46,8 ± 3,7 лет) составили 10 здоровых мужчин. Пациентам подгруппы 2а (n = 10) проводили стандартное лечение, подгруппы 2б (n = 10) — стандартное лечение и малую аутогемоозонотерапию (МАГОТ) при концентрации озона 20 мг/л. В динамике на 7-е, 30-е, 90-е сутки определяли интенсивность консолидации (по шкале RUST), С-концевые телопептиды коллагена I типа (bCTx, пг/мл) в крови, С-концевой пропептид проколлагена I типа (PICP, нг/мл). Результаты оценки по шкале RUST в подгруппах 2а и 2б на 7-е сутки — 4 балла, на 30-е сутки — 6,5 и 8,7 баллов, на 90-е — 10 и 11,5 баллов соответственно. На фоне МАГОТ минеральная плотность костной ткани в подгруппе 2б на 90-е сутки достигала 90% против 78% в подгруппе 2а, что отражает значимо высокие темпы консолидации. На фоне МАГОТ bCTx на 30-е сутки был выше, чем в подгруппе 2а (соответственно 2289,4 [2145,3; 2365,4] против 1894,6 [1745,3; 2098,2], PICP значимо повышался в сравнении с подгруппой 2а на 7-е сутки, с максимумом на 30-е и 90-е сутки наблюдения (30-е сутки: 268,3 [231,2; 286,3] против 183,2 [174,6; 195,6], 90-е сутки: 584,6 [512,3; 589,3] против 351,2 [312,3; 369,4]. Применение МАГОТ оказывает позитивное влияние на качество и интенсивность формирования костного регенерата у мужчин с закрытым неосложненным изолированным переломом диафиза бедренной кости.

Ключевые слова: закрытый изолированный перелом диафиза бедра, озонотерапия, маркеры ремоделирования костной ткани

Вклад авторов: М. В. Осиков — концепция и дизайн исследования, анализ полученных данных, написание текста, редактирование рукописи; Е. В. Давыдова — концепция и дизайн исследования, анализ полученных данных, написание текста; К. С. Абрамов — набор клинического материала, анализ результатов, написание текста, редактирование рукописи. Все авторы внесли существенный вклад в проведение исследования и подготовку статьи, прочли и одобрили финальную версию перед публикацией.

Соблюдение этических стандартов: исследование одобрено этическим комитетом Южно-Уральского государственного медицинского университета г. Челябинск (протокол № 4 от 22 мая 2020 г.). Все участники подписали информированное согласие на участие в исследовании.

✉ **Для корреспонденции:** Михаил Владимирович Осиков
ул. Воровского, д. 64, г. Челябинск, 454092; prof.osikov@yandex.ru

Статья получена: 29.12.2020 **Статья принята к печати:** 17.01.2021 **Опубликована онлайн:** 02.02.2021

DOI: 10.24075/vrgmu.2021.003

Traumatic femoral fractures are among the leading causes of morbidity and mortality in low- and middle-income countries. They typically occur in young, working-age individuals [1, 2]. The need to clarify the pathogenesis of trauma-associated conditions and to develop efferent therapies for restoring the biochemical and immune homeostasis in patients with musculoskeletal injuries underscores the significance of studying bone turnover markers. The standard treatment

of orthopedic pathology can be complemented by physical therapy, like ozone therapy. Ozone therapy produces a local pain-relieving, anti-edematous, anti-inflammatory and tissue-regenerative effect, improves circulation, and exerts systemic immunomodulatory, anti-hypoxic, and redox-state-regulating activity. At the immune system level, ozone therapy stimulates the synthesis of pro- and anti-inflammatory cytokines and growth factors, contributing to tissue healing and remodeling [3]. When administered at therapeutic concentrations, ozone actively participates in the mitochondrial respiratory chain, accelerates glycolysis through the activation of phosphofructokinase and boosts the synthesis of ATP and 2,3-diphosphoglycerate, thereby improving oxygen uptake. It is reported that ozone therapy is effective in treating musculoskeletal disorders, such as rheumatoid arthritis, subacromial and other types of bursitis, osteoarthritis, capsulitis, temporomandibular joint pathology, etc. [4]. According to some authors, intravenous and intraarticular ozone injections benefit patients with osteoarthritis [5]. The aim of this study was to investigate the dynamics of bone turnover markers at different stages of simple (closed) femoral shaft fracture consolidation in the setting of systemic ozone therapy.

METHODS

This pilot study enrolled 20 male patients admitted to Chelyabinsk Regional Clinical Hospital for isolated closed displaced midshaft femoral fractures coded as 32A or 32B according to the AO/ASIF classification and as S72.3 according to ICD-10 [6]. The mean age of the participants, who formed group 2, was 47.8 ± 3.5 years. The following inclusion criteria were applied: age between 35 and 55 years; an isolated closed midshaft femoral fracture sustained 5–7 days before admission. Patients with acute pathology, cancer, lymphoproliferative disorders or osteoporosis were excluded from the study. The control group (group 1) comprised 10 healthy males aged 46.8 ± 3.7 years; their levels of bone turnover markers were used as a reference. All patients from group 2 underwent surgery on day 5–7 after the injury. The surgical procedure was performed using the standard surgical approach and involved closed reduction followed by intramedullary fixation with self-locking nails. Postoperatively, both groups received conventional treatment with antibiotics and non-steroid anti-inflammatory drugs.

Immediately after the surgical intervention, patients from the main group (n = 20, group 2) were randomized into 2 equally sized subgroups 2a and 2b (10 persons per group). Group 2a was assigned to receive standard therapy; group 2b was assigned to receive standard therapy complemented by minor autohemotherapy (MAHT), i.e. injections of ozone-enriched autologous blood. The ozone-oxygen mixture (OOM) was prepared using an automated UOTA-60-01 machine (Medozone; Russia) fitted with an ozone destructor. Ozone concentrations in the ozone-oxygen mixture were 20 mg/L. First, the medical grade gas was collected in a 20-ml syringe; then it was combined 10 ml of venous blood drawn from the cubital vein. The blood was combined with OOM by vigorous stirring for 2–3 seconds; the resultant mixture was injected deep into the gluteal or femoral muscles. The regimen consisted of 7–9 injections on alternate days. None of the patients developed adverse reactions to ozone therapy (fever, chills, malaise, infiltration at the injection site).

On admission and during treatment, the severity of pain at the fracture site was assessed using a visual analog scale (VAS) [7]. This scale is an ungraded 10cm-long line, the left and right ends of which represent no pain and extreme pain, respectively. Pain scores were measured immediately after the surgical procedure, prior to administering pain killers. Postoperatively, general condition was assessed every day; the patients were monitored for a fever and local signs of inflammation (edema, hyperemia, tissue infiltration, wound discharge). The day after surgery, each patient underwent a CT scan to rule out systemic osteoporosis and check the adequacy of the applied surgical technique. The scans were performed using a SOMATOM Definition Edge scanner (Siemens; Germany). Bone mineral density (BMD) measured in the paracortical bone at the fracture site was expressed in Hounsfield units (HU) and compared to BMD of the cortical bone in the contralateral leg. Follow-up CT scans were performed on days 7, 30 and 90 after the injury. In addition, the RUST scale [8] was applied to assess bone healing in each of 4 cortices (anterior, posterior, medial, lateral). The total score of 4 points was interpreted as the absence of consolidation; the total score of 10–12 points was interpreted as complete bony union. Clinical criteria for consolidation included the absence of edema or soft tissue infiltration and no pain on axial, ipsilateral and rotational loading.

Bone turnover markers were measured in fasting venous blood samples collected on days 7, 30 and 90 after the injury. Bone resorption was assessed from the levels of C-terminal telopeptides of type I collagen (bCTx, Beta-Crosslaps, pg/ml) measured by ELISA (ProteinsAntibodies; Russia). Bone formation was assessed from the levels of procollagen type I carboxy-terminal propeptide (PICP, ng/ml) (ProteinsAntibodies; Russia). The measurements were conducted in a Multiskan Multisoft plate reader (Labsystems Oy; Finland) at the corresponding wavelength.

Statistical analysis was carried out in IBM SPSS Statistics 19 (IBM; USA). Below, the data are presented as median (Me) values and quartiles [Q_{25}; Q_{75}]. The significance of differences between the groups was assessed with the Wilcoxon, Kruskal–Wallis, Mann–Whitney and Wild–Wolfowitz tests. Correlations between the studied parameters were tested using Spearman's rank correlation coefficient (R). The discovered differences were considered significant at $p < 0.05$.

RESULTS

VAS pain scores measured on days 5–7 after the injury (prior to surgery) were above average (5.6 [4.8–6.4] points), i.e. subjectively the pain was moderately severe, persistent, and

Table 1. Bone mineral density and RUST scores for the periosteal callus in patients with a closed isolated femoral shaft fracture, (Me [Q_{25}; Q_{75}])

Parameter	Healthy leg (cortical bone) (n = 10)	Fractured leg, (subgroup 2a, n = 10)					
		Day 7		Day 30		Day 90	
BMD	1956.5 [1789.5; 2035.8]	HU units	%	HU units	%	HU units	%
		0.5*	0	354. 4 [327; 368.8]*	18	1544. 2 [1468.2; 1632.1]*	1544. 2 [1468.2; 1632.1]*
Total RUST score	12.0 [12.0; 12.0]	4.0 [4.0; 4.0]*		6.5 [5.5; 7.0]*		10.0 [9.0; 11.0]	

Note: * — differences are significant ($p < 0.05$; the Mann–Whitney, Kruskal–Wallis, Wilcoxon and Wild–Wolfowitz tests) for comparison with the healthy leg.

Table 2. Bone mineral density and RUST scores at the site of the periosteal callus in patients with an isolated closed femoral shaft fracture in the setting of ozone therapy (Me [Q_{25}; Q_{75}])

Paramater	Healthy leg (cortical bone) (n = 20)	Fractured leg (n = 20)					
		Day 7 (immediately after surgery), HU, un. (%)		Day 30, HU, un. (%)		Day 90, HU, un. (%)	
		No O_3 (subgroup 2a)	MAHT (subgroup 2b)	No O_3 (subgroup 2a)	MAHT (subgroup 2b)	No O_3 (subgroup 2a)	MAHT (subgroup 2b)
BMD	1956.5 [1789.5; 2035.8]	0.5* (0%)	0.6* (0%)	354. 4 [327.3; 368.8] (18%)*	372.8 [262.5; 381.4] (19%)*	1544. 2 [1468.2; 1632.1] (78.2%)*	1825.3 [1726.1; 1911.3] 90%*#
Total RUST score	12.0 [12.0; 12.0]	4.0 [4.0; 4.0]*	4.0 [4.0; 4.0]*	6.5 [5.5; 7.0]*	8.7 [5.9; 8.9]#	10.0 [9.0; 11.0]	11.5 [10.5; 2.0]#

Note: * — differences are significant (p < 0.05; the Mann–Whitney, Kruskal–Wallis, Wilcoxon and Wild–Wolfowitz tests) for comparison with the healthy leg; # — differences are significant for comparison with subgroup 2a.

interfered with any activity or mental concentration. The patients could ignore the pain for several minutes at the longest. After the surgical intervention, the pain reached its intensity peak and was assessed as 8–9 points on the visual analog scale. Now, the pain became intense, excruciating, and was a serious constraint on physical activity. According to the CT scans performed on the day after the surgical procedure (i.e., on day 7 after the injury), none of the patients had osteoporosis. No visual signs of inflammation in the affected limb were detected on physical examination. On days 30 and 90, VAS scores were as low as 1.2 [0.9–1.4] and 0.8 [0.6–0.9] points, respectively.

Throughout the entire observation period, bone fragments retained a stable position and no signs of intramedullary nail dislocation were detected on CT scans in both subgroups (2a and 2b) of the main group. On day 7, the radiographic assessment of BMD showed an almost complete absence of the periosteal callus in subgroup 2a (standard treatment; Table 1), also indicated by the low total score on the RUST scale. On day 30, the periosteal callus was visualized as a distinct nebulous area of newly formed tissue; its BMD was 18% (relative to the cortical bone of the healthy contralateral limb). The average RUST score was 6.5, suggesting the ongoing process of callus formation. On day 90, there were no clinical signs of soft tissue infiltration and no pain on axial, ipsilateral and rotational loading. The callus BMD value was close to that of the cortical bone in the healthy contralateral limb, equaling 78% on average. The RUST score for fracture consolidation was 10 points, confirming complete bony union.

C-terminal telopeptides of type I collagen (bCTx, Beta-Crosslaps) are known markers of bone resorption. They are the products of collagen helix degradation; importantly, collagen makes up 90% of the bone matrix. Procollagen type I carboxy-terminal propeptide (PICP) is the marker of bone formation; its C(carboxyl) and N(amino) termini are cleaved by proteinases, resulting in collagen formation and its integration into the bone matrix. The cleaved C- and N-terminal fragments join extracellular fluid and enter the bloodstream. PICP levels in the blood are directly proportional to the amount of newly synthesized collagen in the bone. The dynamics of bone turnover markers are shown in Tables 3 and 4.

The analysis of Tables 3 and 4 reveals that bone metabolism (bone resorption and formation) was more active in patients from subgroup 2a at all stages of the observation period (days 7, 30, 90) than in the healthy males of the same age; this suggests the intensity of metabolic processes throughout the entire healing period.

The standard postoperative therapeutic regimen applied in subgroup 2a was complemented by systemic ozone therapy (MAHT) in group 2b. Subjectively, on day 7 (immediately after surgery) VAS pain scores in subgroup 2b were as high as in group 2a (8–9 points). By days 30 and 90, pain intensity in group 2b had declined to its minimal values (1.1 [0.8–1.2] and 0.4 [0.2–0.6], respectively) and did not differ from pain scores in group 2a.

The bone mineral density test showed the absence of the periosteal callus in subgroup 2b on day 7 (Table 2); RUST scores reflecting the degree of fracture consolidation were low (4 points). CT findings on day 30 indicated the presence of an actively forming periosteal callus. BMD was 19% relative to the cortical bone in the healthy contralateral limb and did no differ significantly from BMD values in subgroup 2a. The average RUST score (8.7) was also suggestive of active periosteal callus formation. On day 90, the patients from subgroup 2b had no pain on axial, ipsilateral and rotational loading. The average RUST score was 11.5, indicating complete bony union. The mineral density of the periosteal callus was about 90% vs. 78.2% in subgroup 2a and did not differ significantly from the density of the cortical bone in the healthy contralateral limb, suggesting the stimulating effect of ozone therapy on bone metabolism.

The levels of bone turnover markers also changed following the administration of systemic ozone therapy (see Tables 3 and 4).

On day 30, bCTx levels (marker of bone resorption) were significantly higher in subgroup 2b (ozone therapy) than in subgroup 2a. PICP levels (marker of bone formation) were significantly higher in group 2b than in group 2a starting from day 7 and then on days 30 and 90. This suggests fast bone tissue repair continuing in the setting of the clinical signs of bony union.

Table 3. Levels of C-terminal telopeptides of type I collagen in patients with an isolated femoral fracture undergoing ozone therapy (Me [Q_{25}; Q_{75}])

bCTx, pg/ml					
Control group, n = 10	Subgroups of the main group (n = 20)	Day of observation	Day 7	Day 30	Day 90
355,6 [324,5; 378,6]	Subgroup 2a (n = 10)		1572.3 [1452.3; 1638.4]*	1894.6 [1745.3; 2098.2]*	851.3 [745.9; 870.2]*
	Subgroup 2b MAHT (n = 10)		1505.2 [1356.2; 1624.7]*	2289.4 [2145.3; 2365.4]*#	915 [868.3; 925.4]*

Note: * — differences are significant (p < 0.05; the Mann–Whitney, Kruskal–Wallis, Wilcoxon and Wild–Wolfowitz tests) for comparison with the control group; # — differences are significant for comparison with subgroup 2a.

Table 4. Levels of procollagen type I carboxy-terminal propeptide (PICP) in patients with an isolated femoral fracture undergoing ozone therapy (Me [Q_{25}; Q_{75}])

PICP, ng/ml					
Control group, *n* = 10	Subgroups of the main group (*n* = 20)	Day of observation	Day 7	Day 30	Day 90
41.4 [38.6; 43.6]	Subgroup 2a (*n* = 10)		55.9 [49.1; 76.6]*	183.2 [174.6; 195.6]*	351.2 [312.3; 369.4]*
	Subgroup 2b MAHT (*n* = 10)		106.5 [75.3; 138.6]*#	268.3 [231.2; 286.3]*#	584.6 [512.3; 589.3]*#

Note: * — differences are significant ($p < 0.05$; the Mann–Whitney, Kruskal–Wallis, Wilcoxon and Wild–Wolfowitz tests) for comparison with the control group; # — differences are significant for comparison with subgroup 2a.

DISCUSSION

According to the currently held view, bone tissue is an active, dynamic metabolic system ensuring continuous bone remodeling. Bone healing consists of a few consecutive stages of resorption and repair [9]. During the first 5 days after a traumatic injury, fibroblasts, endothelial cells, leukocytes and monocytes migrate to the injury site and promote necrosis of damaged tissue. At the same time, molecules released by these cells trigger the process of granulation tissue formation; this granulation tissue includes elements of mesenchymal, osseous, cartilage and vascular tissues. Necrosis of dead or damaged cells in soft and bone tissues is accompanied by intense pain. According to the International Association for the Study of Pain (IASP), it is not only the actual tissue damage during a traumatic injury that causes pain but also the inflicted emotional stress which reflects the changed mental state of an injured individual. Pain experienced during high-energy long-bone fractures results from the hyperalgesia of the nociceptive system due to the effects exerted by inflammatory mediators (proinflammatory cytokines, chemokines, bradykinin) and the efferent effects of the sympathoadrenal axis.

The outer (the most massive) layer of the callus is derived from the cambium layer of the periosteum rich in fibroblasts, blood vessels and osteoblasts. During the first 5 weeks after a traumatic injury, a fibrocartilage callus is formed. In the next 3 to 4 months, the callus remodels. This process can be distinctly visualized on CT scans and identified during clinical examinations. The intensity of bone metabolism (bone resorption and formation) at all stages of our observation (days 7, 30, 90) was significantly higher than in the healthy men of the same age. This suggests active metabolic processes unfolding in the bone throughout the entire healing period.

The applied physical therapy (minor autohemotherapy) included in the regimen to complement the standard treatment of a closed femoral shaft fracture produced a number of positive effects on bone healing that were associated with the multimodal properties of molecular ozone derivatives. In minor autohemotherapy with ozonated blood, ozone molecules and their derivatives do not enter the bloodstream, so ozone cannot reach its molecular targets. However, when a small volume of blood is combined with the ozone-oxygen gas in a syringe, ozone molecules start to interact with the unsaturated fatty acids of blood cell membranes and plasma components; this results in the production of aldehydes and hydroperoxides (ozone peroxide) and their subsequent transformation into H_2O_2 and 4-hydroxynonenal (4-HNE), one of the most active aldehydes [10, 11]. Endogenous hydrogen peroxide and 4-HNE are secondary messengers that modulate the activity of immune cells and hematopoietic tissue and participate in the regulation of cellular antioxidant systems [10, 11]. It is known that H_2O_2 is capable of entering the cytoplasm of mononuclear cells (monocytes, macrophages) and modulates the activity of the nuclear factor kappa B (NF-κB) [10].

There is ongoing debate about the pluripotent effects of 4-HNE on the immune system that are mediated by the regulatory effect on the NF-κB pathway [10, 11]. This pathway triggers release of proinflammatory cytokines (TNFα, INFγ, IL1β, IL6, and IL8) and expression of proinflammatory genes, such as the cyclooxygenase-2 gene (COX-2) and the inducible nitric oxide synthase gene (iNOS) [10, 11]. The therapeutic dose of O_3 blocks NF-κB signaling, thereby reducing inflammation. The hormetic role of ozone is definitive in the regulation of inflammatory/proinflammatory responses. This underscores the therapeutic potential of ozone against a variety of pathologies.

The literature also mentions the analgesic effect of ozone therapy linked to the ozone derivatives-based oxidative modification of inflammatory mediators involved in the transmission of the nociceptive signal to CNS, balance restoration between pro- and antioxidant systems, and the declining levels of toxic molecular lipid peroxidation products [12]. Our study demonstrates the effects of ozone therapy on the optimization of bone repair confirmed by follow-up CT scans: on day 30, the total RUST score (fracture consolidation) was higher for the group receiving ozone therapy, indicating faster bone healing. However, it was only by day 90 that differences in the periosteal callus BMD between subgroups 2a (no ozone therapy) and 2b had reached statistical significance. The complex biochemical processes unfolding at the hematoma site create the conditions for bone tissue regeneration. Here, the special regulatory role is played by activated T cells and osteoclasts. In bone tissue, the majority of the regulatory mechanisms mediated by the immune system promote bone resorption [13, 14]. The key role in this process is played by the receptor activator of NF-κB (RANK), its ligand (RANKL) and osteoprotegerin (OPG) responsible for osteoclastogenesis, regulation of bone resorption and bone remodeling at the stages of fracture consolidation [15]. Some studies report that bCTx reaches its peak levels (3 times higher the age norm) 3–4 months after the sustained injury and declines substantially 6 months later [15]. Similar data were obtained during the study of bone turnover markers in patients with concomitant spinal and femoral fractures: the levels of bCTx and other bone resorption markers (OPG and RANKL) peaked at weeks 6–12 after the injury [16]. Some authors hold the opinion that OPG production by osteocytes is required to regulate the balance between bone remodeling and receptor-dependent activation of RANKL [16]. We think that the regulatory role of ozone is mediated by the non-classic secondary messenger 4-HNE and consists in the ability of ozone to modulate bone remodeling [17]. This supposition is indirectly confirmed by the increase in the mineral density of the periosteal callus in patients receiving ozone therapy, elevated bCTx on day 30 (relative to the values

observed in group 2a) and the increase in PICP levels (bone formation marker) on days 7, 30 and 90, which suggests a higher level of bone tissue metabolism at the earliest stages of bone repair.

Thus, our study demonstrates the positive effect of systemic ozone therapy on bone tissue metabolism at the stages of bone formation in patients with isolated closed femoral shaft fracture, which is indicated by the relative increase in bone mineral density and the high total RUST score reflecting fracture consolidation.

CONCLUSION

Our study reached its goal and showed that systemic ozone therapy used as an adjunct to the standard treatment regimen for a closed isolated femoral shaft fracture produces a positive effect on the quality and intensity of bone repair, leading to significant changes in BMD, a higher total RUST score, and faster bone remodeling. MAHT can be used as an auxiliary method of efferent physical therapy in the combination treatment of the abovementioned pathology.

References

1. Bommakanti K, Feldhaus I, Motwani G, Dicker RA, Juillard C. Trauma registry implementation in low- and middle-income countries: challenges and opportunities. J Surg Res. 2018 Mar; 223: 72–86.
2. Agarwal-Harding KJ, Meara JG, Greenberg SL, Hagander LE, Zurakowski D, Dyer GS. Estimating the global incidence of femoral fracture from road traffic collisions: a literature review. J Bone Joint Surg Am. 2015 Mar 18; 97 (6): e31. DOI: 10.2106/JBJS.N.00314.
3. Bocci VA. Scientific and medical aspects of ozone therapy. State of the art. Arch Med Res. 2006; 37: 425–35.
4. Omar Seyam, Noel L. Smith, Inefta Reid, Jason Gandhi, Wendy Jiang, Sardar Ali Khan. Clinical utility of ozone therapy for musculoskeletal disorders. Med Gas Res. 2018 Jul-Sep; 8 (3): 103–10.
5. Manoto SL, Maepa MJ, Motaung SK. Medical ozone therapy as a potential treatment modality for regeneration of damaged articular cartilage in osteoarthritis. Saudi J Biol Sci. 2018 May; 25 (4): 672–9.
6. Pomogaeva EV, redaktor. Sovremennye klassifikacii perelomov kostej nizhnej konechnosti. Ekaterinburg: Izd-vo UGMU, 2016; 56 s. Russian.
7. Huskisson EC. Measurement of pain. The Lancet. 1974; 9 (2): 1127–31.
8. Leow JM, Clement ND, Tawonsawatruk T, Simpson CJ, Simpson RW. The radiographic union scale in tibial (RUST) fractures. J Bone & Joint Research. 2016; 5 (4): 116–21.
9. Hismatullina ZN. Factors influencing the metabolism of bone tissue and leading to diseases of the bone system. Bulletin of the Kazan technological University. 2015; 22. Available from: https://cyberleninka.ru/article/n/faktory-okazyvayuschie-vliyanie-na-metabolizm-kostnoy-tkani-i-privodyaschie-k-zabolevaniyam-kostnoy-sistemy (data obrashhenija: 20.12.2020). Russian.
10. Bernardino C, Martínez-Sánchez FG, Llontop P, Aguiar-Bujanda D, Fernández-Pérez R, Santana-Rodríguez N. Modulation of Oxidative Stress by Ozone Therapy in the Prevention and Treatment of Chemotherapy-Induced Toxicity: Review and Prospects Antioxidants (Basel). 2019 Dec; 8 (12): 588. DOI: 10.3390/antiox8120588.
11. Bocci V, Valacchi G. Nrf2 activation as target to implement therapeutic treatments. Front Chem. 2015; 3: 4.
12. Osikov MV, Davydova EV, Abramov KS. Innate immunity in isolated femoral fractures. Modern problems of science and education. 2019; 1. Available from: http://www.science-education.ru/article/view?id=28540 (data obrashhenija: 20.01.2020). Russian.
13. Korshunova AC, Yuryevna E, Lebedev VF. The role of interferons in the regulation of osteogenic and osteoresorptive processes. Acta Biomedica Scientifica. 2012; 5–2 (87). Available from: https://cyberleninka.ru/article/n/rol-interferonov-v-regulyatsii-osteogennyh-i-osteorezorbtivnyh-protsessov.
14. Mashejko IV. Biohimicheskie markery v ocenke processov remodelirovanija kostnoj tkani pri osteopenii i osteoporoze. Zhurnal GrGMU. 2017; 2. Available from: https://cyberleninka.ru/article/n/biohimicheskie-markery-v-otsenke-protsessov-remodelirovaniya-kostnoy-tkani-pri-osteopenii-i-osteoporoze (data obrashhenija: 01.12.2020). Russian.
15. Aganov DS, Tyrenko VV, Cygan EN, Toporkov MM, Bologov SG. Rol' citokinovoj sistemy RANKL/RANK/OPG v reguljacii mineral'nogo obmena kostnoj tkani. Geny i kletki. 2014; 4. Available from: https://cyberleninka.ru/article/n/rol-tsitokinovoy-sistemy-rankl-rank-opg-v-regulyatsii-mineralnogo-obmena-kostnoy-tkani (data obrashhenija: 20.12.2020). Russian.
16. Sousa K, Dias I, Lopez-Peña M, Camassa J, Lourenço P. Bone turnover markers for early detection of fracture healing disturbances: A review of the scientific literature. Annals of the Brazilian Academy of Sciences. 2015; 87 (2): 1049–1061. Available from: http://dx.doi.org/10.1590/0001-3765201520150008.
17. Thakkar P, Naveen B. Prakash, Tharion G, Shetty Sh, Paul V, Bondu J, Yadav B. Evaluating Bone Loss with Bone Turnover Markers Following Acute Spinal Cord InjuryAsian Spine Journal 2020; 14 (1): 97–105. Available from: https://doi.org/10.31616/asj.2019.0004.

Литература

1. Bommakanti K, Feldhaus I, Motwani G, Dicker RA, Juillard C. Trauma registry implementation in low- and middle-income countries: challenges and opportunities. J Surg Res. 2018 Mar; 223: 72–86.
2. Agarwal-Harding KJ, Meara JG, Greenberg SL, Hagander LE, Zurakowski D, Dyer GS. Estimating the global incidence of femoral fracture from road traffic collisions: a literature review. J Bone Joint Surg Am. 2015 Mar 18; 97 (6): e31. DOI: 10.2106/JBJS.N.00314.
3. Bocci VA. Scientific and medical aspects of ozone therapy. State of the art. Arch Med Res. 2006; 37: 425–35.
4. Omar Seyam, Noel L. Smith, Inefta Reid, Jason Gandhi, Wendy Jiang, Sardar Ali Khan. Clinical utility of ozone therapy for musculoskeletal disorders. Med Gas Res. 2018 Jul-Sep; 8 (3): 103–10.
5. Manoto SL, Maepa MJ, Motaung SK. Medical ozone therapy as a potential treatment modality for regeneration of damaged articular cartilage in osteoarthritis. Saudi J Biol Sci. 2018 May; 25 (4): 672–9.
6. Помогаева Е. В., редактор. Современные классификации переломов костей нижней конечности. Екатеринбург: Изд-во УГМУ, 2016; 56 с.
7. Huskisson EC. Measurement of pain. The Lancet. 1974; 9 (2): 1127–31.
8. Leow JM, Clement ND, Tawonsawatruk T, Simpson CJ, Simpson RW. The radiographic union scale in tibial (RUST) fractures. J Bone & Joint Research. 2016; 5 (4): 116–21.
9. Хисматуллина З. Н. Факторы, оказывающие влияние на метаболизм костной ткани и приводящие к заболеваниям костной системы. Вестник Казанского технологического университета. 2015; 22. Доступно по ссылке: https://cyberleninka.ru/article/n/faktory-okazyvayuschie-vliyanie-na-metabolizm-kostnoy-tkani-i-privodyaschie-k-zabolevaniyam-kostnoy-sistemy (дата обращения: 20.12.2020).

10. Bernardino C, Martínez-Sánchez FG, Llontop P, Aguiar-Bujanda D, Fernández-Pérez R, Santana-Rodríguez N. Modulation of Oxidative Stress by Ozone Therapy in the Prevention and Treatment of Chemotherapy-Induced Toxicity: Review and Prospects Antioxidants (Basel). 2019 Dec; 8 (12): 588. DOI: 10.3390/antiox8120588.
11. Bocci V, Valacchi G. Nrf2 activation as target to implement therapeutic treatments. Front Chem. 2015; 3: 4.
12. Осиков М. В., Давыдова Е. В., Абрамов К. С. Врожденный иммунитет при изолированных переломах бедренной кости. Современные проблемы науки и образования. 2019; 1. Доступно по ссылке: http://www.science-education.ru/article/view?id=28540 (дата обращения: 20.01.2020).
13. Korshunova AC, Yuryevna E, Lebedev VF. The role of interferons in the regulation of osteogenic and osteoresorptive processes. Acta Biomedica Scientifica. 2012; 5–2 (87). Available from: https://cyberleninka.ru/article/n/rol-interferonov-v-regulyatsii-osteogennyh-i-osteorezorbtivnyh-protsessov.
14. Машейко И. В. Биохимические маркеры в оценке процессов ремоделирования костной ткани при остеопении и остеопорозе. Журнал ГрГМУ. 2017; 2. Доступно по ссылке: https://cyberleninka.ru/article/n/biohimicheskie-markery-v-otsenke-protsessov-remodelirovaniya-kostnoy-tkani-pri-osteopenii-i-osteoporoze (дата обращения: 01.12.2020).
15. Аганов Д. С., Тыренко В. В., Цыган Е. Н., Топорков М. М., Бологов С. Г. Роль цитокиновой системы RANKL/RANK/OPG в регуляции минерального обмена костной ткани. Гены и клетки. 2014; 4. Доступно по ссылке: https://cyberleninka.ru/article/n/rol-tsitokinovoy-sistemy-rankl-rank-opg-v-regulyatsii-mineralnogo-obmena-kostnoy-tkani (дата обращения: 20.12.2020).
16. Sousa K, Dias I, Lopez-Peña M, Camassa J, Lourenço P. Bone turnover markers for early detection of fracture healing disturbances: A review of the scientific literature. Annals of the Brazilian Academy of Sciences. 2015; 87 (2): 1049–1061. Available from: http://dx.doi.org/10.1590/0001-3765201520150008.
17. Thakkar P, Naveen B. Prakash, Tharion G, Shetty Sh, Paul V, Bondu J, Yadav B. Evaluating Bone Loss with Bone Turnover Markers Following Acute Spinal Cord InjuryAsian Spine Journal 2020; 14 (1): 97–105. Available from: https://doi.org/10.31616/asj.2019.0004.

REFINEMENT OF NONINVASIVE METHODS FOR DIAGNOSING PRECANCER AND CANCER OF ORAL MUCOSA IN GENERAL DENTAL PRACTICE

Postnikov MA[1], Gabrielyan AG[1,2] ✉, Trunin DA[1], Kaganov OI[1,2], Kirillova VP[1], Khamadeeva AM[1], Osokin OV[2] , Kopetskiy IS[3], Eremin DA[3]

[1] Samara State Medical University, Samara, Russia

[2] Samara Regional Clinical Cancer Center, Samara, Russia

[3] Pirogov Russian National Research Medical University, Moscow, Russia

The search for and the application of available noninvasive methods for early diagnosis of oral mucosa (OM) neoplasia is a clinically significant problem. The aim of this study was to evaluate the effectiveness of the original score-based algorithm for assessing clinical data generated by a conventional and an autofluorescence-based examination in diagnosing OM cancer and assessing indications for a biopsy. We analyzed 134 medical histories and pathology reports of patients with oral neoplasia. The patients were assigned to 2 groups: the control group included 63 patients who underwent a standard visual and tactile examination with history taking and then were referred for an incisional biopsy followed by a histopathological examination of the specimens. In the main group consisting of 71 patients, a standard visual and tactile examination was complemented by an autofluorescence-based examination and the original score-based algorithm with the original index of required histopathological verification (RHV) were used to assess indications for a biopsy. In both groups, the most commonly affected site was the tongue (72.4%). The histopathological examination revealed that 28 patients from the main group and 14 patients from the control group had OM cancer (p = 0.051). Histologically, early-stage cancer was diagnosed in 17 patients from the main group and in 4 patients from the control group (p = 0.004). The proposed algorithm allowed us to effectively (in 90% of cases) diagnose precancer and cancer and avoid unnecessary biopsies.

Keywords: oral mucosa, precancer, cancer, required histological verification index (RHV)

Author contribution: Postnikov MA — literature analysis; Gabrielyan AG — study planning; Trunin DA, Kopetskiy IS, Eremin DA — analysis of the obtained data; Kaganov OI — manuscript draft; Kirillova VP — analysis of patients' records; Khamadeeva AM — interpretation of the obtained results; Osokin OV — data acquisition.

Compliance with ethical standards: the study was approved by the Ethics Committee of Samara State Medial University (Protocol № 27 dated February 12, 2018).

✉ **Correspondence should be addressed:** Alexey G. Gabrielyan
Michurina, 138, kv. 85, Samara, 443086; gabriel_002@mail.ru

Received: 18.12.2020 **Accepted:** 29.01.2021 **Published online:** 18.02.2021

DOI: 10.24075/brsmu.2021.005

СОВЕРШЕНСТВОВАНИЕ НЕИНВАЗИВНЫХ МЕТОДОВ ДИАГНОСТИКИ ПРЕДРАКОВЫХ И ЗЛОКАЧЕСТВЕННЫХ ЗАБОЛЕВАНИЙ СЛИЗИСТОЙ ОБОЛОЧКИ РТА НА ПРИЕМЕ У СТОМАТОЛОГА

М. А. Постников[1], А. Г. Габриелян[1,2] ✉, Д. А. Трунин[1], О. И. Каганов[1,2], В. П. Кириллова[1], А. М. Хамадеева[1], О. В. Осокин[2], И. С. Копецкий[3], Д. А. Еремин[3]

[1] Самарский государственный медицинский университет, Самара, Россия

[2] Самарский областной клинический онкологический диспансер, Самара, Россия

[3] Российский научно-исследовательский медицинский университет имени Н. И. Пирогова, Москва, Россия

Поиск и применение доступных неинвазивных методов ранней диагностики новообразований слизистой оболочки рта (СОР) является актуальной задачей. Целью работы было выявить эффективность использования разработанного алгоритма балльной оценки данных клинического обследования в сочетании с проведением аутофлуросцентной стоматоскопии (АФС) для постановки диагноза злокачественных новообразований СОР и принятия решения о необходимости проведения биопсии. Проведен анализ 134 амбулаторных карт больных, которым выполняли биопсию. Пациенты были разделены на две группы: в контрольную группу вошли 63 человека, которым после проведенного традиционного обследования (опроса, осмотра, пальпации) проводили инцизионную биопсию с последующим морфологическим исследованием; у 71 пациента основной группы применяли (ИНГВ). Установлено, что патологические состояния СОР локализовались в большей степени на языке у 72,4% пациентов в обеих группах. После выполненных биопсий в основной группе злокачественные опухоли СОР были диагностированы у 28 пациентов, в контрольной — у 14 (p = 0,051). В основной группе начальные стадии рака СОР установлены у 17 человек после биопсии, в контрольной — у 4 (p = 0,004). Использование разработанного алгоритма позволило с высоким процентом точности (90%) диагностировать предраковые и злокачественные новообразования и проводить инвазивные методы исследования (биопсию) строго по показаниям.

Ключевые слова: слизистая оболочка рта, СОР, предрак, злокачественное образование, индекс необходимости гистологической верификации, ИНГВ

Вклад авторов: М. А. Постников — анализ литературы; А. Г. Габриелян — планирование исследования; Д. А. Трунин, И. С. Копецкий, Д. А. Еремин — анализ данных; О. И. Каганов — подготовка черновика рукописи; В. П. Кириллова — обработка и анализ первичной документации; А. М. Хамадеева — интерпретация данных; О. В. Осокин — сбор данных.

Соблюдение этических стандартов: исследование одобрено этическим комитетом Самарского государственного медицинского университета (протокол № 27 от 12 февраля 2018 г.).

✉ **Для корреспонденции:** Алексей Григорьевич Габриелян
ул. Мичурина, д. 138, кв. 85, г. Самара, 443086; gabriel_002@mail.ru

Статья получена: 18.12.2020 **Статья принята к печати:** 29.01.2021 **Опубликована онлайн:** 18.02.2021

DOI: 10.24075/vrgmu.2021.005

According to statistics, over 300,000 new cases of oral cancer are reported worldwide annually [1]. In Russia, over 9,000 patients were diagnosed with oral mucosal (OM) malignancies in 2018; of them, 199 were residents of Samara region. OM cancer is the 18th most common cancer; this malignancy is histologically confirmed in 97% of suspected cases [2]. Although OM cancer develops on external body surfaces, 62% of Russian patients and 63% of patients residing in Samara region present with advanced stages. Delays in diagnosis are associated with a number of factors, including low suspicion by dentists, the lack of awareness among patients, and the absence of screening programs. General dentists working in secondary prevention do not have a clear diagnostic algorithm for oral cancer screening and often misdiagnose their patients [3–5]. A physical examination remains the main screening (but not diagnostic) test for oral cancer [6–8]. Most patients with suspicious lesions are referred for a biopsy. This may result in overdiagnosis [9–11]. A biopsy is an invasive method of tissue sampling. Biopsied specimens of oral mucosa are subjected to a histopathological examination performed to establish a differential and a final diagnosis. An oral tissue biopsy poses a risk of adverse events, so a patient should be referred for this procedure only when he/she has clear indications for it, including a suspicious lesion. A pathology report plays a critical role in establishing a definitive diagnosis, choosing an adequate treatment and predicting a patient's outcome. This is why an OM biopsy should be performed only when clearly indicated and required for a differential diagnosis. Autofluorescence-based visualization of the oral cavity is a well-known method of oral cancer detection [12–14]. There has been a wealth of studies investigating this diagnostic method, but none of them looked at the integrated approach combining a conventional clinical examination and autofluorescence-based visualization [15–18]. In 2020, we patented a simple noninvasive method for assessing indications for biopsy in patients with a suspected vermillion lip border neoplasm that can be used in general dental practice [19].

The aim of this study was to evaluate the effectiveness of the original score-based algorithm in diagnosing OM precancer and cancer and assessing indications for biopsy during a standard clinical examination complemented by autofluorescence-based visualization of the oral cavity.

METHODS

We analyzed 134 medical histories and pathology reports of patients with oral neoplasia who had been referred to Samara Regional Clinical Cancer Center by the general dentists of Samara clinics between 2014 and 2019.

The patients were divided into 2 groups according to the method of clinical examination. The control group (M2) comprised 63 patients with suspicious oral mucosal lesions (preliminary diagnosis: oral neoplasia) who had been referred to the Cancer Center by their dentists between 2014 and 2019. At the Center, the patients underwent a standard visual and tactile examination, and their medical histories were taken; then, the patients underwent an incisional biopsy. The collected specimens were studied by a pathologist at the Center's laboratory. In the main group (M1) consisting of 71 patients, a standard visual and tactile examination was complemented by an autofluorescence-based examination and the original score-based algorithm with the original index of required histopathological verification (RHV) were used to assess indications for a biopsy. This algorithm allows discriminating between inflammation or precancer and cancer (Fig. 1). In both groups, incisional biopsies were performed under local anesthesia using conchotomes; the obtained specimens were subjected to a histopathological examination (Fig. 2). In the main group incisional biopsy was performed on those patients whose RHV index was above 5.

The following inclusion criteria were applied: any age or sex; superficial oral cavity neoplasia; first-time referral to an oncologist by a general dentist. Patients who had been referred to an oncologist by other specialists, self-referred patients, those who had submucosal malignancies and those who refused to participate were excluded from the study.

The patients were comparable in terms of sex (M : F = 3 : 1; $p = 0.858$), age (63 ± 2.8 years in the control group, 71 ± 2.8 years in the main group) and lesion site (Table 1). The original protocol for cancer detection applied in the main group consisted in taking a medical history, conducting a visual and tactile examination of the oral cavity, and a visual autofluorescence-based examination with an AFS400 handpiece (Polironik; Russia). Results produced by each component of the protocol are expressed as points and are then summated and expressed in the form of the RHV index. The index value specified in the oral cavity assessment form must contain a letter indicating the site of the detected lesion. The RHV index must be calculated for each detected lesion. There must be a separate assessment form for each detected lesion. If the RHV index value is below 5, a patient should receive treatment and be invited for a follow-up examination. If the RHV index value is 5 or above, a biopsy is recommended. The pathology report concluding precancer or cancer is the main criterion

Table 1. Lesions sites in the main and control groups

Site	Groups			
	Control M2 *n* = 63		Main M1 *n* = 71	
	n	%	*n*	%
Tongue	29	46	33	47
Upper alveolus	1	2	–	0
Lower alveolus	3	5	1	1
Mouth floor	14	22	17	24
Hard palate	2	3	3	4
Soft palate	1	2	2	3
Cheek	13	20	15	21
Total	63	100	71	100

Note: Pearson's coefficient = 2.7567; $p = 0.8386$.

Date: First visit/followup visit (underline as appropriate)	POINTS	**Protocol for visual, tactile and autofluorescence-based examination of vermillion lip border and oral mucosa**
Patient's full name		
Date of birth		a) lip, vermillion border / labial mucosa, corner upper / lower / right / left b) mouth vestibule upper / lower / right / left c) vestibular alveolar mucosa upper / lower jaw, right / left / front d) buccal mucosa right / left e) labial alveolar mucosa upper / lower jaw, right / left / front f) retromolar space right / left g) floor mouth mucosa frontal / lateral / right / left h) ventral surface of tongue right / left i) lateral border of tongue right / left j) tip of tongue k) dorsal surface of tongue right / left l) base of tongue right / left m) hard palate mucosa right / left n) soft palate mucosa right / left o) anterior faucial pillars right / left Note: underline as appropriate
History (underline as appropriate) Any symptoms — 0.25 points, no symptoms — 0 points Onset of symptoms — 14 days ago or earlier — 0.25 points Less than 14 days ago — 0 points Any unhealthy lifestyle habits (except smoking) — 0.25 points Smoking — 0.5 points No unhealthy lifestyle habits — 0 points Occasional exposure to occupational hazards — 0.25 points No exposure to occupational hazards — 0 points	0,25 0,25 0 0	
Visual examination (underline as appropriate) Erosions, excoriation, aphthae, ulceration, chapping or cracking, scarring, hyperkeratosis — 2 points Discoloration, nodules, bumps, vesicles, abscesses, cysts — 1 point No lesions — 0 points Does not require dental care — 0 points Requires dental care — 0.25 points	2 0,25	
Tactile examination (underline as appropriate) No palpable growth — 0 points Palpable growth — 1 point Palpable regional lymph nodes — 0.5 points Regional lymph nodes not palpable — 0 points	1 0	
Autofluorescence-based examination (underline as appropriate) Dark-brown fluorescence — 2 points Pinkish red fluorescence — 1 point Green fluorescence — 0 points	2	
RHV index	ИНГВ = 5,75j	

Fig. 1. An algorithm for assessing indications for biopsy in patients with vermillion lip border and oral mucosa neoplasia presenting to a dentist for a clinical examination

indicating the efficacy of the proposed algorithm. Fig. 1–4 show a visual examination of the patient with a tongue neoplasm conducted under natural light and with an AFS handpiece. The following variables were compared between the main and control groups: presenting complaints, pathologies detected on examination, the proportion of precancerous conditions and malignancies, histologically identified stages of cancer. Multivariate logistic regression models were applied to analyze the data of patients with OM malignancies. Differences were considered significant at $p < 0.05$ Statistical analysis was carried out in Statistica 10.0 (Dell; USA).

RESULTS

The groups differed in terms of frequency of complaints. In the main group, complaints of a suspicious growth were more frequent than in the control group (0.54 vs. 1.17 times, respectively). Pain was reported by 23.9% of patients from M1 and by 47.6% of patients from M2. In both groups, discomfort was very pronounced; a burning sensation and itching were

Fig. 2. Biopsy of a buccal mucosa lesion

Table 2. Presenting complaints in the main (M1) and control (M2) groups

Groups	Complaints	Suspicious growth	Pain	Discomfort	Burning sensation	Itching	Bleeding
M1	Detected	35.2%	23.9%	64.8%	40.8%	29.6%	7.04%
	Not detected	64.8%	76.1%	35.2%	59.2%	70.4%	92.96%
	Difference	0.54 times	3.17 times	1.84 times	1.45 times	0.98 times	13.2 times
M2	Detected	53.9%	47.6%	47.6%	42.9%	39.7%	22.2%
	Not detected	46.1%	52.4%	19.1%	57.1%	60.3%	77.8%
	Difference	1.17 times	1.1 times	4.25 times	1.33 times	1.52 times	3.5 times

reported at the same frequency (Fig. 5). Table 3 compares the clinical manifestations of the pathology between groups M1 and M2. Mucosal discoloration was observed 0.82 times more often in the main group than in the control group (54.9% vs. 28.4%). A coated tongue was present in 62.0% and 60.3% of patients from the main and control groups, respectively. Hyperkeratosis was detected in 45.1% and 58.7% of patients, respectively. Erosions prevailed in the control group (55.6% vs. 36.6%). Hyperplasia and atrophy were detected in 11.1% to 31.0% of cases.

The histopathological examination confirmed precancer in 18 and 36 patients from the main and control groups, respectively (p = 0.016). Oral cancer was confirmed in 28 patients from the control group and only 14 patients from the main groups (p = 0.051). According to the pathology reports, 7 patients in the main group and 31 patients in the control group had inflammation (p = 0.001) (Fig. 6). Early-stage cancer was detected in 17 patients from the main group and 4 patients from the control group (p = 0.004). There were no significant differences in the frequency of late-stage cancer between the groups: advanced cancer was detected in 11 and 10 patients from the main and control groups, respectively (Fig. 7).

DISCUSSION

Pain, discomfort and a burning sensation were more pronounced in the control group than in the main group; erosions were also more common for the control group. By contrast, a coated tongue and dysplasia were more prevalent in the main group. The tongue was the most commonly affected site in both groups (46% and 47% in the control and main groups, respectively), which is consistent with the literature [2, 5]. Patients with OM inflammation pose the main diagnostic challenge for primary care dentists. They are often referred for invasive diagnostic procedures for no justified reason. The proposed score-based assessment of biopsy indications in patients with suspicious growths on the vermillion border or oral cavity mucosa during a conventional clinical examination complemented by autofluorescence-based visualization allowed us to confirm precancerous conditions and cancer in 90% of patients in the main group

Fig. 3. Lingual mucosa lesion detected on clinical examination

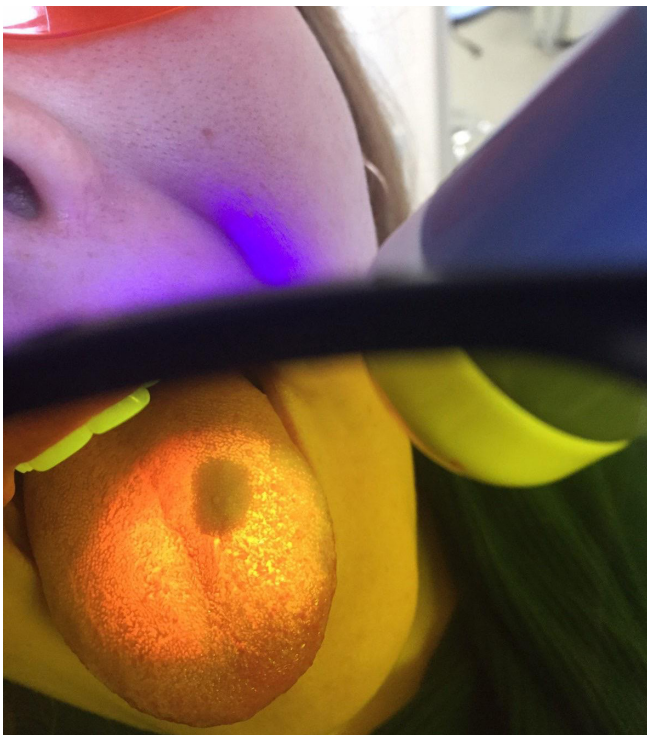

Fig. 4. Brown autofluorescence of lingual mucosa under AFS400 light

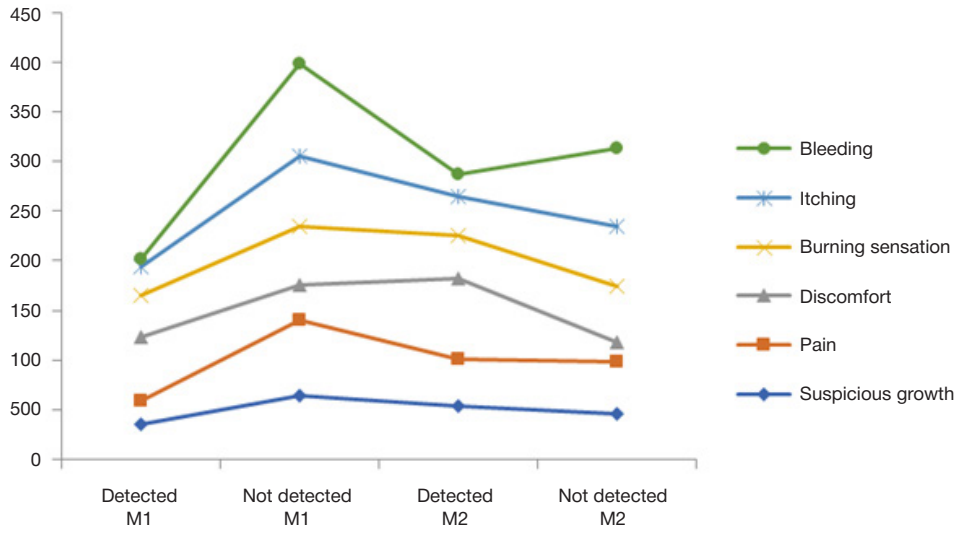

Fig. 5. Distribution of presenting complaints in the main (M1) and control (M2) groups on clinical examination

Table 3. Clinical manifestations detected on examination in the main (M1) and control (M2) groups (under natural light)

Oral mucosa examination		Mucosal discoloration	Moist, glossy mucosa	Coated tongue			Signs of pathology			
				Present	Removable	Non-removable	Hyperkeratosis	Hyperplasia	Atrophy	Erosion/ ulceration
M1	Detected	54.9%	43.7%	62.0%	31.0%	28.2%	45.1%	31.0%	12.7%	36.6%
	Not detected	45.1%	56.3%	38.0%	69.0%	71.8%	54.9%	69.0%	87.3%	63.4%
	Difference	0.82 times	1.29 times	1.63 times	2.23 times	2.55 times	1.22 times	2.23 times	6.9 times	1.73 times
M2	Detected	28.4%	53.9%	60.3%	33.8%	36.5%	58.7%	17.5%	11.1%	55.6%
	Not detected	71.4%	46.1%	39.7%	66.2%	63.5%	41.3%	82.5%	88.9%	44.4%
	Difference	2.5 times	1.17 times	1.52 times	3.2 times	1.7 times	1.42 times	4.7 times	8.0 times	1.25 times

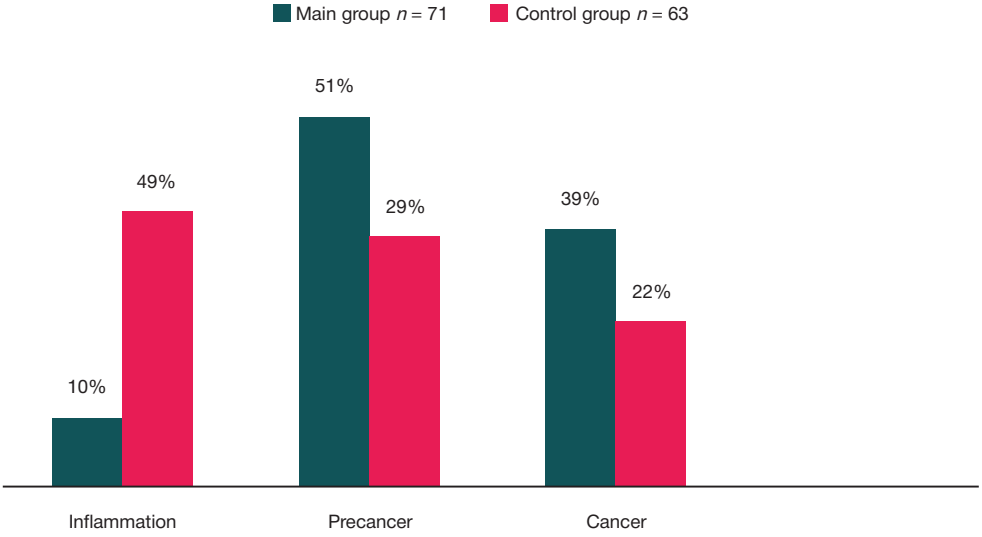

Fig. 6. Distribution of patients in the groups by histologically verified diagnoses

and 51% of patients in the control group (p = 0.001). The proposed method has advantages over the conventional examination in terms of early cancer detection and secondary prevention because it can be used by general dentists. According to the literature, a physical examination cannot be used as a diagnostic test for establishing a differential diagnosis and should be complemented by fluorescence-based and other methods. Our study demonstrates the effectiveness of such methods used as an adjunct to traditional procedures [12, 14–16].

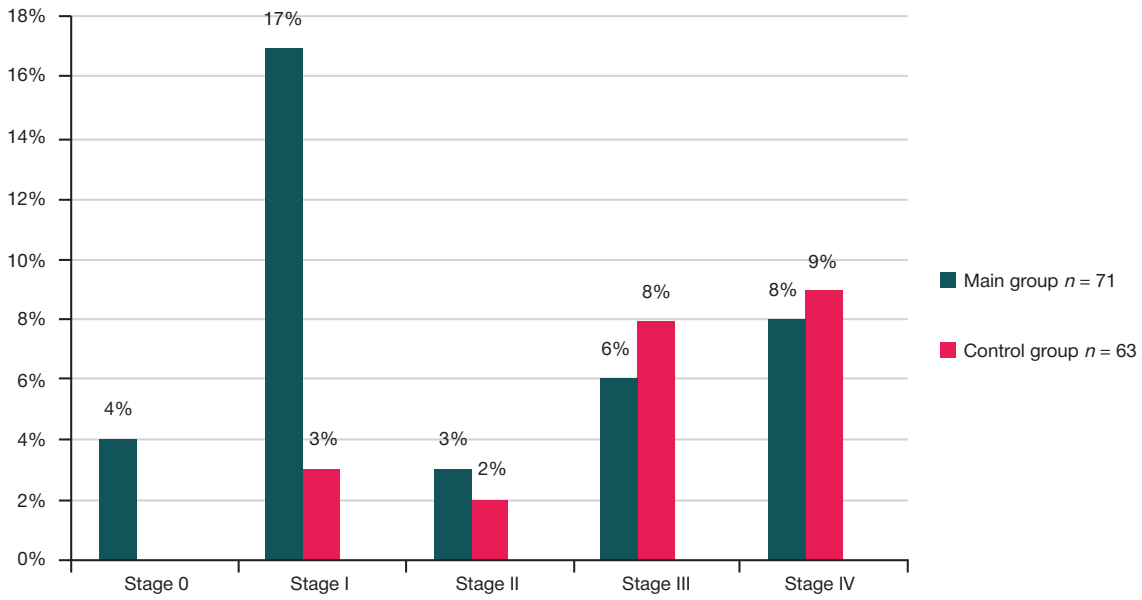

Fig. 7. Distribution of patients in the groups by cancer stages

CONCLUSION

Our score-based assessment of data yielded by a conventional clinical examination complemented by an autofluorescence-based examination allowed us to effectively (in 90% of cases) diagnose precancer and cancer, better detect early-stage OM cancer in comparison with traditional examinations (24% and 5% respectively) and avoid unnecessary biopsies.

References

1. Global Cancer Statistics 2018: GLOBOCAN Estimates of Incidence and Mortality Worldwide for 36 Cancers in 185 Countries.
2. Kaprin AD, Starinskii VV, Shakhzadovoi AO. Sostojanie onkologicheskoj pomoshhi naseleniju Rossii v 2019 godu. M.: MNIOI im. P. A. Gercena — filial FGBU «NMIC radiologii» Minzdrava Rossii, 2020; s. 239. Russian.
3. Starikov VI. Opuholi golovy i shei: uchebnoe posobie dlja studentov IV kursa stomatologicheskogo fakul'teta. Har'kov: 2014; s. 73. Russian.
4. Domanin AA, Solnyshkina AF. Diagnostika predraka slizistoj obolochki polosti rta. Privolzhskij onkologicheskij vestnik. 2011; 1: 45–46. Russian.
5. Kostina IN. Struktura, lokalizacija opuholevyh i opuholepodobnyh zabolevanij polosti rta. Problemy stomatologii. 2014; 4: 33–39. Russian.
6. Nikolenko V. N. i dr. Sovremennyj vzgljad na diagnostiku i lechenie raka slizistoj obolochki polosti rta. Golova i sheja. 2018; 4: 36–42. Russian.
7. Stepanov DA, Fedorova MG, Averkin NS. Morfologicheskie issledovanija v stomatologii. Vestnik Penzenskogo gosudarstvennogo universiteta. 2019; 1 (25): 80–85. Russian.
8. Filimonova LB, Mezhevikina GS, Marshuba LO. Ispol'zovanie autofluorescentnoj stomatoskopii kak skriningovogo metoda diagnostiki predrakovyh sostojanij i onkologicheskih zabolevanij slizistoj obolochki rta na stomatologicheskom prieme. Nauka molodyh. 2020; 8 (1): 80–85. Russian.
9. Mezhevikina GS, Gluhova EA. Sovremennye metody diagnostiki predrakovyh i rakovyh izmenenij slizistoj obolochki rta. Nauka molodyh. 2018; 6 (4): 600–6. Russian.
10. Ephros H. Oral Tissue Biopsy. Medscape. 2018: 1–13.
11. Leonteva ES, Egorov MA, Kuznecova RG. Immunogistohimicheskie markery v diagnostike predrakovyh porazhenij slizistoj obolochki polosti rta i krasnoj kajmy gub. Prakticheskaja medicina. 2012; 1: 20–22. Russian.
12. Maksimovskaya LN, Erk AA, Bulgakova NN, Zubov BV. Primenenie autofluorescentnoj stomatoskopii dlja onkoskrininga zabolevanij slizistoj obolochki polosti rta. Stomatologija dlja vseh. 2016; 4 (77): 34–37. 13. Pursanova AE, Kazarina LN, Gushhina OO, Serhel EV, Belozerov AE, Abaev ZM. Kliniko-immunologicheskie osobennosti predrakovyh zabolevanij slizistoj obolochki rta i krasnoj kajmy gub. Stomatologija. 2018; 5: 23–26.
14. Pozdnyakova TI, Smirnova YuA, Volkov EA, Bulgakova NN. Vozmozhnosti autofluorescentnoj spektroskopii v vyjavlenii predrakovyh zabolevanij slizistoj obolochki polosti rta. Dental-Revju. 2013; 2: 46–47.
15. Amirchaghmaghi M, Mohtasham N, Delavarian Z, Shakeri MT, Hatami M, Mozafari PM. The diagnostic value of the native fluorescence visualization device for early detection of premalignant/malignant lesions of the oral cavity. Photodiagnosis Photodyn Ther. 2018; 21: 19–27.
16. Simonato LE, Tomo S, Navarro RS, Villaverde AGJB. Fluorescence visualization improves the detection of oral, potentially malignant, disorders in population screening. Photodiagnosis Photodyn Ther. 2019; 27: 74–8.
17. Meleti M, Giovannacci I, Vescovi P, Pedrazzi G, Govoni P, Magnoni C. Histopathological determinants of autofluorescence patterns in oral carcinoma. Oral Dis. 2020.
18. Shuhorova YuA, Tkach TM, Burakshaev SA, Postnikov MA. Onkonastorozhennost v praktike vracha-stomatologa na ambulatornom prieme. Institut stomatologii. 2020; 3 (88): 20–22.
19. Orlov AE, Kaganov OI, Postnikov MA, Vozdvizhensky MO, Trunin DA, Makhonin AA, Gabrielyan AG, Tkachev MV, Kirilova VP, Osokin OV, Kerosirov AP, Akhmadieva EO, Baranov RA, Shurygina OV, avtory. Sposob opredelenija pokazanij dlja vypolnenija gistologicheskoj verifikacii obrazovanija krasnoj kajmy gub i slizistoj polosti rta u bol'nogo na prieme u vracha stomatologa. Patent RF # 2019133760. 22.10.2019.

Литература

1. Global Cancer Statistics 2018: GLOBOCAN Estimates of Incidence and Mortality Worldwide for 36 Cancers in 185 Countries.
2. Каприн А. Д., Старинский В. В., Шахзадовой А. О. Состояние онкологической помощи населению России в 2019 году. М.: МНИОИ им. П. А. Герцена — филиал ФГБУ «НМИЦ радиологии» Минздрава России, 2020; с. 239.
3. Стариков В. И. Опухоли головы и шеи: учебное пособие для студентов IV курса стоматологического факультета. Харьков: 2014; с. 73.
4. Доманин А. А., Солнышкина А. Ф. Диагностика предрака слизистой оболочки полости рта. Приволжский онкологический вестник. 2011; 1: 45–46.
5. Костина И. Н. Структура, локализация опухолевых и опухолеподобных заболеваний полости рта. Проблемы стоматологии. 2014; 4: 33–39.
6. Николенко В. Н. и др. Современный взгляд на диагностику и лечение рака слизистой оболочки полости рта. Голова и шея. 2018; 4: 36–42.
7. Степанов Д. А., Федорова М. Г., Аверкин Н. С. Морфологические исследования в стоматологии. Вестник Пензенского государственного университета. 2019; 1 (25): 80–85.
8. Филимонова Л. Б., Межевикина Г. С, Маршуба Л. О. Использование аутофлуоресцентной стоматоскопии как скринингового метода диагностики предраковых состояний и онкологических заболеваний слизистой оболочки рта на стоматологическом приеме. Наука молодых. 2020; 8 (1): 80–85.
9. Межевикина Г. С., Глухова Е. А. Современные методы диагностики предраковых и раковых изменений слизистой оболочки рта. Наука молодых. 2018; 6 (4): 600–6.
10. Ephros H. Oral Tissue Biopsy. Medscape. 2018: 1–13.
11. Леонтьева Е. С., Егоров М. А., Кузнецова Р. Г. Иммуногистохимические маркеры в диагностике предраковых поражений слизистой оболочки полости рта и красной каймы губ. Практическая медицина. 2012; 1: 20–22.
12. Максимовская Л. Н, Эрк А. А., Булгакова Н. Н., Зубов Б. В. Применение аутофлуоресцентной стоматоскопии для онкоскрининга заболеваний слизистой оболочки полости рта. Стоматология для всех. 2016; 4 (77): 34–37.
13. Пурсанова А. Е., Казарина Л. Н., Гущина О. О., Серхель Е. В., Белозеров А. Е., Абаев З. М. Клинико-иммунологические особенности предраковых заболеваний слизистой оболочки рта и красной каймы губ. Стоматология. 2018; 5: 23–26.
14. Позднякова Т. И, Смирнова Ю. А, Волков Е. А, Булгакова Н. Н. Возможности аутофлуоресцентной спектроскопии в выявлении предраковых заболеваний слизистой оболочки полости рта. Дентал-Ревю. 2013; 2: 46–47.
15. Amirchaghmaghi M, Mohtasham N, Delavarian Z, Shakeri MT, Hatami M, Mozafari PM. The diagnostic value of the native fluorescence visualization device for early detection of premalignant/malignant lesions of the oral cavity. Photodiagnosis Photodyn Ther. 2018; 21: 19–27.
16. Simonato LE, Tomo S, Navarro RS, Villaverde AGJB. Fluorescence visualization improves the detection of oral, potentially malignant, disorders in population screening. Photodiagnosis Photodyn Ther. 2019; 27: 74–8.
17. Meleti M, Giovannacci I, Vescovi P, Pedrazzi G, Govoni P, Magnoni C. Histopathological determinants of autofluorescence patterns in oral carcinoma. Oral Dis. 2020.
18. Шухорова Ю. А., Ткач Т. М., Буракшаев С. А., Постников М. А. Онконастороженность в практике врача-стоматолога на амбулаторном приеме. Институт стоматологии. 2020; 3 (88): 20–22.
19. Орлов А. Е., Каганов О. И., Постников М. А., Воздвиженский М. О., Трунин Д. А., Махонин А.А., Габриелян А. Г, Ткачев М. В., Кирилова В. П., Осокин О. В., Керосиров А. П., Ахмадиева Е. О., Баранов Р. А., Шурыгина О. В., авторы. Способ определения показаний для выполнения гистологической верификации образования красной каймы губ и слизистой полости рта у больного на приеме у врача стоматолога. Патент РФ № 2019133760. 22.10.2019.